



รายงานวิจัยฉบับสมบูรณ์

โครงการ

การพัฒนาชุดสมการสำหรับทำนายความหนาแน่นของพลังงานคลื่น ผิวน้ำพร้อมการประยุกต์งานใช้สำหรับชายฝั่งทะเลของประเทศไทย (Development of predictive equations for surface wave power density with practical application in the coastal ocean of Thailand)

โดย

รองศาสตราจารย์ ดร.ชัชวิน ศรีสุวรรณ (Associate Professor Dr. Chatchawin Srisuwan)

> พฤษภาคม 2563 (MAY 2020)

สัญญาเลขที่ MRG6180102

รายงานวิจัยฉบับสมบูรณ์

โครงการ

การพัฒนาชุดสมการสำหรับทำนายความหนาแน่นของพลังงานคลื่น ผิวน้ำพร้อมการประยุกต์งานใช้สำหรับชายฝั่งทะเลของประเทศไทย (Development of predictive equations for surface wave power density with practical application in the coastal ocean of Thailand)

โดย

รศ.ดร.ชัชวิน ศรีสุวรรณ

(Associate Professor Dr. Chatchawin Srisuwan)

สนับสนุนโดยสำนักงานคณะกรรมการส่งเสริมการวิจัย และสำนักงานคณะกรรมการการอุดมศึกษา

(ความเห็นในรายงานนี้เป็นของผู้วิจัย หน่วยงานที่สนับสนุนและต้นสังกัดไม่จำเป็นต้องเห็นด้วยเสมอไป) Project Code: MRG6180102

Project Title: Development of predictive equations for surface wave power density with

practical application in the coastal ocean of Thailand

Investigator: Associate Professor Dr. Chatchawin Srisuwan,

Department of Civil Engineering, Faculty of Engineering, Prince of Songkla University

E-mail Address : chatchawin.s@psu.ac.th

Project Period: 24 Months (MAY2018 - MAY2020)

Abstract

Surface water waves develop and grow as wind blows across a flat ocean surface. The present research project aims at developing a new set of analytical expressions of wave energy fluxes which attribute to the total amount of wave power at a particular location. The new expression is applied for estimating wave power potential in the coastal ocean of Thailand. This application part is incited by insufficiency of information regarding feasibility in harvesting ocean wave power in Thailand. To achieve the goal, under the concept of spectral wave parameterization, a new estimation formula is introduced capitalizing the advantages of both the numerical method and the closed-form solution. The formula was verified using synthetic wave data in which its applicable condition was revealed to be in the mid-intermediate to deep water environment. Validation against reliable field wave data showed that the new solution may outperform the representative wave approach by allowing lower estimation errors of up to 25%. The new formula was then applied for a practical estimation of wave power in Thailand. While the wave power magnitudes were found to be relatively low around 0.3 to 1.5 kW/m, the utility of the new solution can be warranted according to its consistency with the full numerical technique. This encouraging outcome is achievable as the deviation of the resulting estimates is limited and symmetric about a neutral mean. In summary, the superiority of the new analytical formula can be attributed to its dependable replication of typical random wave field and its adaptability to some irregular wave energy distribution in the nature.

Keywords: surface water waves, phase-averaged wave parameters, wave energy spectra, parameterized wave spectra, renewable ocean energy, wave energy flux, wave power density, ocean wave modeling.

รหัสสัญญาเลขที่ MRG6180102

ชื่อโครงการ: การพัฒนาชุดสมการสำหรับทำนายความหนาแน่นของพลังงานคลื่นผิวน้ำพร้อมการ ประยุกต์งานใช้สำหรับชายฝั่งทะเลของประเทศไทย

ชื่อหักวิจัย: รศ.ดร.ชัชวิห ศรีสุวรรณ ภาควิชาวิศวกรรมโยธา คณะวิศวกรรมศาสตร์ มหาวิทยาลัยสงขลานครินทร์

E-mail Address : chatchawin.s@psu.ac.th

ระยะเวลาโครงการ: 24 เดือน (พฤษภาคม 2561 – พฤษภาคม 2563)

บทคัดย่อ

คลื่นผิวน้ำก่อกำเนิดขึ้นเมื่อได้รับอิทธิพลจากการพัดผ่านของลมบนผิวน้ำในมหาสมุทร โครงการศึกษาวิจัยนี้ มุ่งเน้นการพัฒนาสูตรคำนวณสำหรับค่าพลังงานคลื่นรวม ณ จุดใดๆในท้องทะเล และสูตรใหม่นี้จะใช้สำหรับ การประมาณค่าพลังงานคลื่นที่พบได้ในเขตท้องทะเลไทยซึ่งมีอยู่บ้างแต่ขาดความครบถ้วนในปัจจุบัน โดย ข้อมูลนี้จะเป็นประโยชน์ต่อการศึกษาความเป็นไปได้ในการเก็บเกี่ยวพลังงานดังกล่าวเพื่อการใช้งานจริง ใน การพัฒนาสูตรนั้นหลักการของค่าสเปกตรัมพลังงานคลื่นสังเคราะห์ได้ถูกนำมาใช้เพื่ออำนวยให้มีการ พิจารณาคลื่นแบบสุ่มในท้องทะเล สูตรใหม่ได้รับการพิสูจน์กับค่าคลื่นต่างๆและพบว่าสูตรสามารถใช้งานได้ ในบริเวณระดับน้ำปานกลางถึงระดับน้ำลึก ในการประเมินความแม่นยำค่าตัวแปรที่คำนวนได้จากสมการ ใหม่ได้ถูกเปรียบเทียบกับค่าตัวแปรที่คลื่นที่ได้จากการตรวจวัดภาคสนาม โดยพบว่าสูตรใหม่นั้นสามารถให้ ความแม่นยำที่สูงขึ้นกว่า 25% เมื่อเทียบกับวิธีตั้งเดิมที่ใช้ หลังจากนั้นเมื่อนำสูตรไปหาค่าพลังงานคลื่นใน เขตท้องทะเลไทยนั้นพบว่าพลังงานรวมโดยทั่วไปมีค่าไม่สูงนักในช่วง 0.3 to 1.5 kW/m อย่างไรก็ตาม ประสิทธิภาพของสูตรคำนวนนั้นสามารถยืนยันได้จากการเปรียบเทียบกับสูตรคำนวนเชิงตัวเลขที่ให้ค่า แม่นยำสูง โดยพบว่าค่าจากทั้งสองสูตรนั้นมีค่าที่เกือบจะเท่ากันทั้งนี้เพราะค่าจากสูตรใหม่นั้นมีการ เบียงเบนที่สมมาตรและให้ค่าเฉลี่ยของพลังงานที่เป็นกลาง โดยข้อสรุปคือสูตรใหม่ให้ประสิทธิภาพตาม เป้าหมายได้เนื่องจากสามารถที่จะจำลองรูปแบบของสเปกตรัมพลังงานคลื่นและความผันผวนตามที่เกิดขึ้น จริงในธรรมชาติได้

คำหลัก: คลื่นผิวน้ำ, ค่าตัวแปรคลื่นเฉลี่ย, ค่าสเปกตรัมพลังงานคลื่น, ค่าสเปกตรัมพลังงานคลื่นสังเคราะห์, พลังงานทางเลือกทางมหาสมุทร, ความหนาแน่นของพลังงานคลื่น, แบบจำลองคลื่นในมหาสมุทร

${\bf Contents}$

	List	of Figures and Tables	iii
	Syn	nbols and Abbreviations	v
	Exe	ecutive Summary	vii
1	Inti	roduction	1
2	${ m Lit}\epsilon$	erature Review	2
	2.1	Background and Relevant Study	2
	2.2	Basic Theory	3
	2.3	Traditional Estimation Technique	7
3	\mathbf{Pro}	posed Study	9
	3.1	Objectives	9
	3.2	Expected Benefits	9
4	Acc	quisition of Wave Data	10
	4.1	Data Collection and Analysis	10
	4.2	Data from Other Sources	29
5	Dev	velopment of Analytical Formulas	30
	5.1	Estimation of power density of random waves	30
	5.2	Problem Formulation	37
	5.3	Evaluation of analytical formula	39
6	Ver	ification	41
	6.1	Comparison to Exact Solutions	41
	6.2	Investigation using Synthetic Wave Data	44
7	Val	idation	46
	7.1	Investigation against Nearshore Wave Buoy Data	46
	7.2	Investigation based on Offshore Wave Buoy Data	51
8	Pra	ctical Application of the Study	5 5
	8.1	Site Selection and Power Estimation	55
Cl	natch	awin S.	j

$\cap \cap$	T	\mathbf{T}	ביע.	т	10
CO	אני	\perp	$_{\text{CJ}}$	L	. O

	8.2 Potential Power along the Coasts	59
9	Conclusion of the Study	63
10	REFERENCES	67
	Appendix I: Output from the Research Project	A
	Appendix II: Article Published in Ocean Engineering	\mathbf{D}

List of Figures and Tables

Figures

2.1	Definition sketch of basic parameters of surface waves propagating over	
	impermeable seafloor	4
2.2	Directionality of energy fluxes of random waves and the unit-circle concept	
	of wave power estimation	7
4.1	Location at which Tybee Road wave bouy was deployed to collect wave spectra.	29
4.2	Triaxy's solar-powered and telemetry-equipped wave buoy	30
4.3	Example of NOAA wave buoy deploy in the Atlantic coast of USA (Station	
	ID: 41004)	31
4.4	Example of NOAA wave buoy deploy in the Gulf of Mexico (Station ID: 42306).	32
5.1	Elevation view of waves propagating towards the shoreline and the unit-circle	
	estimation concept	34
5.2	Exact values from the full hyperbolic term compared to approximates allowed	
	by asymptotic formulas employed in the new expression	38
6.1	Comparison between exact and approximation solutions of dispersion rela-	
	tion. Percent error (Δ) is shown respect to the right axis	42
6.2	Comparison on resulting magnitudes of wave power estimated by use of	
	possible techniques and simplifications	43
6.3	Relative density of evaluation results on wave power P based on $26,000$	
	synthetic tests given as functions of estimation errors and ranges of relative	
	water depth $k_p h$	45
6.4	Root-mean-square deviation (RMSD) found in the synthetic tests on the two	
	different techniques given as a function of relative water depth k_ph	46
7.1	Estimation errors as a function of relative water depth k_ph found in the	
	validation of the two techniques against in-situ wave buoy data	48
7.2	Variation of the estimation errors found in the sensitivity tests based on two	
	influential spectral factors: including (a) random-sea steepness factor S_p , and	
	(b) spectral width parameter ν	49
7.3	Comparison between resulting values of total wave power P estimated using	
	the two different techniques at two intermediate-deep water sites. Summary	
	on the comparison based on all of the data sets may be found in Table 7.2.	53

7.4	Comparison between resulting values of total wave power P at two deep-	
	water sites estimated using the two different techniques. See Figure 7.3 for	
	details	54
8.1	Locations along the coastline of Thailand where the potential wave power is	
	evaluated. Specific details including coordinates and depths can be found in	
	Table 8.1	56
8.2	Evaluation on the magnitudes of wave power at Location "A" (Narathiwas)	
	and estimated errors from the two different techniques	58
8.3	Evaluation on the magnitudes of wave power at Location "N" (Phuket) and	
	estimated errors from the two different techniques	60
8.4	Average wave power potential found during the monsoon season of each of the	
	locations. The southern Thai Gulf is evaluated under the northwest monsoon	
	from Nov 2017 to April 2018; the other two zones are evaluated under the	
	southeast monsoon from Jun 2017 to Sep 2017	61
Ta	able	
4.1	Definitions of the bulk wave parameters derived from a surface wave energy	
	spectrum.	11
4.2	Details of NDBC stations from which spectral wave data were utilized for	
	validation and verification of the new analytical formulas	33
7.1	Statistical factors computed per values of total wave power P yielded by the	
	two different techniques. \mathbb{R}^2 is the coefficient of determination, Err is the	
	mean error in percent, Std is the standard deviation of error as percentage	
	of the mean	50
7.2	Information of NDBC stations and statistical indicators found in the	
	validation of the new analytical formula. Note that positive differences (Δ)	
	indicate smaller values found in the new solution	54
8.1	Information of 16 locations in the coastal ocean of Thailand considered for	
	practical application of the new formula	63

Symbols and Abbreviations

η	instantaneous water surface level	L
γ^{δ}	peak enhancement factor in JONSWAP spectrum	[-]
ω	wave angular frequency	T^{-1}
ϕ_k	depth-dependency factor in TMA spectrum	[-]
ϑ	coefficient in parametrized wave spectrum	[-]
\vec{u}	total flow velocity due both wave and current	$ m LT^{-1}$
C	wave celerity	$ m LT^{-1}$
C_g	wave group celerity	$ m LT^{-1}$
D	directional spreading function of wave spectrum	[-]
E(f,	θ) directional spectrum of surface wave energy density	${ m L}^2{ m T}$
E_T	total energy of surface water wave	$ m ML^2~T^{-2}$
f	wave frequency	T^{-1}
f_H	high frequency cutoff	T^{-1}
f_L	low frequency cutoff	T^{-1}
f_p	peak wave frequency	T^{-1}
F_x , F	\overline{Y}_y wave-induced mass flux in x or y direction	$ m ML^2~T^{-3}$
F_{α}	wave energy flux in α direction	$ m ML^2~T^{-3}$
H	surface wave height	L
h	mean water depth	L
H_s	significant wave height	L

H_{rms}	root-mean-square height of random waves	I
k	wave number	L^{-1}
k_p	wave number evaluated at peak wave frequency	L^{-1}
L	wave length	Ι
P	total wave power density of the wave field	$\mathrm{ML^2~T}^{-3}$
R^2	coefficient of determination	[-]
$S_{\eta}(f)$	nondirectional spectrum of surface wave energy density	$\mathrm{L}^2\mathrm{T}$
T_e	energy period of the wave field	Τ
u	nondimensional parameter equal to $(\omega^2 h)/g$	[-]
u_H	nondimensional parameter u evaluated at f_H	[-]
u_L	nondimensional parameter u evaluated at f_L	[-]
BIAS	slope of a linear line fitted through comparison between two data sets	[-]
Err.	error in estimation as percentage of mean measured value	%
RMSI	O root-mean-square deviation as percentage of mean measured value	%
Std.	standard deviation of Err. as percentage of mean measured value	%

Chatchawin S. vi

Executive Summary

Renewable energy accounts for around 19% of the world energy consumption nowadays, with biomass, hydropower, wind, and solar power as the leading sources. Alternative energy from the ocean still contributes to a rather intangible fraction of less than 0.1% of the entire renewables, with most of the present development projects only found in few European countries. Prior to any harvesting decision, the actual potential at a site must be estimated in terms of wave power density. Typical means for the estimation are based on the basic parameters of sinusoidal waves described by Airy wave theory. A numerical integration may be considered for random waves with different magnitudes and frequencies, but this method can be adopted only where wave energy spectra are available.

In the present research effort, the ultimate goal is to introduce a novel set of analytical solutions for the estimation of wave power density. These new solutions are presented in closed form while considering incremental components of wave energy in the random sea, imitating an estimate based on a full random wave spectrum. Therefore, the efficient aspects of the representative wave approach and the spectral-based numerical integration are capitalized. The new formula is utilized to provide an outlook of wave power potential of Thailand which had ever been attempted before. The key technique in the formulation is the utilization of a parameterized wave spectrum for imitating the random sea. A few implicit terms and functions in the full spectral expression are then simplified using an alternative wave dispersion relation and mathematical asymptotes. The derivation is finally achieved via an integration relying on the linear wave theory to obtain the new analytical formula from which the total wave power can be estimated based on the water depth and basic wave parameters including statistical wave height and wave period.

The new solution was verified by investigating all of the steps involved in its formulation. The verification revels that the simplification and asymptotic techniques applied can induce some errors but their effects on the resulting wave power are insignificant. Besides, a large set of synthetic wave spectra based on up to 26,000 realizations were applied to evaluate the new formula under different conditions of random waves. In comparison to the representative wave approach, the synthetic test proves that the new solution can offer greater estimation accuracy and precision in the mid-intermediate to deep water condition indicated by a relative water depth factor.

The new formula was also validated using two reliable sources of field wave spectra. First, its estimation performance and sensitivity on diverse sea states were investigated

Chatchawin S. vii

with available data from a nearshore wave buoy. It was demonstrated that the new solution can estimate the total wave power within about $\pm 12\%$ errors while the representative wave approach can produce up to 40% errors. The performance of the new formula seems to be affected by the sea steepness and the spectral width factors but such an impact should be limited within the applicable range of new solution declared in terms of the relative water depth. For more than 90% of the tests, regardless of the sea states, the new formula still allow more accurate estimates than the representative wave approach. The second validation of new formula employed eight independent sets of wave energy spectra recorded by the National Data Buoy Center (NDBC) along the US Atlantic Coast and the Gulf of Mexico. In this case, the superior of the new formula to the representative wave approach can be confirmed once again based on the offsets in the mean estimation errors and the standard deviations of around 15% and 3%, respectively.

After the verification and the validation, the new formula was demonstrated for practical use in the estimation of wave power in the coastal sea of Thailand. A modeling suit was adopted to simulate hourly wave data over a year at 16 locations along both sides of the national coast. An initial analysis based on the data leads to an important remark that only the waves under two regional monsoons should be considered as their power delivery could be up to 3 times higher than that of the off-season waves. For the main purpose in this study, hourly estimates of wave power from the representative wave approach, the numerical integration, and the new analytical solution were first compared at each of the locations. In general, the new solution was found to produce around $\pm 15\%$ errors while the representative approach was associated with errors in a range of 0 to 30%. Both of such error ranges were found to be narrower in deeper water, in terms of the relative water depth, which are in accordance with the other findings based on synthetic and available measured wave spectra.

For all of the locations considered, average magnitudes of wave power during the monsoon seasons were computed and the resulting power potentials were found to be relatively low, ranging from 0.3 to 1.5 kW/m, as opposed to the maximum daily average which could be as high as 10 kW/m. Initially, this fact implies that the standard deviations of the power can be multiple times of the average values. Beside the temporal fluctuation, the power magnitudes also differ greatly among the locations. The Southern Thai Gulf is the region that sees the greatest spatial variation of the wave power potentials, including the most promising spot at Location E and a few very low potential sites such as Locations B and C. Most of the locations in the Eastern Thai Gulf do not offer any impressive magnitude

Chatchawin S. viii

of the potential with the zonal maximum found to be slightly lower than 0.7 kW/m. The sites in the Andaman Sea may not seem to offer much greater potentials but the resulting mean values between 0.6 to 1.0 kW/m can be considerable and are also the most invariant numbers in a particular coastal zone. The true potential of wave power in this region is still widely open for a more detailed evaluation. The temporal and spatial coverages certainly need to be extended and a more circumspect investigation is required on their variations. A complete multi-dimensional, statistical analysis is possibly the most appropriate approach for any further attempts on the problem.

For the main purpose on the application of the new solution, the magnitudes of wave power potentials yielded by the three available methods are compared. The comparison result shows that the representative wave approach tends to provide around 10 to 15% higher estimates than the other two techniques. Surprisingly, the estimation results allowed by the new analytical solution almost match with those of the numerical integration at every location investigated. This encouraging outcome is possible as a consequence of the estimation with symmetrical biases, from which a neutral mean can be determined. Since the underlying wave spectra were also simulated, the numerical technique may not provide actual values of the power but such resulting potentials should still be accepted as the best estimates. That is, the wave model is believed to allow an accurate random wave field in the sea. This given hypothesis can be met to different degrees in practical, but its effectiveness over the narrow-banded assumption can always be warranted. For the objective here in determining the wave power potential, the performances of the new analytical solution and the numerical technique should therefore be considered to be equal as they both provide almost identical results.

The resulting numbers and the facts discovered here can be digested to summarize several interesting cases on the capabilities of the new solution and the traditional representative wave approach. One is when the energy distribution in the random sea perfectly follows the form of a narrow-banned spectrum. In this idealistic case, both of the techniques will perform equally well as the actual spectrum can be represented based on their underlying principles, i.e. using some bulk wave parameters or a parameterized wave spectrum. Another case, the most common in nature, occurs when the random wave field features a typical pattern of energy distribution but with some irregularities. Almost all of the test cases in this study fall into this scenario and therefore, according to the results shown thus far, the mean accuracy of the new solution can be pronounced to be up to 15% superior than that of the representative wave approach. It is also a valid question whether

Chatchawin S. ix

the new solution can be outperformed in any circumstance. This unfavorable case is, in fact, possible but only when the sea spectrum is so irregular that no assumption can be made for its representation. Under this rare condition, accounting for only 3% to 8% in all of the analyzes in this study, the representative wave approach can offer a more accurate result but only by random chance rather than by its basis principle. With all these facts, the new analytical solution can be confidently applied in any practical estimation, especially for wave power as possible errors from discrete estimates can be averaged-out when reproducing the mean potential power.

The new analytical formula obtained in this study should be able to serve as an effective tool in the estimation of surface wave power in the ocean. Besides, this type of solution can also be incorporated in a module of wave power estimation for input or computing parameters in any wave modeling system. In standalone form, the new formula which appears in a closed analytical form can readily be executed by coastal and ocean engineers in many nearshore hydrodynamic problems. The new body of knowledge achieved in this study is expected to be extended in two principal directions. One is on the improvement of the new formula itself, focusing on enhancing its applicable range and estimation performance. The other is on a very widely-open topic in the assessment of wave power potential of Thailand which was conducted initially here to demonstrate the use of the new formula. A complete evaluation on the magnitude and variation of the wave power in this region is still certainly needed, at least for a critical justification on whether such an alternative power around the equator is worth considering despite being infamous for its low wave power density.

Journal article published based on the research work:

"Srisuwan, C., Rattanamanee, P., Rattanapitikon, W. (2020). Analytical formula for estimation of surface wave power with application in the coastal ocean of Thailand. Ocean Engineering (ELSEVIER), Vol. 204, 107273."

Database: ISI Web of Science

Quartile: 1st, all listed fields (CIVIL/MARINE/OCEAN)

5-Year Impact Factor: 3.067

Link: https://www.sciencedirect.com/science/article/pii/S0029801820303206

1 Introduction

The great fear of energy crisis in the past might largely be influenced by the cyclical cost of fossil fuels. Sustainability and environmental impact of the energy utilization may later appear as part of the concern. Regardless of such debatable reasons, the human intellect and motive are behind the aim in discovering safer, easier, and better cost-effective means of supplying energy for the rapid global civilization. As of 2016, renewable energy accounts for around 19% of the world energy consumption with biomass, hydropower, wind, and solar power as the leading sources (Sawin et al., 2016).

Alternative energy from the ocean still contributes to a rather intangible fraction of less than 0.1% of the entire renewables, with most of the present development projects only found in few European countries (Mofor et al., 2014; Sawin et al., 2015). Tidal power is to date the most advanced topic in the field since tides are deterministic and featuring greatest magnitudes close to the shoreline, adding some reliability and practicality to the energy conversion (e.g. Define et al. 2011; Lawless and Rodger 2013; Work et al. 2013). The harvest of energy from irregular surface waves usually has to be performed in a harsh environment under some random conditions. States-of-the-art technologies have recently been developed to allow conversion of renewable energy from the waves which are induced everywhere in the ocean that covers more than 70% of the earth surface (e.g. Sørensen and Russell 2006; Thomson et al. 2011).

Prior to any harvesting decision, the actual potential at a site must be estimated in terms of wave power density. In current practice, typical means for the estimation are based on the basic parameters of sinusoidal waves described by Airy wave theory. A numerical integration may be considered for random waves with different magnitudes and frequencies, but the method can only be adopted where wave energy spectra are available (e.g. van Nieuwkoop et al. 2013; Gonçalves et al. 2014). Thus, the assumption of a narrow-banded wave field with some nominal leading waves is commonly applied (e.g. Hughes and Heap 2010). Such a representative wave approach will allow a closed-form equation for the computation of the total energy fluxes of the wave field. Two obvious improvable bases of this typical technique lie in the fact that a linear sinusoidal waveform nor a perfect narrow-banded wave field has ever existed in the nature.

In the present research project, the ultimate goal is to introduce a novel set of analytical solutions for the estimation of wave power density. These new solutions are presented in closed form while considering incremental components of wave energy in the random sea,

imitating an estimate based on a full random wave spectrum. The assumption on the linear form of surface wave profile is to be revisited. The new solutions are verified to assure their estimation capability in comparison to the existing representative wave technique. An application of the new solutions is also demonstrated by estimating wave power density along the coastline of Thailand. A field wave measurement campaign was launched to collect data for validating the estimation results. Finally, an outlook of wave power potential is presented and discussed for the country where, to the applicant's knowledge, no characterizing or mapping of nearshore wave power had ever been attempted before.

2 Literature Review

2.1 Background and Relevant Study

Ocean wave energy is associated with relatively high spatial and temporal variations but, in general, is more persistent than wind and solar energy (Falnes, 2007; Reikard, 2013). A feasibility study in a region always involves characterization and mapping of the available energy as initial tasks, allowing optimization for the energy converting scheme, and minimizing risk in the operation (Iglesias and Carballo, 2011). Magnitudes, time periods, and propagation directions of waves are primary factors required in the estimation of wave energy flux and its total, non-directional quantity that represents the local wave power density (Jacobson et al., 2011). These physical wave parameters differ among individual random waves in the ocean but all of them can be obtained accurately using modern measurement devices (e.g. URS 2009; Lindroth and Leijon 2011). Advanced numerical models have also been introduced for predicting these parameters, mainly to overcome spatial limitation in launching a field wave measurement campaign (e.g. Arinaga and Cheung 2012; Reikard et al. 2015; Sierra et al. 2016).

Two typical means are in current practice for the estimation of wave power density, both of which are based the basic wave parameters described by Airy wave theory. A numerical solution can be executed to integrate energy fluxes contributed by random waves with different magnitudes and frequencies. This method is usually applied where wave energy spectra are available in the target area (e.g. van Nieuwkoop et al. 2013; Gonçalves et al. 2014). The other common implementation relies on the assumption of a narrow-banded wave field with some nominal leading waves (e.g. Hughes and Heap 2010). This latter technique, commonly referred to as a representative wave approach, allows a closed-form equation for the computation of the total energy flux of the wave field. For deep water

waves, the approach can further be simplified and only the nominal wave height and wave period are required in the computation (e.g. Cornett et al. 2008; Fernández et al. 2015).

A scarcity of quality spectral wave data often leads to an application of the representative wave approach which offers an ease of use and practicality. In such a case, an adjusting factor may be required in the computation to adjust the estimated wave power to match that of the actual random wave field. Define et al. (2009) performed a regression analysis and found that a reduction factor of 0.61 was appropriate in the estimation where the significant wave height and mean wave period were the nominal wave parameters. The adjustment may alternatively be achieved via an introduction of an energy period defined as the period of a single wave with a total amount of energy identical to that of the sea, also determined following a theoretical spectral shape (e.g. Boronowski et al. 2010). Various analyzes based on field wave data, however, reveals that this conversion technique could lead to an underestimation of wave power by up to 18% since the relationship between the nominal wave and the actual energy spectrum does not always hold in the random sea (Cahill and Lewis, 2014). This possible room of improvement has therefore encouraged an introduction of a novel formula for the estimation in which the entire sea spectrum can be considered via an analytical technique.

2.2 Basic Theory

A comprehensive review on the research problem is given here starting from basic attempts to describe energy and power associated with surface water waves. Some of the most recent techniques are then discussed for the estimation of the total amount of wave energy fluxes and wave power density.

As surface waves propagate, the fluid mass which is serving as the medium displaces. The heave of surface water and the orbit of water particle underneath the waves are two evidences of the displacement. A definition sketch of this problem in two dimensions is shown in Figure 2.1. Under linear wave theory, the wave motion is governed by the Laplace equation of irrotational flow

$$\nabla^2 \Phi = 0 \tag{2.1}$$

in which Φ is the velocity potential and ∇ indicates the parameter gradient. Meanwhile, the relationships among the fluid pressure, the potential head, and the velocity potential must conform to the unsteady Bernoulli equation that follows

$$\frac{P}{\rho} + \frac{1}{2}\nabla\Phi \cdot \nabla\Phi + \frac{\partial\Phi}{\partial t} + gz = 0 \tag{2.2}$$

where P is the pressure and t is the instantaneous time. Equations (2.1) and (2.2) can be solved with appropriate boundary conditions to yield (e.g. Dean and Dalrymple 1991)

$$\eta(x,t) = \frac{H}{2}\cos(kx - \omega t) \tag{2.3}$$

$$u(x, z, t) = \frac{\omega H}{2} \left[\frac{\cosh k(h+z)}{\sinh(kh)} \right] \cos(kx - \omega t)$$

$$w(x, z, t) = \frac{\omega H}{2} \left[\frac{\sinh k(h+z)}{\sinh(kh)} \right] \sin(kx - \omega t)$$
(2.4)

$$w(x,z,t) = \frac{\omega H}{2} \left[\frac{\sinh k(h+z)}{\sinh(kh)} \right] \sin(kx - \omega t)$$
 (2.5)

in which H is the wave height; k is the wave number; ω is the angular wave frequency. The surface heave (η) and the water particle velocities (u and w) are as sketched in Figure 2.1.

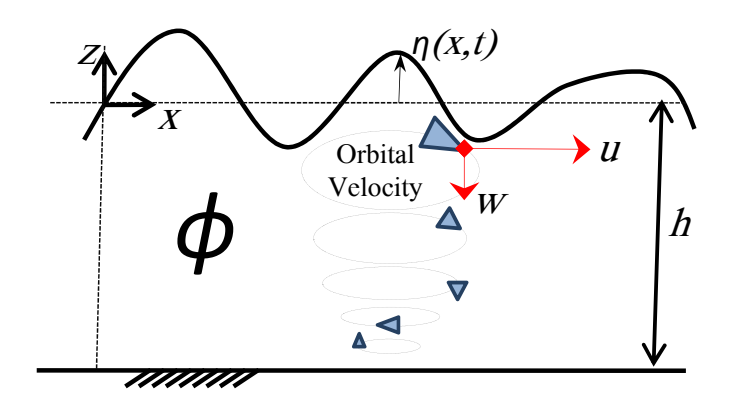


Figure 2.1: Definition sketch of basic parameters of surface waves propagating over impermeable seafloor.

The displacement of the fluid mass against its vertical equilibrium certainly results in gravitational potential energy E_{LP} , which can be written per an elemental part of the water column as

$$d(E_{LP}) = \rho g(h+\eta) \left(\frac{h+\eta}{2}\right) dx \tag{2.6}$$

The oscillatory wave-induced velocities that cause water particle to orbit also initiate an element of kinetic energy E_{LK} following

$$d(E_{LK}) = \rho\left(\frac{u^2 + w^2}{2}\right)dzdx \tag{2.7}$$

where dzdx indicates a volume of the cubic element per unit width (along the wave crest). Using the expressions of wave parameters in Equations (2.3) to (2.5), the total amount of each type of energy underneath the wave can be rewritten in the integral form as

$$\overline{E_{LP}} = \frac{\rho g}{2L} \int_0^L \left(h^2 + hH \cos(kx - \omega t) + \left[\frac{H}{2} \cos(kx - \omega t) \right]^2 \right) dx \tag{2.8}$$

and for the kinetic energy

$$\overline{E_{LK}} = \frac{\rho}{L} \left(\frac{gkH}{4\omega \cosh(kh)} \right)^2 \int_0^L \int_{-h}^0 \cosh[2k(h+z)] + \cos[2(kx-\omega t)] dz dx \tag{2.9}$$

in which L is the wavelength and k is the wave number $(2\pi/L)$. The overbars indicate wave-averaged quantities. Each of the integrals can be evaluated (e.g. Svendsen 2006) to reveal that the potential energy is equal to the kinetic energy, and the net amount of wave energy \overline{E}_L is equal to

$$\overline{E_L} = \left(\overline{E_{LP}} + \overline{E_{LK}}\right) = \frac{1}{8}\rho g H^2 \tag{2.10}$$

which is represented in the unit of energy per unit horizontal area of the water surface, e.g. J/m^2 .

In the estimation of wave power, the rate at which the wave energy is transferred with the propagating wave also needs to be considered. This rate is equal to the work being done due to the presence of the wave, often referred to as a wave energy flux described following

$$F_{\alpha,t} = \int_{-h}^{\eta} \left[P + \rho gz + \frac{\rho}{2} (\vec{u} \cdot \vec{u}) \right] u_{\alpha} dz \, n_{\alpha}$$
 (2.11)

where P is the wave-induced pressure; and \vec{u} is the total flow velocity. The horizontal direction of interest is denoted by the subscript α with n_{α} as its normal unit vector. These directional aspects imply that the resulting value of the flux F depends on both the wave propagation direction and the orientation of a referenced feature such as a bathymetric contour or the coastline.

Considering an x coordinate normal to the shoreline (see Figure 2.2), the use of the linear wave theory can aid the evaluation of the energy flux to yield the simple relationships

$$\overline{F_x} = \overline{E_L} \cdot C_q \cos(\theta); \quad \text{and} \quad \overline{F_y} = \overline{E_L} \cdot C_q \sin(\theta)$$
 (2.12)

in which θ is the wave direction; $\overline{F_x}$ and $\overline{F_y}$ are the shore-normal and shore-parallel components of the energy flux, respectively. The group celerity C_g represents the speed at which the energy is being transmitted, which is given as

$$C_g = \frac{1}{2} \left[1 + \frac{2kh}{\sinh(2kh)} \right] \tag{2.13}$$

Each component of the energy flux given in Equation (2.12) has a unit of watt per unit meter of wave crest. The amount of the total power (P_w) available in the wave can therefore be represented by $P_w = \sqrt{F_x^2 + F_y^2}$. This quantity is often referred to as "wave power density" of the sea surface which is widely accepted as a standard parameter in the estimation of wave energy resources all over the world (e.g. Pontes 1998; Define et al. 2009; Mork et al. 2010).

All of the expressions above, which are meant for monochromatic waves, may be modified for a random wave field with waves of different frequencies and directions. For example, by use of the concept of wave energy spectra, the shore-normal component of energy flux given earlier in Equation (2.12) can be revised to

$$\overline{F_x} = \rho g \int_0^{2\pi} \int_0^{\infty} E(f, \theta) C_g(f) \cos \theta \, d\theta \, df$$
 (2.14)

where C_g is now the frequency-dependent wave group celerity, and the directional wave spectrum is described as

$$E(f,\theta) = S_{\eta}(f) D(f,\theta)$$
(2.15)

where S_{η} is a non-directional energy spectrum, and D is a directional spreading function.

At a particular location, a scalar sum of random wave energy fluxes will resemble a sink of transmitted wave energy across a circular domain with one unit diameter (Jacobson et al. 2011, see also Figure 2.2). Under this unit-circle concept, the local wave power density can

be obtained by integrating the energy fluxes over all possible wave directions under the constraint that

$$\int_0^{2\pi} D(f,\theta) \, d\theta = 1 \tag{2.16}$$

which subsequently allows the expression of the total wave power density to follow

$$P_w = \int_0^\infty S_\eta(f) C_g(f) df \qquad (2.17)$$

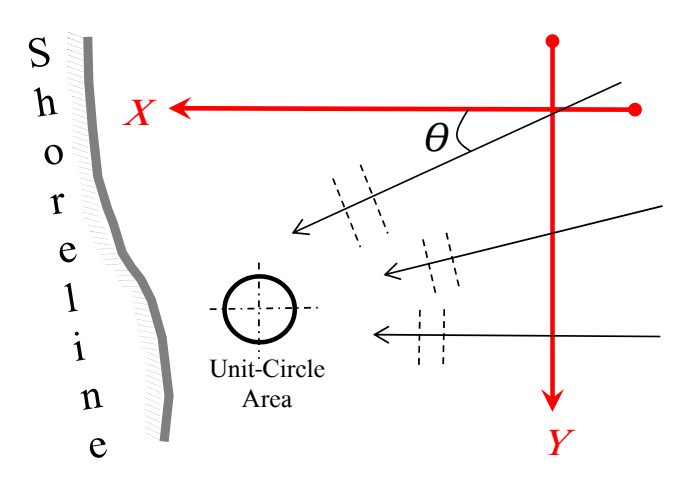


Figure 2.2: Directionality of energy fluxes of random waves and the unit-circle concept of wave power estimation.

2.3 Traditional Estimation Technique

By use of Equation (2.17), an accurate estimation of the wave power density can be achieved if the local wave energy spectra are made available. Many advanced techniques can be launched to serve to measure the wave spectra but eventually they will be limited by spatial and temporal scopes of the measurement. This limitation often leads to an application of the so-called "representative wave approach". For example, the wave energy spectrum S_{η} can be assumed to be narrowed-banded, represented through the root-mean-squared wave height (H_{rms}) , which subsequently allows an approximate of wave power density

$$P_w = \frac{1}{8} \rho g H_{rms}^2 C_g(f_m)$$
 (2.18)

in which C_g is the wave group celerity evaluated at the energy-weighted mean wave frequency (f_m) .

Other types of nominal waves are also employed in the literature with many discrepancies reported among the choices. Define et al. (2009) performed a regression analysis and found that a reduction factor of 0.61 was required in the estimation where the significant wave height and the mean wave period were nominal wave parameters. An alternative for the adjustment may be achieved via introduction of an energy period defined as the period of a single wave having the same total amount of energy as that of the sea (e.g. Boronowski et al. 2010). Various analyses based on field wave data, however, reveal that this conversion technique could still lead to an underestimation of wave power by up to 18% since the relationship between the nominal wave and the actual energy spectrum does not always hold in the random sea (Cahill and Lewis, 2014).

Further simplification of Equation (2.18) has been applied under deep water condition where all of the waves are non-dispersive with depth-independent phase speeds (e.g. Iglesias and Carballo 2011). This characteristic thus eliminates the dependency of water depth on the wave group celerity and, with a revision on the wave energy spectrum in Equation (2.15), will finally lead to

$$P = \frac{\rho g^2 H_s^2 T_e}{64\pi} \tag{2.19}$$

in which H_s is the significant wave height approximately equal to $\sqrt{2}H_{rms}$; and T_e is the energy period of the wave field. By definition, T_e should be equal to the period of a monochromatic wave that features the same amount of wave power as the random sea of interest. It is often related to a spectral wave period, for example $T_e = \delta T_m$, where δ is an adjusting factor and T_m is the mean wave period. Cahill and Lewis (2014) found that the value of δ could range from 1.21 to 1.38 based on an analysis on wave spectra at 12 stations along the US coasts.

Disagreement between an estimate and the actual wave power density mostly originates since the representative wave parameters cannot really account for contributions of all waves in the random field. Various site characteristics and prevailing wave conditions are some major reasons as to why such a representation, for example based on the narrow-banded spectrum, can be misleading. This fact has motivated the present research project for developing a new set of analytical expressions for the estimation purpose. The assumption of a linear sinusoidal waveform is also set to be reinvestigated if it could lead to any

misestimation. Major objectives and methodology in carrying out the research project are outlined in the next sections.

3 Proposed Study

3.1 Objectives

This research project is accomplished as the newly-developed solutions have been warranted for their performance and their utility to serve as a predictive tool of potential wave power in the coastal ocean of Thailand. Such an accomplishment was subject to the following objectives:

- 1. to develop a new set of analytical solutions for estimating total wave energy fluxes;
- 2. to test the new solutions against available exact means of calculation for accuracy and precision;
- 3. to apply the new solutions for estimating wave power potential along the coastlines of Thailand;
- 4. to launch field wave measurement schemes to collect a validation set of wave data;
- 5. to verify and validation the new solutions with available and reliable wave data;
- 6. to prove that the new solutions are superior to other estimation techniques in terms of estimation performance and practical utility.

The concluding output from the project is a research article published in a prestigious journal. All of the contents in the article (see appendix) can reflect essential facts discovered upon the completion of the tasks above.

3.2 Expected Benefits

The accomplishment in this research project will deliver a new body of knowledge in coastal and ocean engineering regarding components of wave energy and wave power density. Tangible outputs from the project include:

 Novel sets of analytical solutions for estimation of wave energy fluxes and wave power density;

- Assembled sets of data of surface wave energy spectra in Thailand;
- Field database as validation sets of data for available wave information in Thailand;
- Article published in a prestigious journal with the highlights on
 - New equations for expression and estimation of wave power density;
 - National map of wave power potential, generated using the new equations.

The above outputs should be considered as some significant contributions in the subject field, as the practical applications and benefits of them may allow:

- Execution of the new formulas for predicting wave power density to
 - provide accurate estimation for surface waves as a renewable source of energy,
 - help reduce the need for complex surface wave measurement scheme,
- Incorporation of the new formulas in numerical modeling systems to
 - increase accuracy and reduce computational demand,
 - permit modeling of cases without available full spectral wave information,
- Use of new field data sets as part of regional wave climate database to
 - enable validation of available modeling results,
 - provide numerical modeling inputs.

4 Acquisition of Wave Data

4.1 Data Collection and Analysis

The test against field wave data was set as a major focus for demonstrating practical application of the new formulas. With this reason, several field measurement efforts were attempted in the coastal ocean of Thailand.

Before illustrating and discussing about the measurement campaigns, it is worth reviewing basic theory applied in the collection and analysis of wave data. For a measurement of wave spectra at a specific location, a set of pressure sensors need to be deployed for data acquisition. Each sensor was set to continuously record absolute pressure under the wave field which, for a monochromatic wave, will be appearing to an observer as

$$P(t) = \frac{\rho g H}{2} \left[\frac{\cosh k(h+z)}{\cosh kh} \right] \exp\{i[(k\cos\alpha)x + (k\sin\alpha)y - \omega t]\}$$
(4.1)

where α is the wave direction with respect to shore normal. For random waves, all of this record at the four sensors can be converted into surface wave energy spectra $S_{\eta}(f)$ using a fast Fourier transform algorithm based on the relation

$$P_{l}(x_{p}, y_{q}, t) = \sum_{m=0}^{M} \sum_{n=0}^{N} \left[a_{nm} \cos(\Psi_{nm} + \omega_{n}t) + b_{nm} \sin(\Psi_{nm} + \omega_{n}t) \right] \left[\frac{\cosh k_{n}(h+z)}{\cosh k_{n}h} \right]$$
(4.2)

in which l indicates the device number with corresponding location x_p and y_q ; while wave frequency and direction are denoted by n and m respectively. The factor Ψ_{nm} represents the phase function $[(k_n \cos \alpha_m)x_p + (k_n \sin \alpha_m)y_q - \omega t]$.

The spectrum of pressure field is then computed using a Fourier transform technique, and later converted to the spectrum of surface wave energy S(f) via

$$S_{\eta}(f) = S_p(f) / K_p^2(f)$$

where

$$K_p(f) = p/\eta = \frac{2fcosh[k(h+z)]}{sinh[kh]}$$

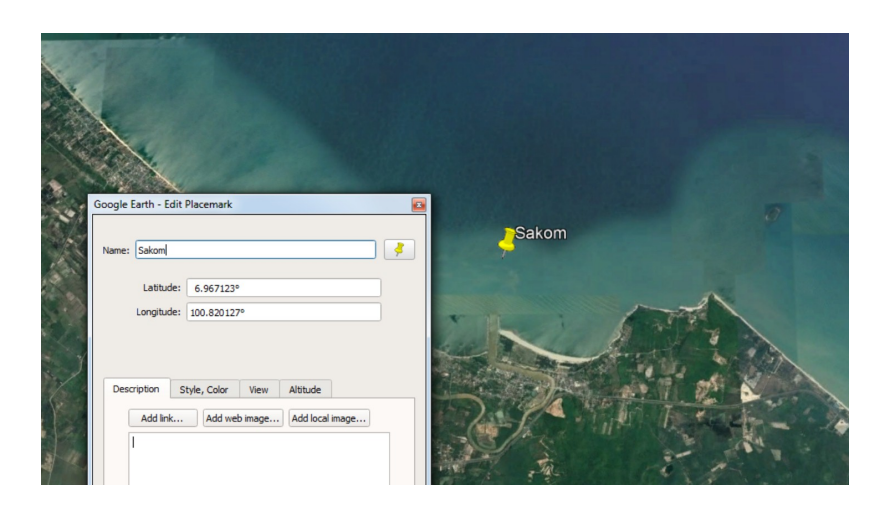
which is the pressure response function. The factor p is wave-induced pressure head; h is mean water depth; h + z is altitude above the bottom; and $S_p(f)$ is the spectrum of the signal which here is the pressure. Meanwhile, important wave parameters based on the wave energy spectrum are estimated according to the definitions given in the Table 4.1 below.

Table 4.1: Definitions of the bulk wave parameters derived from a surface wave energy spectrum.

Wave parameter	Definition		
n^{th} moment of wave energy spectrum	$m_n = \int_0^\infty f^n S_\eta(f) df$		
Significant wave height	$H_{mo} = 4.01\sqrt{m_o}$		
Mean wave period	$T_m = \frac{m_o}{m_1}$		
Peak wave period	$T_p = \frac{1}{f_p}$		

A dedicated measurement platform and the analyzing technique above were adopted in the field data collection efforts carried out at eight different locations in the coastal zone of Thailand. The position and exact coordinate of each location is shown in the geographical figure below. A set of nominal spectral wave parameters were also computed and given, based on the resulting field wave records which include water depth, spectral wave height, wave period, and spectral wave energy.

Location A: Tambon Sakom, Songkhla Province



——Exact position and reference coordinates of the station.—

Principal Results:

• Significant wave height H_{mo}

Mean: 0.136 m.

Max: 0.249 m.

 $\bullet\,$ Energy-weighted wave period T_m

Mean: 4.02 s.

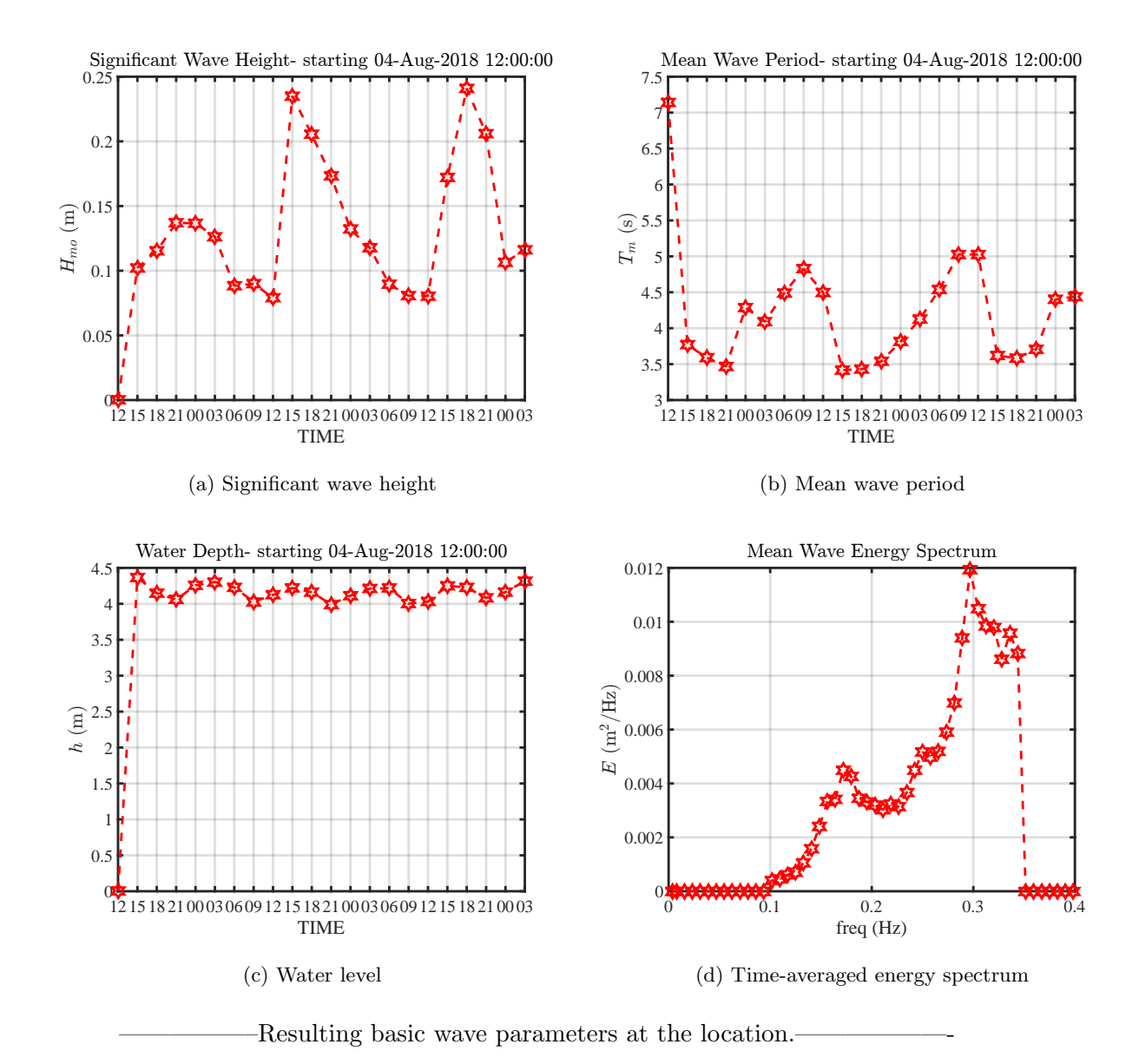
Max: 5.03 s.

ullet Water depth h

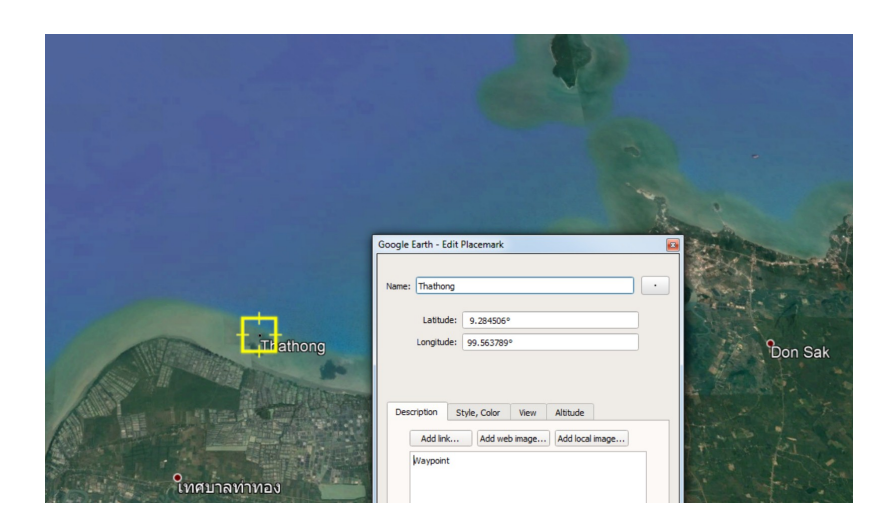
Mean: 4.16 m

Max: 4.01 m

Min: 4.42 m



Location B: Tambon Tha-Thong, Suratthani Province



—Exact position and reference coordinates of the station.—

Principal Results:

• Significant wave height H_{mo}

Mean: 0.046 m.

Max: 0.161 m.

 \bullet Energy-weighted wave period T_m

Mean: 3.80 s.

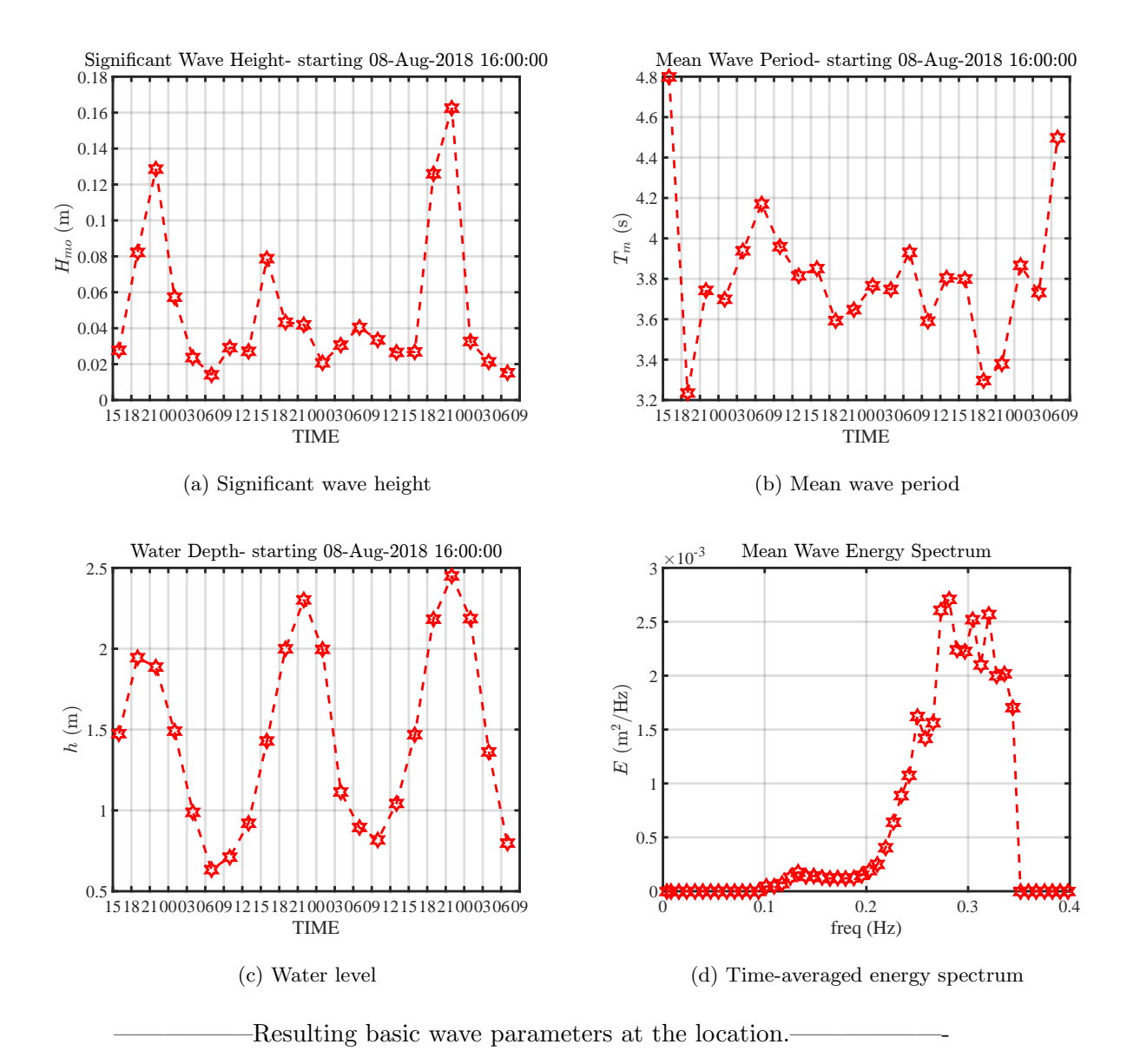
Max: 4.52 s.

 \bullet Water depth h

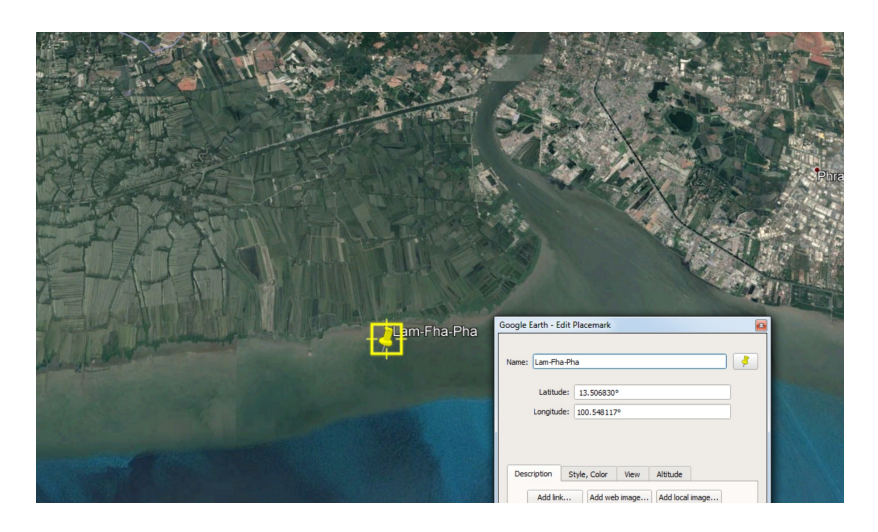
Mean: 1.45 m

Max: 2.48 m

Min: 0.58 m



Location C: Tambon Lam-Fha-Pha, Samutprakarn Province



—Exact position and reference coordinates of the station.

• Significant wave height H_{mo}

Mean: 0.162 m.

Max: 0.51 m.

 \bullet Energy-weighted wave period T_m

Mean: 4.00 s.

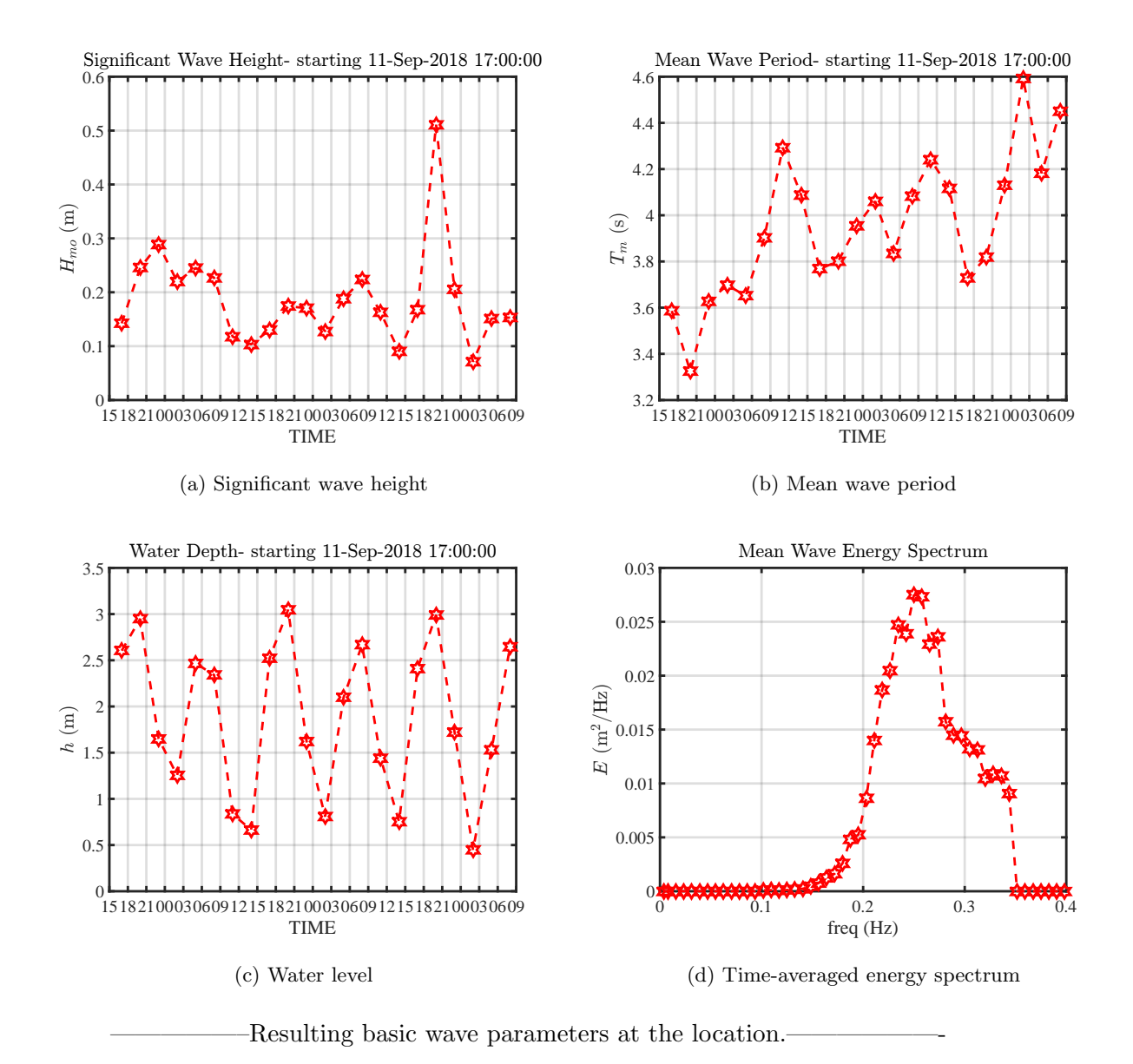
Max: 4.60 s.

 \bullet Water depth h

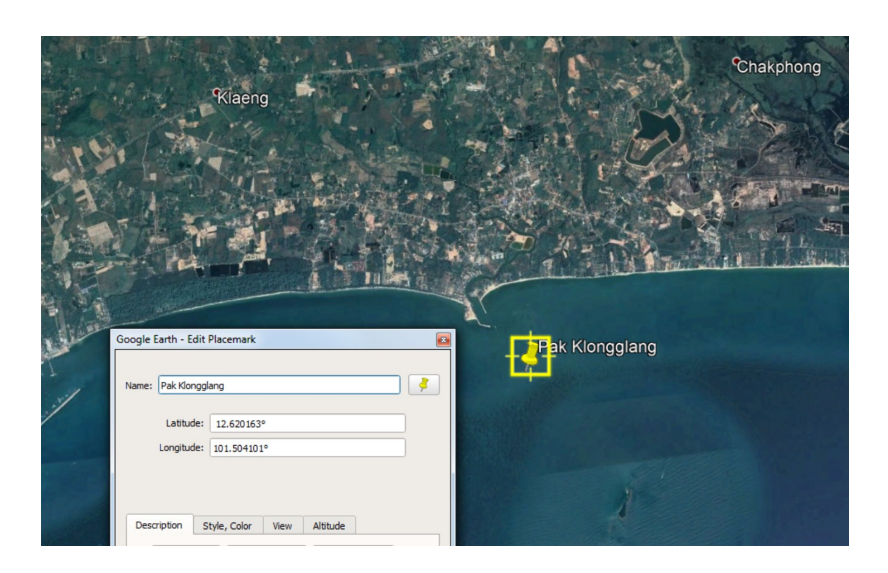
Mean: 1.92 m

Max: 3.05 m

Min: 0.49 m



Location D: Tambon Pak-Klongglang, Rayong Province



—Exact position and reference coordinates of the station.—

Principal Results:

• Significant wave height H_{mo}

Mean: 0.316 m.

Max: 0.429 m.

 \bullet Energy-weighted wave period T_m

Mean: 4.52 s.

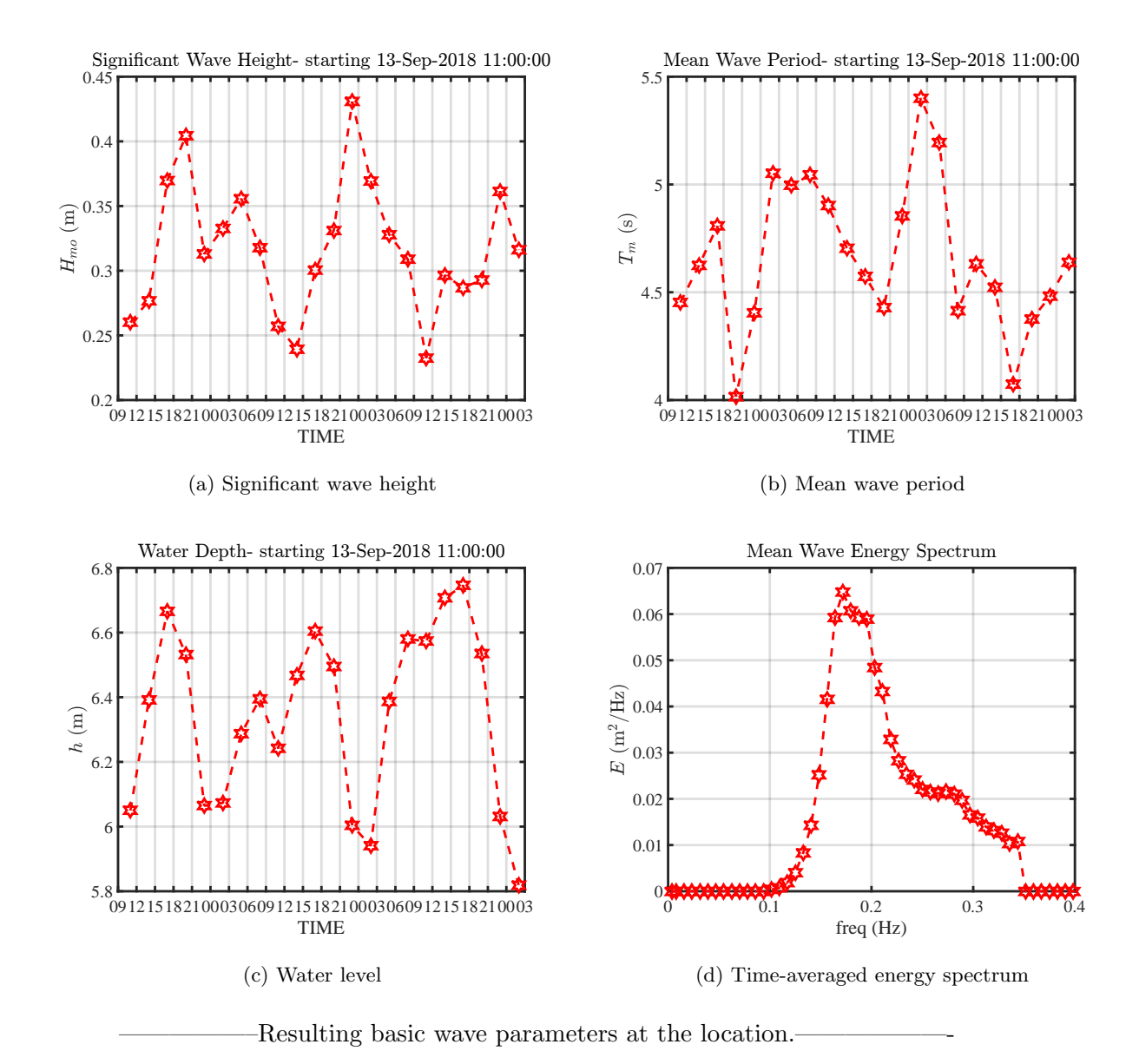
Max: 5.45 s.

 \bullet Water depth h

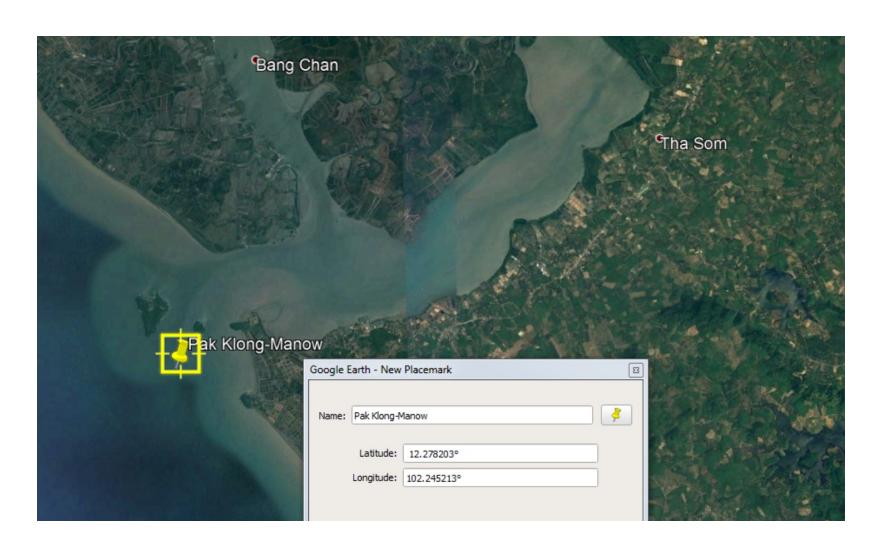
Mean: 6.23 m

Max: 6.76 m

Min: 5.92 m



Location E: Tambon Mai-Route, Trat Province



—Exact position and reference coordinates of the station.—

Principal Results:

• Significant wave height H_{mo}

Mean: 0.360 m.

Max: 0.669 m.

 \bullet Energy-weighted wave period T_m

Mean: 4.75 s.

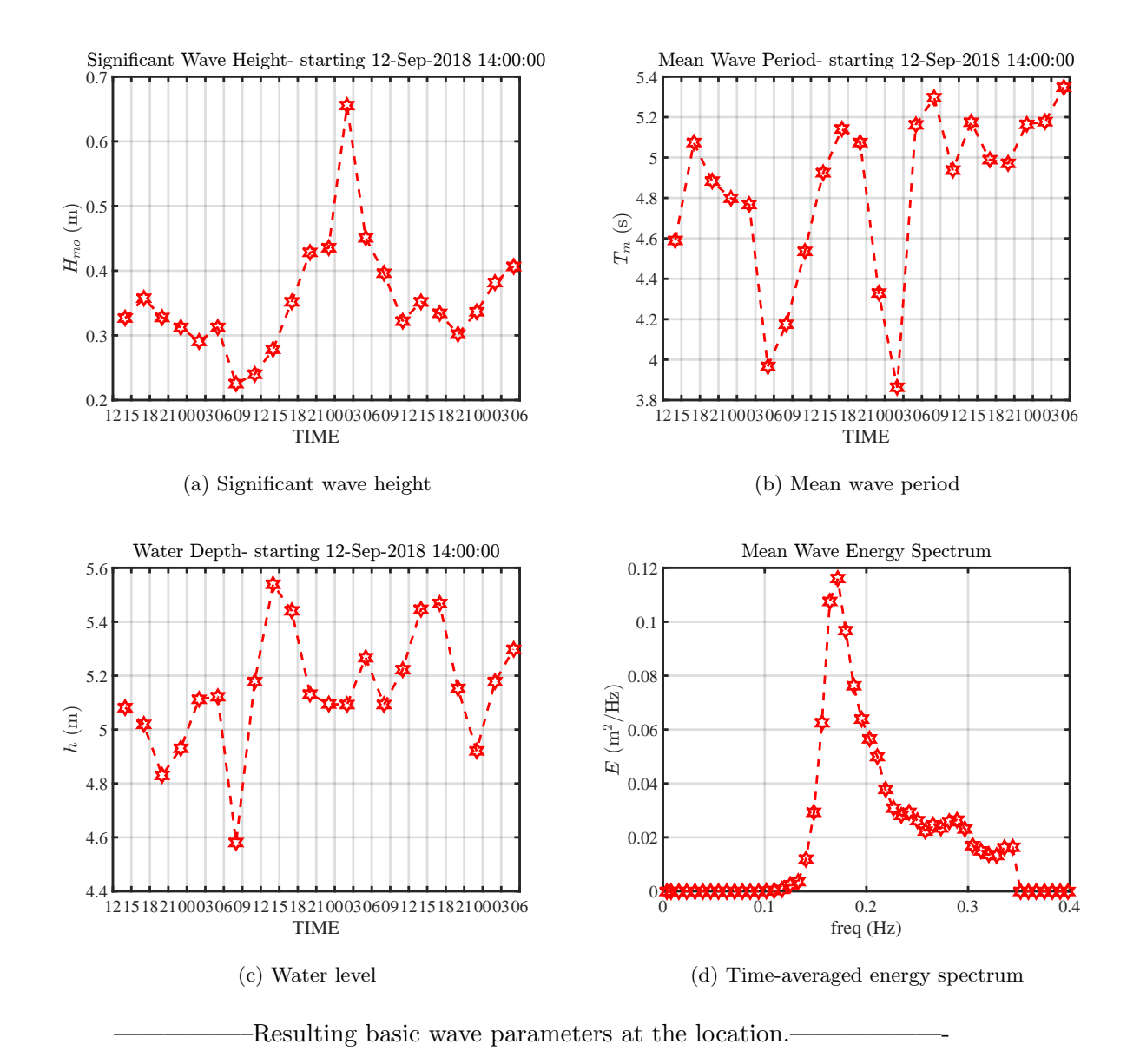
Max: 5.33 s.

 \bullet Water depth h

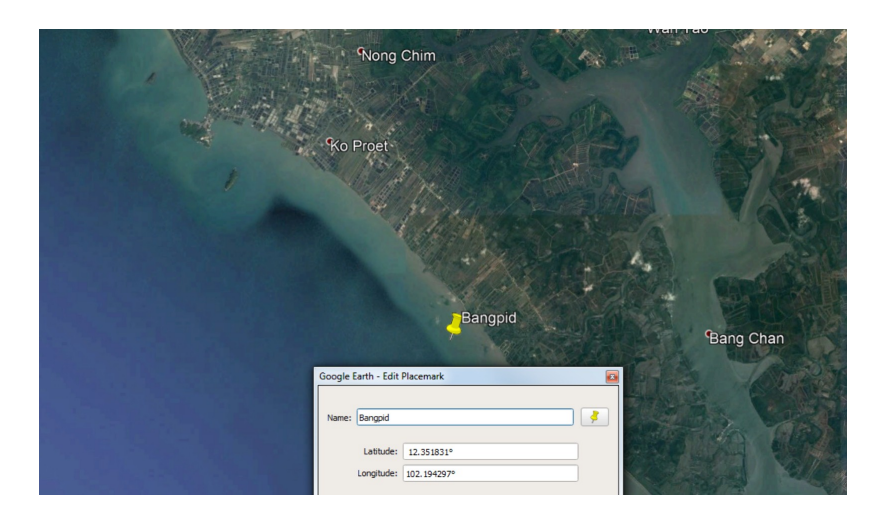
Mean: 5.11 m

Max: 5.85 m

Min: 4.82 m



Location F: Tambon Bangpid, Trat Province



Exact position and reference coordinates of the station.

Principal Results:

• Significant wave height H_{mo}

Mean: 0.361 m.

Max: 0.549 m.

 \bullet Energy-weighted wave period T_m

Mean: 4.62 s.

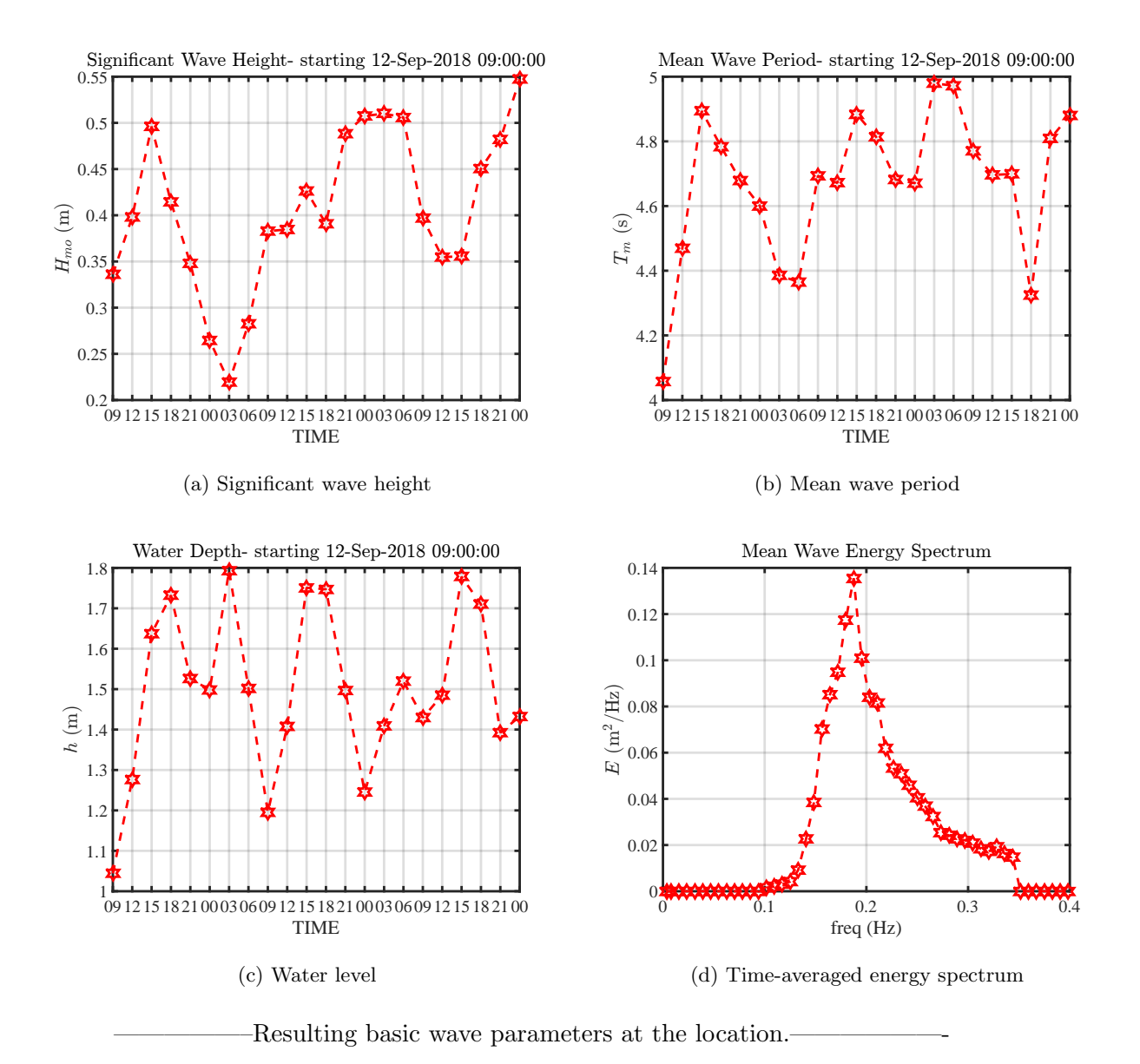
Max: 4.98 s.

ullet Water depth h

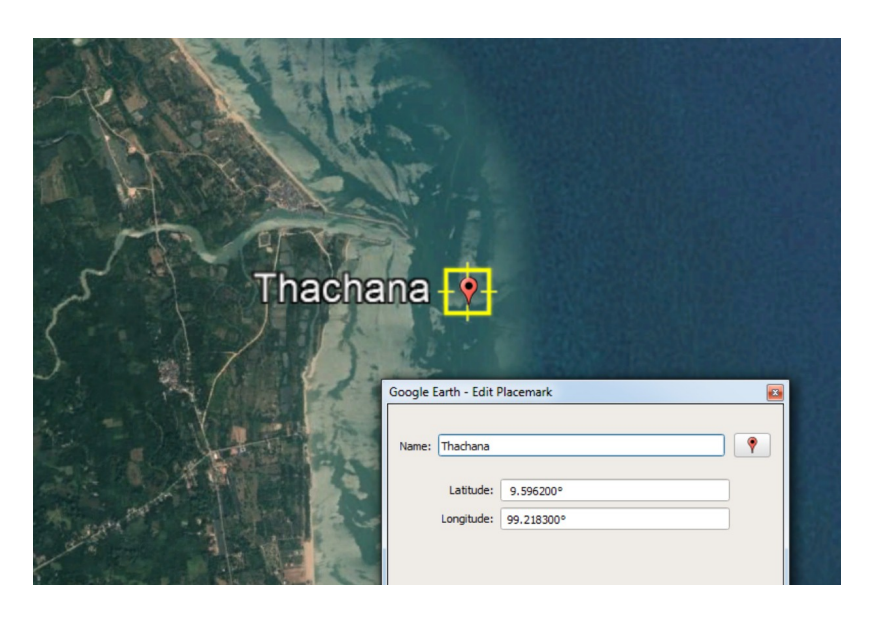
Mean: 1.56 m

Max: 1.79 m

Min: 1.20 m







—Exact position and reference coordinates of the station.——

Principal Results:

• Significant wave height H_{mo}

Mean: 0.045 m.

Max: 0.064 m.

 \bullet Energy-weighted wave period T_m

Mean: 4.16 s.

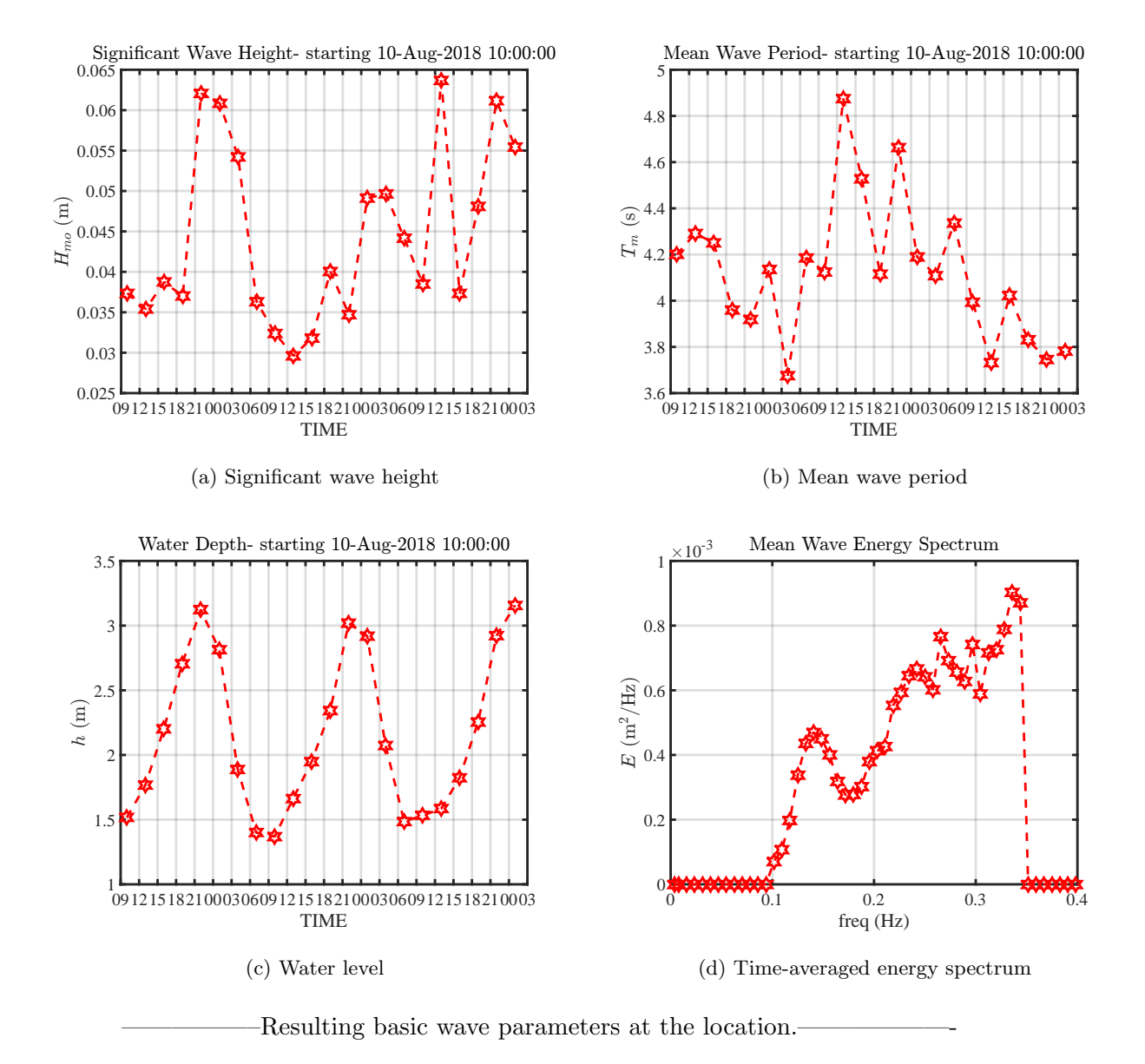
Max: 4.83 s.

 \bullet Water depth h

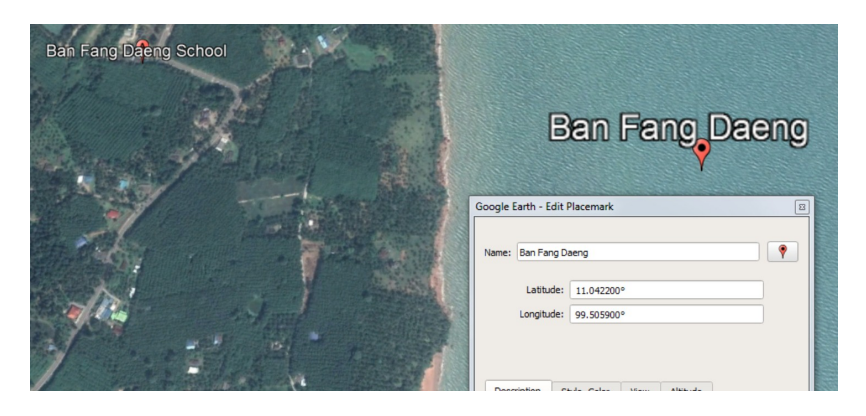
Mean: 2.26 m

 $Max:\ 3.21\ m$

Min: 1.42 m



Location H: Tambon Thachana, Surattani Province



——Exact position and reference coordinates of the station.—

Principal Results:

• Significant wave height H_{mo}

Mean: 0.189 m.

Max: 0.348 m.

• Energy-weighted wave period T_m

Mean: 3.66 s.

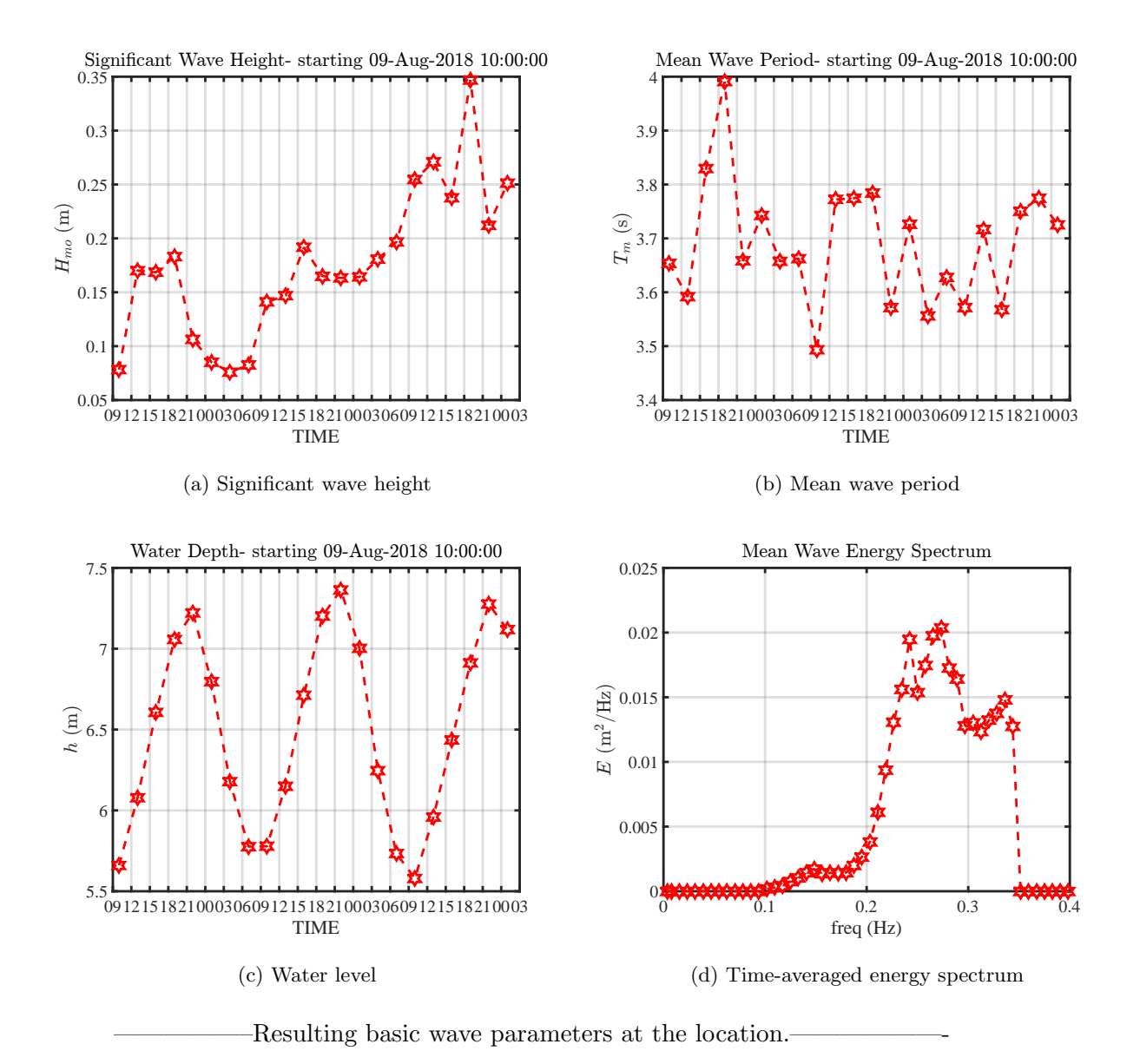
Max: 3.98 s.

 \bullet Water depth h

Mean: 6.48 m

Max: 7.28 m

Min: 5.57 m



4.2 Data from Other Sources

The spectral wave data obtained from the measurement campaign attempted in this project could be spared as part of the verification and validation of the new analytical formulas. However, the total availability and coverage of field conditions were fairly limited and therefore external sources of wave data were explored for fulfilling the need. One primary advantage in considering wave data from other sources lies in the fact that almost all such data were already verified to be accurate and precise upon a certain standard. Two major sources of wave data found in the literature and available as online database were utilized here which can be described below.

The first dataset were from the field measurement by Work (2008) carried out at a site near the Savannah River entrance channel in the State of Georgia, USA, as shown in Figure 4.1. This measurement scheme made use of several Triaxys surface-following wave buoys (Figure 4.2) which reported hourly directional wave energy spectra and wave parameters almost continuously from 2004-2007. The mean water depth at the site is 13.6 m with a tidal range of 2.1 m. For a period of 2.5 months, an acoustic Doppler current profiler (ADCP) was also collocated with the buoy to verify the measured wave spectra. Besides the reliability, the spectral estimates from this work were suitable for testing the new analytical formulas because of the wide variation of their associated relative water depths (k_ph) .

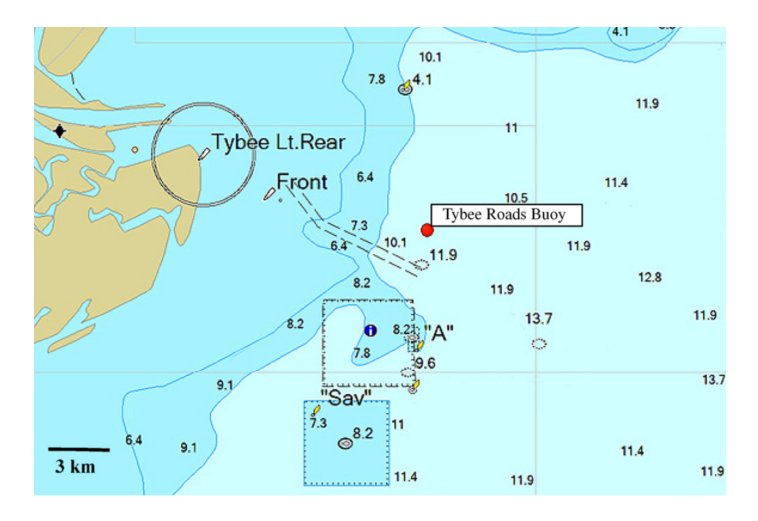


Figure 4.1: Location at which Tybee Road wave bouy was deployed to collect wave spectra.

The other group of wave data were obtained from the National Data Buoy Center (NDBC) of the US National Oceanic and Atmospheric Administration (NOAA), who



Figure 4.2: Triaxy's solar-powered and telemetry-equipped wave buoy.

manages the development, operations, and maintenance of the national data buoy network. At all measurement stations, hourly non-directional wave spectra were recorded and made available to the public routinely. Within this large database, field wave energy spectra available at nine locations along the US Atlantic Coast and the Gulf of Mexico were selected for use for the verification and validation purposes in this research project. Figures 4.3 and 4.4 illustrate examples of wave buoys deployed in each of the two primary locations. Details of all of the measurement stations considered in this study can be found in Table 4.2.

5 Development of Analytical Formulas

Development of the new solution for estimation of wave power density is described in this section. The keys in the problem formulation and the evaluation of the solution are illustrated for the first time below.

5.1 Estimation of power density of random waves

An actual wave field in the ocean consists of random waves with different frequencies (f) and directions (θ) . The linear wave theory can still be applied to describe individual characteristics of all of the waves that contribute to the net available wave power. For



Figure 4.3: Example of NOAA wave buoy deploy in the Atlantic coast of USA (Station ID: 41004).

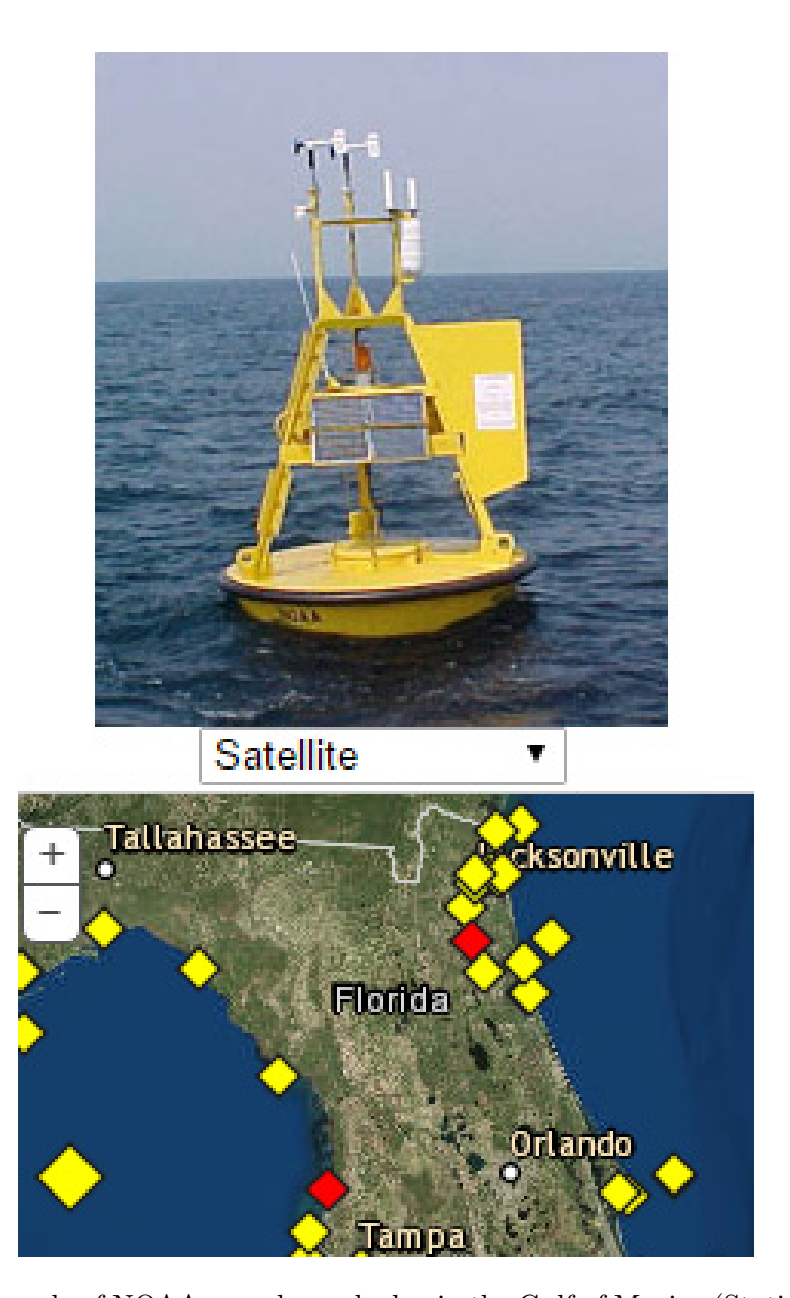


Figure 4.4: Example of NOAA wave buoy deploy in the Gulf of Mexico (Station ID: 42306).

Table 4.2: Details of NDBC stations from which spectral wave data were utilized for validation and verification of the new analytical formulas.

No.	Site Specification					
	Sta. ID.	Position	h (m)	$k_p h$ [-]		
1.	41004	32.501N, 79.099W	38.4	0.90-30.6		
2.	41008	31.400N, 80.868W	19.5	0.52-15.5		
3.	41009	28.522N, 80.188W	40.5	0.85-32.3		
4.	41013	33.436N, 77.743W	23.5	0.68-18.7		
5.	42012	30.065N, 87.555W	27.7	0.68-24.1		
6.	41025	35.006N, 75.402W	68.3	1.53-49.6		
7.	42019	27.907N, 95.352W	82.2	2.84-59.8		
8.	42020	26.968N, 96.694W	79.9	2.76-52.7		
9.	42036	28.500N, 84.517W	50.6	2.07-36.8		

example, by use of the concept of wave energy spectra, the shore-normal component of energy flux given earlier for a monochromatic wave can be revised as

$$F_x = \rho g \int_0^{2\pi} \int_0^{\infty} E(f, \theta) C_g(f) \cos \theta \, d\theta \, df \tag{5.1}$$

where E is the directional wave energy spectrum; and C_g are now the frequency-dependent wave group celerities. The integrals in Equation (5.1) are to be evaluated over all possible wave frequencies f and directions θ . The evaluation result should be referred to as a spectral estimate of the parameter since dynamic wave parameters such as the orbital velocities are not considered directly. In wave measurement and analysis, however, it is always interpreted as measured results due to a lack of means to quantify the energy flux directly.

The total available power in the wave field can still be computed as a scalar sum of energy fluxes of random waves in their propagation directions, i.e. resembling a sink of transmitted wave energy. The wave power density may therefore be redefined as the rate at which the wave energy is aggregated across a circular domain with one meter diameter (Jacobson et al., 2011). Note that wave power density holds the unit of watt per meter which is basically the width of a vertical plane bisecting the unit circle (see also Figure 5.1).

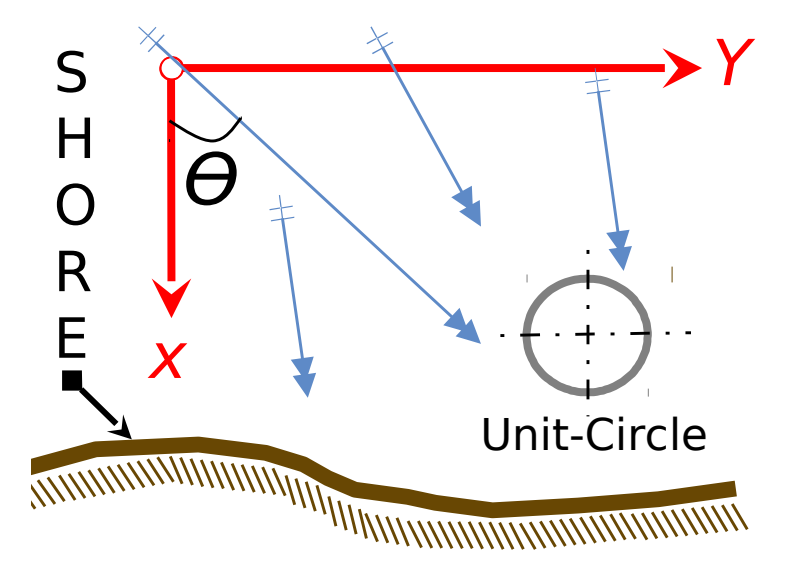


Figure 5.1: Elevation view of waves propagating towards the shoreline and the unit-circle estimation concept.

In practice, the estimation of the wave power density can be achieved via two traditional methods. The first technique is to reproduce the spectral estimates based on available wave energy spectra E which is represented by

$$E(f,\theta) = S_n(f) D(f,\theta)$$
(5.2)

where S_{η} is a non-directional energy spectrum, and $D(f,\theta)$ is a directional spreading function. Under the unit-circle concept, the wave power density can be obtained by integrating the energy fluxes over all possible wave directions under the conservation of wave energy such that

$$\int_0^{2\pi} D(f,\theta) \, d\theta = 1 \tag{5.3}$$

which subsequently allows the expression of the total wave power density to follow

$$P = \int_0^\infty S_{\eta}(f) C_g(f) df \tag{5.4}$$

where $C_g(f)$ is the group celerity of an individual wave with frequency f. By use of this equation, an accurate estimation of the wave power density can be achieved if the local wave energy spectra are made available. Many advanced techniques can be launched to serve to

measure the wave spectra but eventually they will be limited by spatial and temporal extents of the measurement.

Given the limitation, predictive or parameterized equations for the wave spectra may optionally be utilized for the provision of the required wave information. For fully-developed surface waves in deep water, Pierson and Moskowitz (1964) suggested that the distribution of energy with frequency could be described using the well-known Pierson-Moskowitz (PM) wave spectrum

$$S_{\eta}^{PM}(f) = \vartheta g^2 (2\pi)^{-4} f^{-5} \exp\left[-\frac{5}{4} \left(\frac{f}{f_p}\right)^{-4}\right]$$
 (5.5)

in which f_p represents the peak wave frequency, and ϑ is an empirical constant that controls the magnitude of the spectral wave energy. Since its introduction, the PM wave spectrum went through two major modifications. The first adjustment led to the JONSWAP wave spectrum (Hasselman et al., 1973), in which the fetch and duration limits are considered in the formation of the spectrum. The effect of finite water depth on the wave field was later accounted for in the second modification (Bouws et al., 1985), resulting in the TMA spectrum that follows:

$$S_{\eta}^{TMA}(f) = S_{\eta}^{PM} \gamma^{\delta} \phi_k \tag{5.6}$$

in which γ^{δ} is the peak enhancement factor imposed in the JONSWAP spectrum to account for the fetch and the duration. The factor ϕ_k which is introduced into the TMA spectrum to represent the water depth dependency can be expressed as

$$\phi_k(f,h) = \left[k(f,h)^{-3} \frac{\partial k(f,h)}{\partial f} \right] / \left[k(f,\infty)^{-3} \frac{\partial k(f,\infty)}{\partial f} \right]$$
 (5.7)

where k(h) and $k(\infty)$ are the wave numbers evaluated for the local water depth and deep water, respectively. Once parameterized, a wave spectrum can readily be employed for the estimation of wave power density following the integral expression in Equation (5.4). This wave parameterization technique is applied not only for an explicit determination of wave spectra, but also for specification of input waves in many numerical models (e.g. Booij et al. 2004; Kirby et al. 2005).

The other common approach in the estimation of the wave power density is referred to as a representative wave approach in which some leading waves are assumed to represent the random wave field. For example, if the wave energy spectrum S_{η} features a narrowed-banded distribution, the total wave energy can be represented through the root-mean-squared wave height (H_{rms}) which subsequently allows the wave power density that follows

$$P = \frac{1}{8} \rho g H_{rms}^2 C_g(f_m)$$
 (5.8)

in which C_g is the wave group celerity evaluated at the energy-weighted mean wave frequency (f_m) . Under deep water conditions, all of the waves will be non-dispersive with depth-independent phase speeds. This characteristic eliminates the effect of the water on the group celerity in the total wave power, allowing a revision of Equation (5.2) to become

$$P = \frac{\rho g^2 H_s^2 T_e}{64\pi} \tag{5.9}$$

in which H_s is the significant wave height approximately equal to $\sqrt{2}H_{rms}$; and T_e is given as the energy period of the wave field. By definition, T_e should be equal to the period of a monochromatic wave which features the same amount of wave power as the random sea of interest (Iglesias and Carballo, 2011). It is often related to a spectral wave period, for example $T_e = \delta T_m$, where δ is an adjusting factor and T_m is the mean wave period. Based on wave spectra at 12 stations along the US coasts, Cahill and Lewis (2014) found that the value of α could range from 1.21 to 1.38 when the average zero-crossing period was taken as the mean period T_m . This discrepancy was reported to originate as a result of different site characteristics and prevailing wave conditions.

Both of the typical estimation techniques feature advantages and disadvantages. The spectral-based numerical method, while capable of providing accurate results, is often subject to limited availability of local spectral wave data. The method also does not permit a closed-form analytical solution for the estimation even with the parameterization of wave spectra. A straightforward and wider applicability can be found for the representative wave approach in which a simple explicit formula is allowed. This approach, however, may not sufficiently account for contributions from all individual waves in the field. Adjustment to the estimation result may be conducted, but this effort could be subjective since it does not concern different site and wave climate conditions

5.2 Problem Formulation

The efficient aspects of the representative wave approach and the spectral-based numerical integration are capitalized as a major goal in the introduction of the new solution in this study. This consideration requires that the new solution be in closed analytical form while allowing an estimation that is based on the random wave field. The governing equation here therefore follows the spectral-based expression of the wave power density, which can be redefined here for convenience as

$$P = \int_{f_L}^{f_H} S_{\eta}(f) \, C_g(f) \, df \tag{5.10}$$

in which f_L and f_H represent the lower bound and the upper bound of the applicable frequency range, in that order. To determine the wave power density P, an appropriate choice of the energy spectrum S_{η} has to be substituted into Equation (5.10) for an evaluation. Here, the condition of interest is a fully-developed sea in arbitrary water depths. The distribution of wave energy with frequency in this case can be described by aids of the wave-spectrum parameterization technique following

$$S_{\eta}(f) = \vartheta g^2 (2\pi)^{-4} f^{-5} \exp\left(-\frac{5}{4} \left(\frac{f}{f_p}\right)^{-4}\right) \cdot \phi_k(f, h)$$
 (5.11)

where ϕ_k is the depth-dependency factor (Equation (5.7)); and ϑ is the only constant controlling the amount of the energy. For dispersive waves in shallow and intermediate water depths, the factor ϕ_k will cause the wave energy to decrease across the frequency domain, while it approaches unity under the deep water condition.

With the combination of the energy distribution, the depth dependency, and the wave celerity terms, Equation (5.10) will be in a fairly complex form and requires to be reformulated in order for it to allow an analytical closed form solution for the wave power density. The first modification on the original expression is applied on the depth-dependency factor ϕ_k in which the wave number k can be described following the linear wave dispersion relation

$$k = \frac{\omega^2}{q \tanh(kh)} \tag{5.12}$$

which allows the factor ϕ_k to be rearranged into a new form that follows

$$\phi_k(f,h) = \left(\frac{\omega^5}{2g^2}\right) \left(k^{-3} \frac{\partial k}{\partial \omega}\right) \tag{5.13}$$

Despite this substitution, a complete evaluation of the factor ϕ_k is still not viable since the wave number k is not in an explicit form in the dispersion relation. A closed-form expression is therefore needed to be found for a replacement of k in Equation (5.13). This optional expression is selected to be an approximation suggested by Eckart (1952) which follows

$$k = \frac{u}{h\sqrt{\tanh u}} \tag{5.14}$$

where u is a non-dimensional factor equal to $(\omega^2 h)/g$. Using this expression, Figure 5.2 illustrates the approximates and the exact values of the non-dimensional factors k_o/k as a function of kh, where k_o is the wave number of deep water wave. The maximum error is found to be around 5% when the value of kh approaches $\pi/4$. Such an inaccuracy however tends to disappear towards both ends of kh ranging from 0 to π .

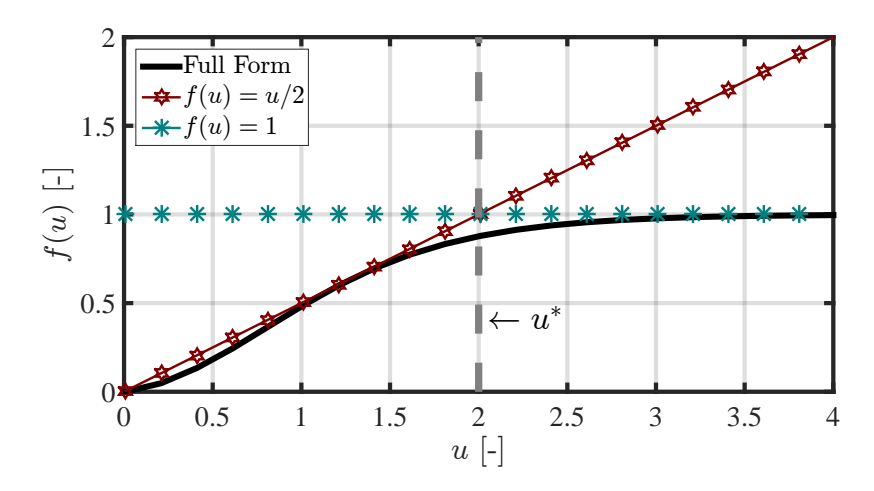


Figure 5.2: Exact values from the full hyperbolic term compared to approximates allowed by asymptotic formulas employed in the new expression.

The fact revealed in Figure 5.2 implies that the errors induced by Equation (5.14) should be minimal for intermediate water depth and should be negligible in the shallow or deep

water regime. Following this approximation, a rearrangement of the derivative term in Equation (5.13) can be achieved to allow

$$\phi_k(f,h) = \tanh(u) + \frac{u}{2} \left[\tanh^2(u) - 1 \right]$$
 (5.15)

This expression can then be inserted into Equation (5.11) for the parameterization of the wave spectrum S_{η} which is one term in the estimation of the wave power density P in Equation (5.10). The other term is the energy transmission speed, or wave group celerity C_g , which may also be expressed in an explicit form by use of Eckart's approximation in Equation (5.14). These attempts will allow a new integral form of the wave power density, given with respect to the non-dimensional factor u as

$$P = A \int_{u_L}^{u_H} u^{-7/2} e^{-Bu^{-2}} \left[(\tanh u)^{3/2} + \frac{u}{2} \left((\tanh u)^{5/2} - (\tanh u)^{1/2} \right) \right] du$$
 (5.16)

in which A and B are groups of constants from the original expressions of S_{η} and C_{g} , and from the transformation of df to du, which follow

$$A = \frac{\vartheta g^{(3/2)} h^{(5/2)}}{4};$$
 and $B = \frac{5h^2}{4\omega_n^{-4} q^2}$ (5.17)

where ω_p is the peak angular wave frequency $(2\pi f_p)$, and the new integral limits u_L and u_H are the values of u at the low and the high frequency cutoffs, respectively. A closed-form analytical solution for the wave power density P can finally be obtained from the evaluation of Equation (5.16) shown in the next section.

5.3 Evaluation of analytical formula

The only task left now is to perform an integration on Equation (5.16) which, however, is not straightforward due to the nonlinear combination of the power, the exponential, and the hyperbolic tangent functions in the equation. To resolve this complexity, an asymptotic analysis will be applied and a nominal expression will be introduced to simplify the equation into an integrable format. This technique will be similar to that of Srisuwan et al. (2017) suggested for another set of waves parameters for different types of application.

The analysis is focused on the group of the hyperbolic tangent functions of which the resulting values are shown in Figure 5.2. Over a wide range of the non-dimensional factor u, the following approximation can be made

$$(\tanh u)^{3/2} + \frac{u}{2} \left((\tanh u)^{5/2} - (\tanh u)^{1/2} \right) \approx \frac{u}{2}, \quad \text{for} \quad 0 < u \le u_*$$
 (5.18)

and

$$(\tanh u)^{3/2} + \frac{u}{2} \left((\tanh u)^{5/2} - (\tanh u)^{1/2} \right) \approx 1, \quad \text{for} \quad u > u_*$$
 (5.19)

where u_* is the threshold value at which the behavior of the function appears to change, which is clearly observed at u=2.0 here. These asymptotes for the tanh terms can be substituted into Equation (5.16) so that the expression of the wave power density is separated into two integral terms following

$$P = A \left[\frac{1}{2} \int_{u_L}^{u_*} u^{-5/2} e^{-Bu^{-2}} du + \int_{u_*}^{u_H} u^{-7/2} e^{-Bu^{-2}} du \right]$$
 (5.20)

These terms can be rearranged for partial integration with substitution of parameters. An aid of special functions is also required to express the definite integrals that involve a nonlinear combination of the power function of u and the exponential function $\exp[f(u)]$. Non-elementary gamma functions can be applied for the purpose here, of which the definitions are given following

$$i\Gamma(\lambda,\beta) = \int_0^\beta e^{-u} u^{(\lambda-1)} du$$
 (5.21)

and

$$\tilde{\Gamma}(\lambda,\beta) = \int_{\beta}^{\infty} e^{-u} u^{(\lambda-1)} du$$
 (5.22)

where Γ and $\tilde{\Gamma}$ are respectively the lower and the upper incomplete gamma functions distinguished by their integral limits. In the present problem with certain integral limits among u_L , u^* , and u_H , a pair of these gamma functions can be employed on each of the integral terms. With all the preparations and the use of these special functions, Equation (5.20) can be evaluated to yield

$$P = \frac{A}{4} \left[\frac{\sqrt{u_H} \exp\left(\frac{-B}{u_*^2}\right) - \sqrt{u_*} \exp\left(\frac{-B}{u_H^2}\right)}{B\sqrt{u_*u_H}} + \frac{i\Gamma\left(\frac{3}{4}, \frac{B}{u_L^2}\right) - i\Gamma\left(\frac{3}{4}, \frac{B}{u_*^2}\right)}{B^{(3/4)}} + \frac{i\Gamma\left(\frac{1}{4}, \frac{B}{u_*^2}\right) - i\Gamma\left(\frac{1}{4}, \frac{B}{u_*^2}\right) - i\Gamma\left(\frac{1}{4}, \frac{B}{u_H^2}\right)}{2B^{(5/4)}} \right]$$
(5.23)

which is a new closed-form, analytical equation for estimation of the wave power density. This full solution can be simplified into a more compact expression if all of the waves in the entire spectrum are considered. In this case, the lower and upper bounds u_L and u_H will respectively shift to 0 and ∞ , allowing the alternative formula that follows

$$P = \frac{A}{4} \left[\frac{-\exp(-B/4)}{B\sqrt{2}} + \frac{\tilde{\Gamma}(3/4, B/4)}{B^{(3/4)}} + \frac{i\Gamma(1/4, B/4)}{2B^{(5/4)}} \right]$$
(5.24)

in which the constant value of u^* is already substituted into the equation. The newly-introduced formulas in Equations (5.23) and (5.24) here can be executed in any programs that include gamma functions which are very common in most scientific computing environments. It is worthwhile to recall that the formulas were derived under the assumption of a fully-developed sea of random waves from all possible propagation directions. The derivation also involves the expressions for the wave energy and its transmission speed that are based on linear wave theory and some simplifications. In the next sections, these adopted techniques will be verified and the new formulas will be validated against various sets of reliable wave data.

6 Verification

The primary goal in this section is to justify for the validity of the new formulas and, if any, limitation in their applications. Three stages were conducted in the testing which can be described below.

6.1 Comparison to Exact Solutions

The derivation of the new analytical formula introduced above involves a few assumptions and approximations. In this section, possible effects from such techniques are investigated focusing on behaviors of a few important terms and the final solution. First of all, the approximate wave dispersion relation in Equation (5.14) needs to be investigated as it is applied throughout the formulation. Figure 6.1 illustrates a non-dimensional wave number k_o/k as a function of the relative water depth (kh), comparing the values yielded by the approximation and the full dispersion relation. The comparison shows that the error induced by the approximation rises almost linearly to 5% as the values of kh increases to $\pi/4$ which is about the mid of the intermediate water range. In the higher part of the intermediate water

regime, $\pi/4 < kh < \pi$, the error continues to increase slightly at the beginning but then starts to decrease and becomes zero at the upper bound. With such a small maximum error of around 5%, any direct use of the approximate expression for determining wave number should be acceptable, provided that eventual impact on the final result is also examined.

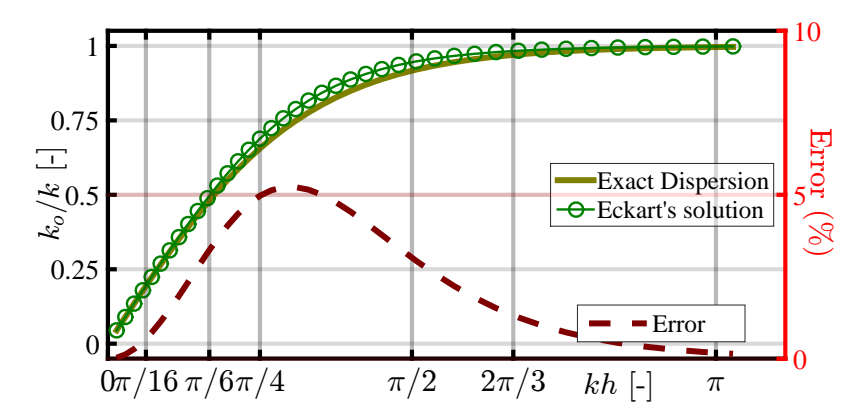


Figure 6.1: Comparison between exact and approximation solutions of dispersion relation. Percent error (Δ) is shown respect to the right axis.

In the formulation of the new solution, the approximate dispersion relation is applied specifically on the hyperbolic tangent $(\tanh(u))$ and the wave celerity (C_g) . Possible influences from such modified terms may be best investigated based on the resulting wave power from several estimation options shown in Figure 6.2a. The magnitudes of wave power allowed by the exact solution is adopted as a basis and the percent differences from the other alternatives are illustrated in Figure 6.2b. Note that random wave spectra are assumed here and a proximal relative water depth k_ph is represented on the basis of the most dominant wave with wave number k_p . For a sole inclusion of the approximated wave group celerity (C_g) , an underestimation of the wave power of up to 30% is found where the relative water depth k_p is equal to $\pi/4$ before it diminishes to zero as the value of k_p approaches 2π . The asymptotic form of tanh, meanwhile, results in around 25% overestimation of the wave power which then plummets to zero, at either end of the k_p limits respectively.

The eventual impact due to the combined asymptotic tangent term and the approximate wave celerity may be investigated considering the performance in estimating the final result. Beyond the mid-intermediate water limit $(k_p > \pi/4)$, the magnitudes of wave power yielded by the new solution are only associated with some errors smaller than 5% (Figure 6.2b). This marginal deviation can occur as the underestimation and the overestimation observed

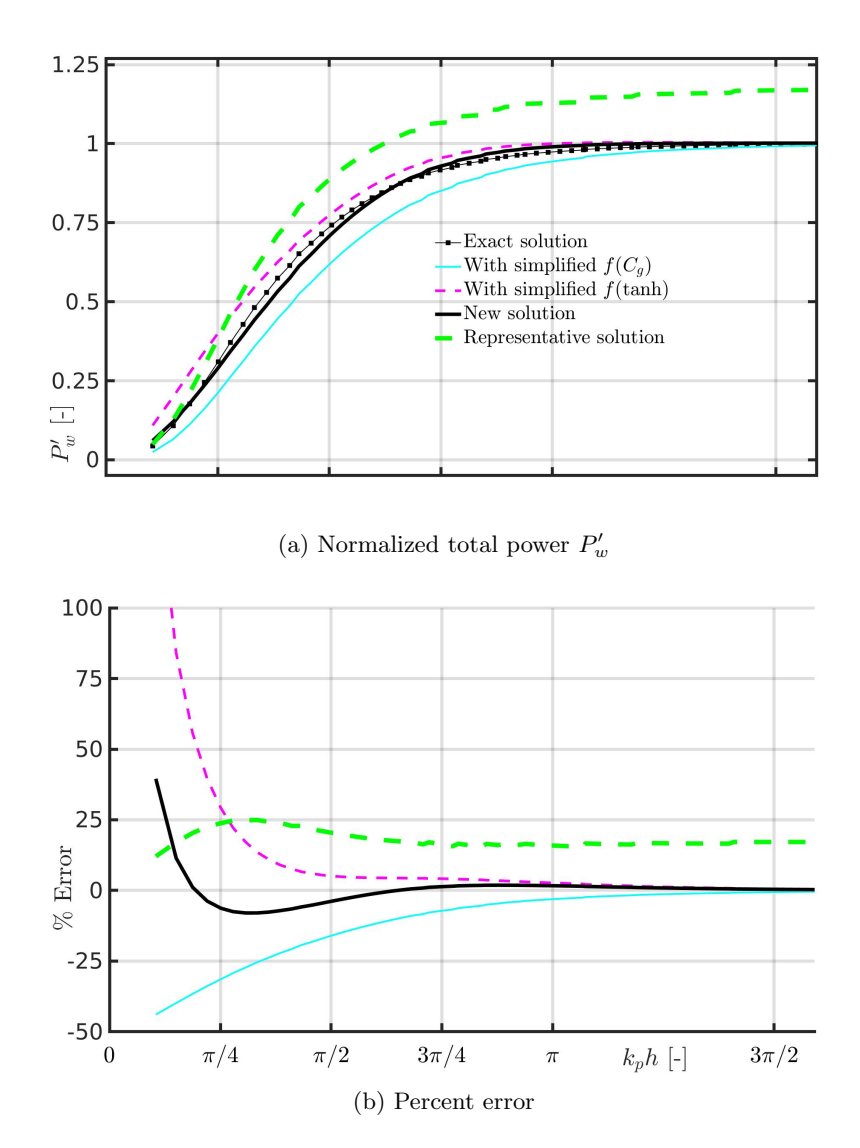


Figure 6.2: Comparison on resulting magnitudes of wave power estimated by use of possible techniques and simplifications.

in each of the two modified terms seem to balance off. For the same condition, the use of representative wave approach results in around 15 to 25% overestimation of the wave power. The comparisons made in Figure 6.2 may lead to two initial findings. One is that the new solution does not perform well in shallower water as the possible error can be excessive. The other conclusion thus far is on the superiority of the new analytical formula over the traditional representative wave approach. Though the latter may be improved via use of an adjusting factor, it will not allow any error lower than that around 5% of the new solution as the variation of its original error itself is already up to 10%.

6.2 Investigation using Synthetic Wave Data

All of the investigations above are achieved theoretically with a primary consideration on behaviors of the terms in the formulation. To reassure its performance and applicability, the new solution in complete form is tested again by use of synthetic wave spectra in which various wave conditions are specified. The dataset consists of 26,000 time series of random waves, each with a different combination of peak wave period (T_p) and water depths (h). One focus here is therefore to investigate the dependencies of the estimation accuracy and precision on the most influential factor which is the proximal relative water depth (k_p) . Figure 6.3 illustrates the relative density or the percentage of cases found according to the computed errors on P for many ranges of k_p . In each case, the results from the new analytical formula are compared to those of the representative wave approach, both evaluated against the exact values of P allowed by the numerical solution.

Starting from the upper range of $k_p h > 5\pi/4$, the new solution tends to lead to a fairly normal distribution of the tests in which the errors are between 25% to -25%, implying overestimation and underestimation respectively. This finding infers that the number of cases found increases as the error decreases, thus the new solution should lead to only some small errors in majority of the cases. Under the same condition, the result allowed by the representative wave approach appears to be similar considering shape of the distribution of which the center, however, dislocates somewhat to the overestimation part. This shifting implies that the representative wave approach overestimates the wave power by 10 to 15% on average. These overall results also seem to uphold in the next range of $5\pi/4 > k_p h > 3\pi/4$, agreeing with the fact that the capabilities of both of the two estimation techniques should be invariant in the upper-intermediate to deep water condition. It may be worth noting that all of the errors being investigated here are due to the difference between the energy distribution assumed in each solution and that of the synthesized waves which include

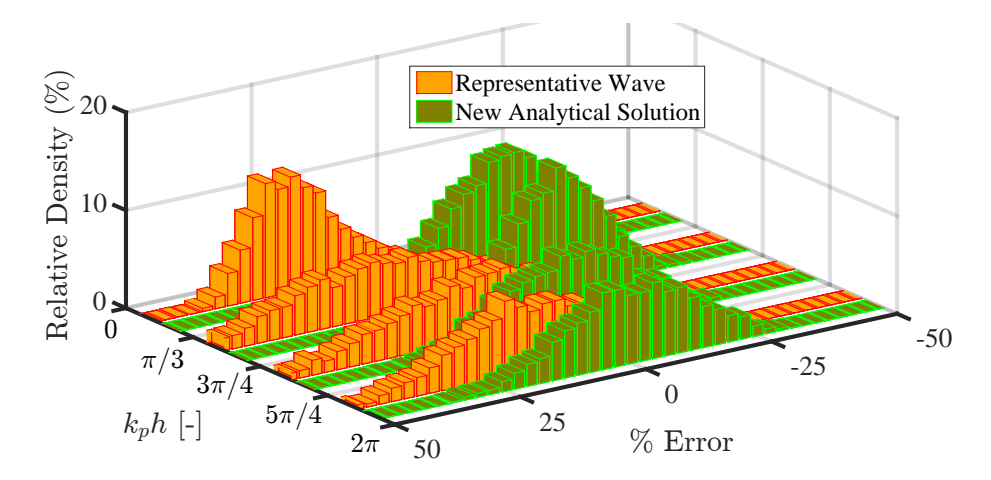


Figure 6.3: Relative density of evaluation results on wave power P based on 26,000 synthetic tests given as functions of estimation errors and ranges of relative water depth k_ph .

randomness. The new solution is based on a more flexible parameterized spectrum which can better constitute the distribution as opposed to the representative approach which relies only on a fixed narrow-banned spectral model.

In the next lower range of $3\pi/4 > k_p h > \pi/3$, the new solution results in a more peaky distribution of the number of tests over the computed errors with a small underestimation bias of around 5 to 10%. These characteristics imply a higher precision in the estimation which, however, comes with a slight decline in the accuracy. Meanwhile, a broader distribution and a higher estimation bias are still found for the result yielded by the representative wave approach in this range. For the lowest part of $k_p h$, the new solution still allows a persisting result while a much narrower distribution of the tests is found in the use of the representative approach. This latter distribution also appears to be asymmetric as the rising part, associated with some higher overestimation, is steeper and leads to a tailing-peak form. All of these findings convince that the new solution is superior to the representative wave approach in all of the tested ranges. To confirm a certain limit in its applicable condition, the results can be evaluated altogether again in terms of the root-mean square deviation (RMSD).

Figure 6.4 shows a comparison between the RMSD values associated with the new solution and the representative approach. Except only when k_ph is smaller than $\pi/4$, the RMSD of the new solution always shows a lower value. The percent difference is found to be 3 to 10% for the range of $\pi/4 < k_ph < 3\pi/4$. Toward the deep water regime, this number

tends to become a constant of around 7 to 8%. For clarity, a certain applicable condition of the new solution may be specified to be where $k_p h > \pi/4$. This limit simply covers midintermediate to deep water environment, according to the thresholds of shallow-water and deep-water waves defined at $kh < \pi/10$ and $kh > \pi$, respectively (Dean and Dalrymple, 1991). In other word, the new solution is not suitable for use wherever the the depth is below the lower intermediate limit. This prohibition should be especially strict for shallower water environment ($k_p h < \pi/10$), due to the low estimation performance as well as the fact that the formulation based on linear wave theory is not intended for describing shallow water waves.

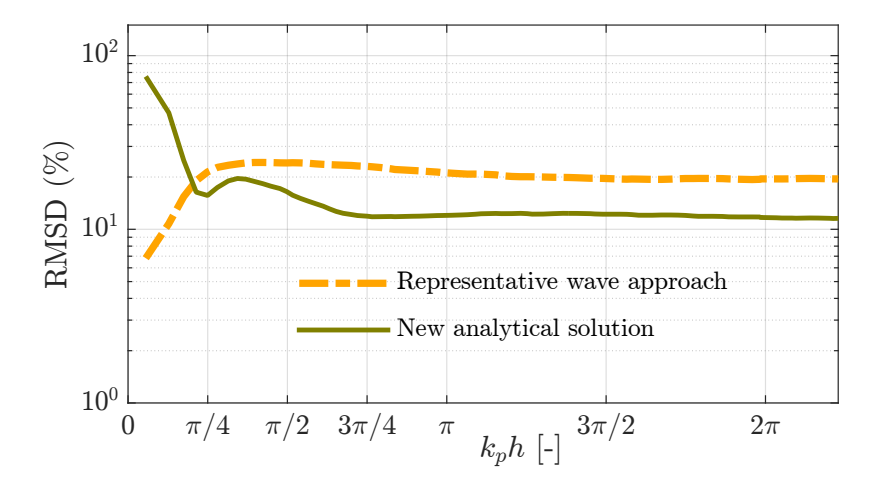


Figure 6.4: Root-mean-square deviation (RMSD) found in the synthetic tests on the two different techniques given as a function of relative water depth k_ph .

7 Validation

In the previous section, the new solution and associated terms are verified analytically and against synthetic data to explore its capability and applicable range. Here, the formula is to be validated using measured wave data from two reliable sources which will help reveal its performance and sensitivity under actual uncertainty and randomness of the wave field.

7.1 Investigation against Nearshore Wave Buoy Data

The first dataset utilized here was acquired by a surface-following wave buoy deployed at a site near the Savannah River inlet in the State of Georgia, USA. It offers more than 16,000

hourly records of spectral waves in a mean water depth of 13.6 m and a tidal range of 1.7 m, covering a wide variety of wave conditions for the proposed validation here. Regarding reliability, the data were also verified by 2.5-month coinciding records from a collocated acoustic Doppler current profiler (ADCP). The full description and detailed analysis on the dateset can be found in Work (2008).

The data preparation here includes a separation of sea and swell components in the original wave spectra. This first step was achieved using the technique outlined by Work and Srisuwan (2010). It was necessary since the new solution was primarily developed to describe the local wind-induced waves or the sea. The instantaneous water depths at the site, not available from the measurement but included in the new solution, were simulated using a tidal harmonic analyzing tool developed by Pawlowicz et al. (2002). The simulation result was also compared to available data from the ADCP and the difference between the two time series was found to be smaller than $\pm 5\%$.

In a strict theory, the magnitude of wave power is actually not known even from the field dataset as it was not measured directly. The most dependable means to obtain such information is still to determine it using the relationship in linear wave theory. Therefore, the wave power reanalyzed from the available wave energy spectra should be referred to as the best estimate of P which is adopted as a basis in evaluating the results yielded by the new solution and the representative approach. In the use of the new solution, the only adjustable coefficient in the formula (ρ) was specified such that the total wave energy was conserved. The estimation errors induced by each of the two techniques are illustrated in Figure 7.1. Initially, the results appear to be fairly similar in terms of the scattering of the errors and their general trends over the proximal water depth regime $(k_p h)$. For $\pi > k_p h > \pi/4$, or mid-intermediate to deep water, both techniques tends to overestimate the values of P, especially the representative wave approach. This overestimation bias appears to decrease fairly quickly toward the deep water limit. Throughout the comparison, the new solution shows up to be the more accurate and more precise tool for the estimation compared to the representative wave approach. This superiority of the new solution can be confirmed considering the statistical numbers summarized in Table 7.1, including the r-square values, the mean percent errors, and the standard deviations found in each range of $k_n h$.

In the table, the percent errors produced in the new solution are between 12 to -14% while the same type of numbers from the representative approach spread over 57 to -17%. In the latter, the values for the standard deviation also appear to be up to 7% higher than those of the new formula. As noticeable in Figure 7.1, both techniques tend to overestimate the

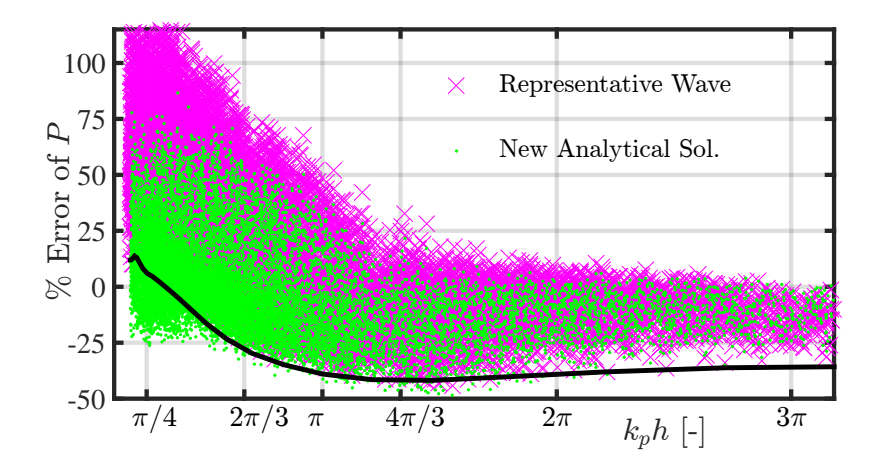


Figure 7.1: Estimation errors as a function of relative water depth $k_p h$ found in the validation of the two techniques against in-situ wave buoy data.

wave power substantially at the lower bound of intermediate water waves. Their capabilities then improve significantly for waves in deeper water, with the best performances found at $\pi/2 > k_p h > 3\pi/4$ and $3\pi/4 > k_p h > \pi/2$, for the new solution and the representative approach, respectively. Beyond these most favorable ranges, the estimation errors still fluctuate but with a decelerating rate. This trend suggests that the two techniques should allow an indistinguishable performance toward the deep water regime. At the lower limit of $k_p h < \pi/4$, the new solution may not be associated with excessive errors but it is still unrecommended for any application within this range, according to the facts in the formulation and behaviors of the important terms discussed earlier in the verification.

The proximal water depth k_ph has been proven thus far to be highly influential to the performance of the new solution, but it could be possible that some other factors may also feature a vital role. The main focus here is on sensitive factors in the random wave spectra as any estimation techniques need to rely on them in some aspects. To investigate the sensitivity, the new solution is tested against two spectral factors which indicate the steepness and the energy-frequency spread in the wave spectrum. The former is referred to straight forwardly as the spectral steepness factor, representing an overall condition of the random wave field via

$$S_p = 2\pi^2 \left(\frac{H_{m0}}{gT_p^2}\right) \tag{7.1}$$

where H_{m0} and T_p are the spectral-based significant wave height and the peak wave period,

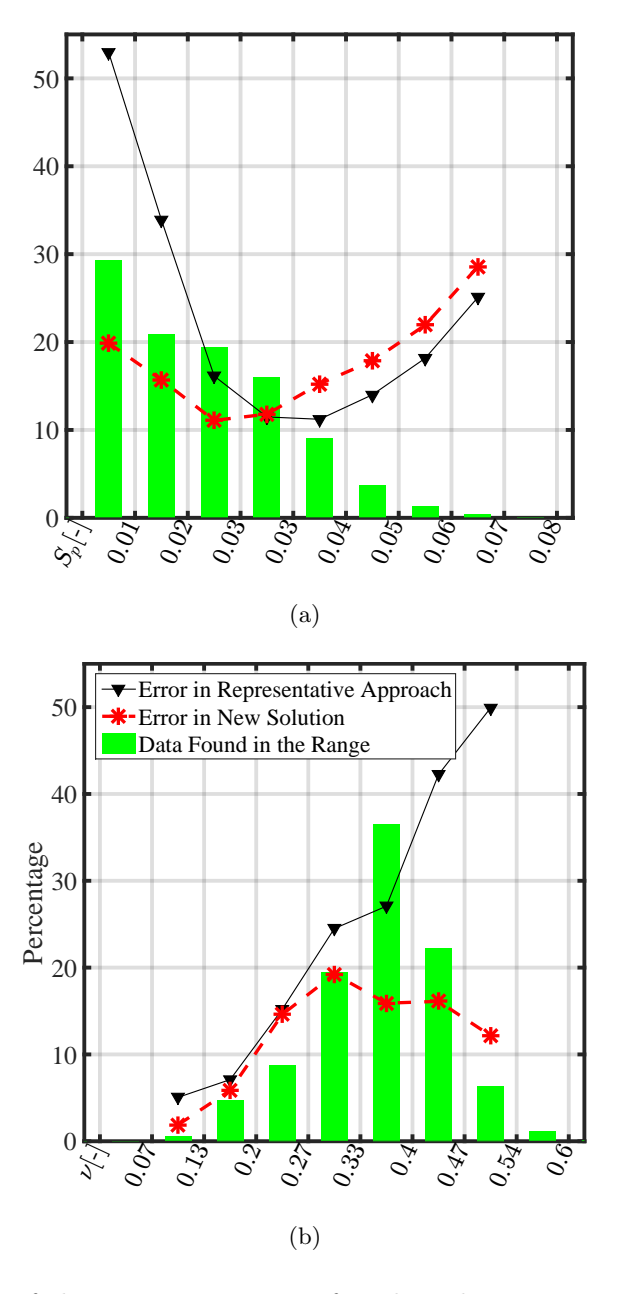


Figure 7.2: Variation of the estimation errors found in the sensitivity tests based on two influential spectral factors: including (a) random-sea steepness factor S_p , and (b) spectral width parameter ν .

respectively. This relationship may be interpreted more easily as a form of wave height to wave length ratio or a non-dimensional steepness of the wave field. The other indicator of interest is proposed for the quantifying the distribution of wave energy over the frequency bands, or simply the spectral width of the sea. Longuet-Higgins (1975) suggested that this physical characteristic can be measured using a single parameter ν which follows

$$\nu = \left(\frac{M_0 M_2}{M_1^2} - 1\right)^{1/2} \tag{7.2}$$

in which M_n is the n^{th} moment of the random wave spectrum. A greater value of ν implies a wider frequency coverage or a more even distribution of wave energy. Values of ν between 0.3 to 0.5 are common for most wind-induced seas, including wave spectra parameterized using the TMA or the JONSWAP technique (e.g. Soares and Carvalho 2003).

Table 7.1: Statistical factors computed per values of total wave power P yielded by the two different techniques. R^2 is the coefficient of determination, Err is the mean error in percent, Std is the standard deviation of error as percentage of the mean.

Analyzing Technique:	Representative Wave			New Analytical Solution		
Range \downarrow / Factor \rightarrow	R^2 [-]	Err. (%)	Std. (%)	R^2 [-]	Err. (%)	Std. (%)
$0 < k_p h \le \pi/4$	0.58	57.74	24.74	0.91	12.68	17.49
$\pi/4 < k_p h \le \pi/2$	0.84	43.70	24.30	0.98	10.43	17.88
$\pi/2 < k_p h \le 3\pi/4$	0.97	17.36	22.41	0.96	2.28	19.30
$3\pi/4 < k_p h \le 3\pi/2$	0.91	-0.83	20.81	0.79	-10.42	18.59
$3\pi/2 < k_p h \le 3\pi$	0.78	-10.17	10.60	0.63	-14.20	10.29
$k_p h > 3\pi$	0.83	-17.34	7.29	0.89	-12.15	7.11

To investigate its influence on the performance of the new solution, each of the hypothesized factors was computed for all of the available wave spectra. The magnitudes of wave power estimated previously are then analyzed as functions of the factors, and the errors associated are illustrated in Figure 7.2. The deviation in the estimation results due to the steepness factor S_p is shown in Figure 7.2a where both types of the estimates produce certain errors in a concave-up pattern over the values of the factor. The errors are greater for very small and very large values of S_p in which the tested wave spectra are believed to be somewhat irregular compared to a parameterized spectrum or a narrow-banded wave model. For example, the spectral shape can be more positively skewed in the case where waves with

lower frequencies are dominant and such long period waves can cause the steepness to be very small. In the opposite condition, a majority of shorter period waves will cause most wave energy to shift to higher frequency bands, potentially forming a fronting peak distribution instead of a tailing peak spectrum of a regular sea.

The influence on the spectral width of the wave field ν is examined in Figure 7.2b considering the estimation errors induced by the new solution and the representative wave approach. As the values of ν increase to around 0.3, both sets of the estimation errors rise at very similar rates from around 5% to 20% with those of the new solution being the lower group. Beyond that limit, the representative approach clearly becomes the less reliable method while the performance of the new solution improves significantly. The errors from either technique soar to 50% and reduce to only around 10%, respectively. It should be recalled that a higher value of ν refers to a scenario with a broader wave energy distribution over the frequency bands. Therefore, it should not be surprising that the representative wave technique provides very poor results as it assumes a narrow-banded wave field. Meanwhile, the greatest capability of the new solution is found for the values of ν between 0.3 to 0.5 as these numbers lie in a common range of the parameterized wave spectra which were adopted as a basis in the solution formulation.

Major findings from the validation using this wave buoy dataset can lead to a few conclusions. First, the best applicable range of the new solution previously specified to be where $k_p h > \pi/4$ could be reconfirmed. The solution might not fail in the test here with $k_p h < \pi/4$, but it is highly not recommended for application due to a reliability reason. While the new formula is clearly most sensitive to $k_p h$, the spectral steepness factor (S_p) and the spectral width factor ν may also be related to the solution performance. For both factors, the relations are fairly straightforward since the new solution performance will enhance if the two factors are within their common ranges specified in the model parameterized spectra. This reliance gives the new solution some flexibility in the estimation and it is the main explanation to its superiority over the representative wave approach that is based solely on a fixed narrow-banded wave model.

7.2 Investigation based on Offshore Wave Buoy Data

The validation with the wave buoy data may provide insightful information but it only covered wave climatology at one location with possibly limited wave characteristics. To ensure its performance under wider field conditions, the new analytical solution is verified again here using wave energy spectra measured at eight locations along the US Atlantic

Coast and the Gulf of Mexico. The data were achieved through a measurement campaign consisting of a network of wave buoys operated by the National Data Buoy Center (NDBC) of the US National Oceanic and Atmospheric Administration (NOAA). Initial details including specific positions of the measurement stations can be found in Table 7.2. About 7,000 hourly wave spectra recorded at each site were employed for the validation here. The preparation techniques follow the same steps applied in the previous validation, except for not including tidal variation which should be insignificant compared to the mean water depths.

The best estimates of wave power were first analyzed from the measured wave spectra using the exact integral method. These principal results were then considered as benchmark to evaluate the estimation results in the representative approach and the new analytical formula. The overall results can be separated into two sets for two groups of stations. The first includes those from Stations 1 to 4 which also feature waves in the mid-intermediate water depth $(k_p h > \pi/4)$. The other set covers those from Stations 6 to 9 in which the waves were in the upper-intermediate water depth and beyond $(k_p h > \pi/2)$. Two examples for the results from the first group are illustrated in Figure 7.3, comparing between the best estimates and the estimated values, on the horizontal axis and the vertical axis, respectively. Scattering and estimation bias are two apparent features which can easily be observed to evaluate the solution performance. The bias may be noticed based on the linear line fitted through the comparison, which would feature a one-to-one slope for equality. In this case, both of the results from the representative approach and the new solution seem to be overestimated as their fitted lines are steeper than the neutral line. However, the new solution appears to be the more accurate and more precise tool as the results are associated with a smaller degree of overestimation and also less scattered.

Another investigation is achieved to validate the new solution against the datasets from the deeper stations (No. 5-8). Two examples from the estimation of the wave power in this case are illustrated in Figure 7.4. The results show that both of the representative wave and the new formulas seem to improve and provide the estimates which are more accurate and more precise than previously allowed for the shallower sites in Figure 7.3. Still, the new analytical solution should be the superior option as its scattering is much narrower and the estimation bias is hardly noticeable. To provide a quantitative comparison, three statistical factors based on all of the results are considered including the mean absolute error, the estimation bias slope, and the standard deviation of the errors in terms of percentage of the mean. The differences between these factors from the representative wave approach and

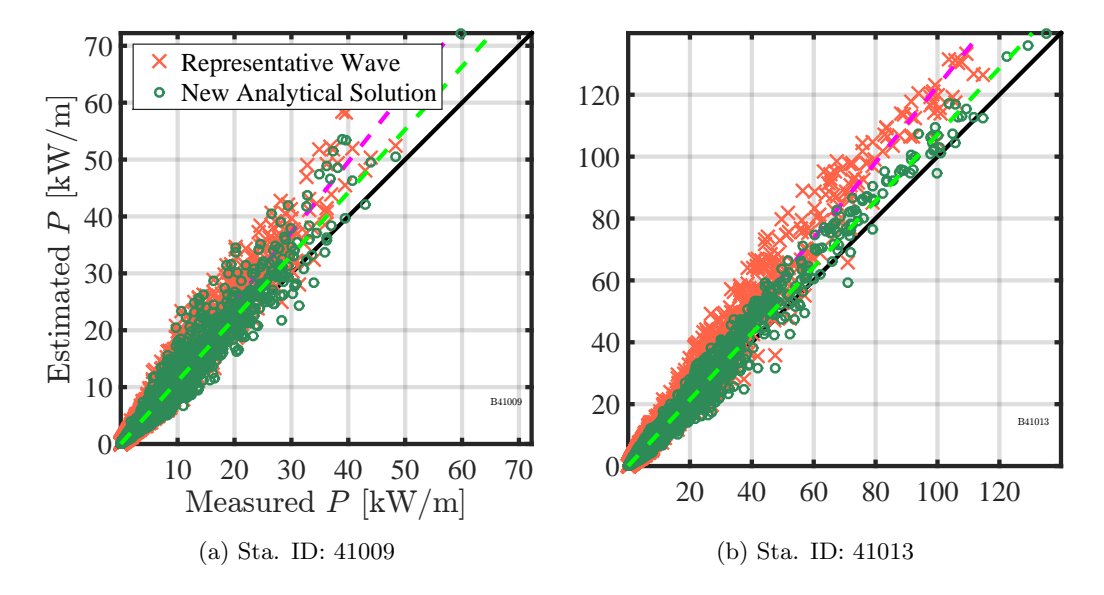


Figure 7.3: Comparison between resulting values of total wave power P estimated using the two different techniques at two intermediate-deep water sites. Summary on the comparison based on all of the data sets may be found in Table 7.2.

the new solution are computed and illustrated in Table 7.2. Note that positive residuals indicate higher values of the representative wave approach.

The indicators presented in Table 7.2 can lead to a very clear conclusion for the gap between the capabilities of the two approaches. Considering the overall investigation, the mean error, the bias, and the standard deviation from the results from the new solution, are respectively about 0.13 to 0.18, 13 to 17%, and 2.3 to 6.6% lower than those of the representative wave approach. These percent differences should be somewhat reliable since their variations are fairly limited in such small ranges despite the fact that they were computed based on datasets from many sites with various wave characteristics. It may be worth noting that the estimation bias and the mean error primarily indicate the estimation performance in average. Meanwhile, a higher standard deviation may imply a greater possibility in seeing some larger errors which should be the case in any application of the representative wave approach. Foreseeably, such an extreme case can occur when a random wave spectrum is pushed away from the original narrow-banded assumption and no nominal wave parameter can be representative for the wave field.

On the other hand, the most supportive attribute in the new solution is its flexibility

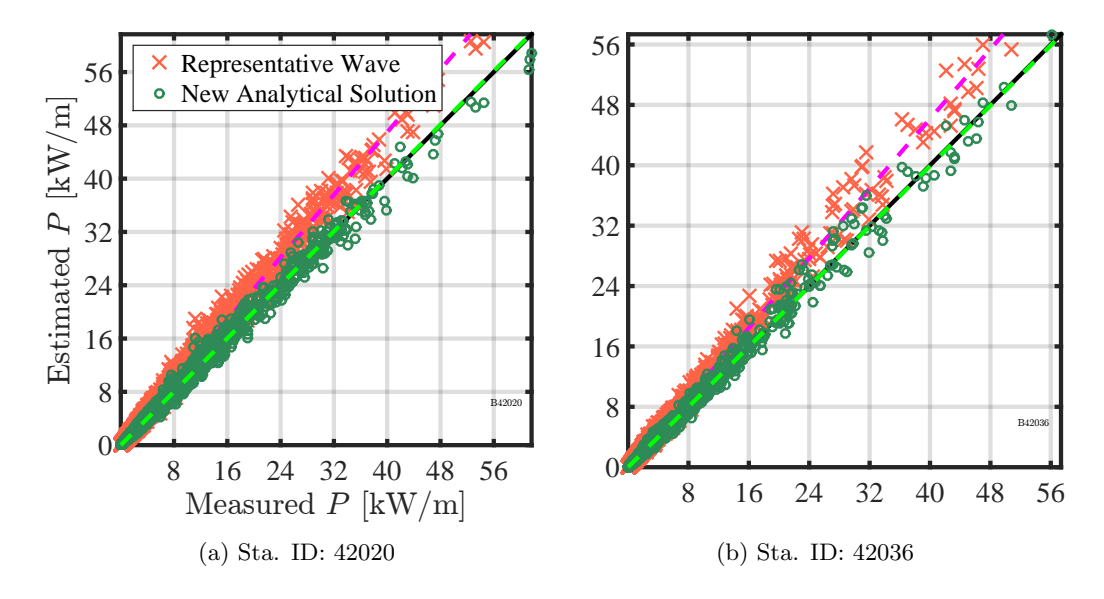


Figure 7.4: Comparison between resulting values of total wave power P at two deep-water sites estimated using the two different techniques. See Figure 7.3 for details.

Table 7.2: Information of NDBC stations and statistical indicators found in the validation of the new analytical formula. Note that positive differences (Δ) indicate smaller values found in the new solution.

No.	Site Specification			Statistical Results			
	Sta. ID.	Position	h (m)	$k_p h$ [-]	Δ BIAS [-]	Δ Error (%)	Δ Std. (%)
1.	41004	32.50N, 79.10W	38.4	0.90-30.6	0.13	14.44	2.29
2.	41008	31.40N, 80.87W	19.5	0.52-15.5	0.17	16.82	6.54
3.	41009	28.52N, 80.19W	40.5	0.85-32.3	0.13	14.62	3.55
4.	41013	33.44N, 77.74W	23.5	0.68-18.7	0.16	13.83	3.18
5.	41025	35.01N, 75.40W	68.3	1.53-49.6	0.18	16.90	3.27
6.	42019	27.91N, 95.35W	82.2	2.84-59.8	0.16	15.83	2.70
7.	42020	26.97N, 96.69W	79.9	2.76-52.7	0.17	16.14	2.56
8.	42036	28.50N, 84.52W	50.6	2.07-36.8	0.15	14.57	2.94

to account for uncertainty and irregularity in the actual wave energy spectra, thus providing the estimate of wave power with higher accuracy and precision compared to the representative wave approach. This fact is especially clear for waves in a transitional water depth. In deep water, the new solution still appears to the superior alternative even though both techniques are very efficient. Regarding the applicable range, the new solution may be proved to deliver satisfactory estimates in any conditions in the validation here, but to adhere to the previous theoretical verification the formula should be preserved for use at the proximal water depth $k_p h > \pi/4$, or the mid-intermediate water depth and beyond. In all of the validation attempts, the findings are rather positive for the capability of the new analytical formula which should now be confident for practical use on any actual sites with available inputs

8 Practical Application of the Study

Having been verified and validated, the new formula can readily be employed for practical use. An example for its application is demonstrated here for the estimation of wave power in the coastal ocean of Thailand.

8.1 Site Selection and Power Estimation

The proposed application was performed at 16 locations in the Gulf of Thailand and the Andaman Sea as shown in Figure 8.1, which are on the east and the west of the nation's coastal ocean, respectively. Specific details including depths and coordinates of the locations can be found in Table 8.1.

The estimation was started by first modeling wind speed and direction over the entire region during May 2017 to April 2018. This initial part was achieved using the Weather Research and Forecasting (WRF) model (Skamarock et al., 2008). With available geographical information of the coastal ocean, the wind data were passed over to the third generation Simulating WAves Nearshore (SWAN) model (SWAN Team, 2011). Two principal processes were simulated including the growth of random waves due to the imposed wind and the transformation of the propagating waves. The latter was achieved via the wave action balance equation which considers important processes such as whitecapping, bottom dissipation, and potential wave breaking (Booij et al., 1999). The final simulation output was in the form of local wave energy spectra which can be processed further for important wave parameters including wave energy and power. Note that all default settings in both

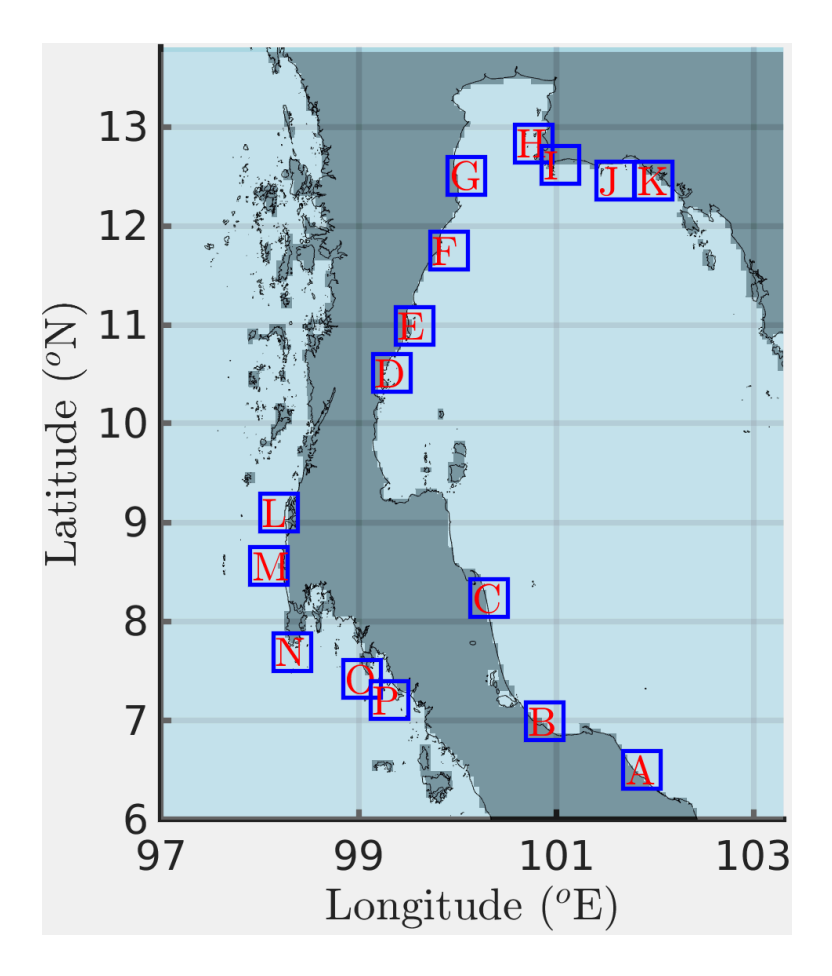


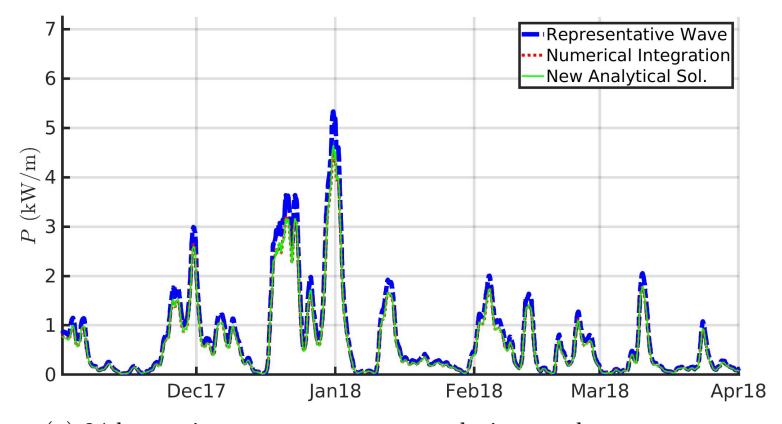
Figure 8.1: Locations along the coastline of Thailand where the potential wave power is evaluated. Specific details including coordinates and depths can be found in Table 8.1.

of the related models were applied as the major purpose here is to demonstrate a practical use of the newly developed formula.

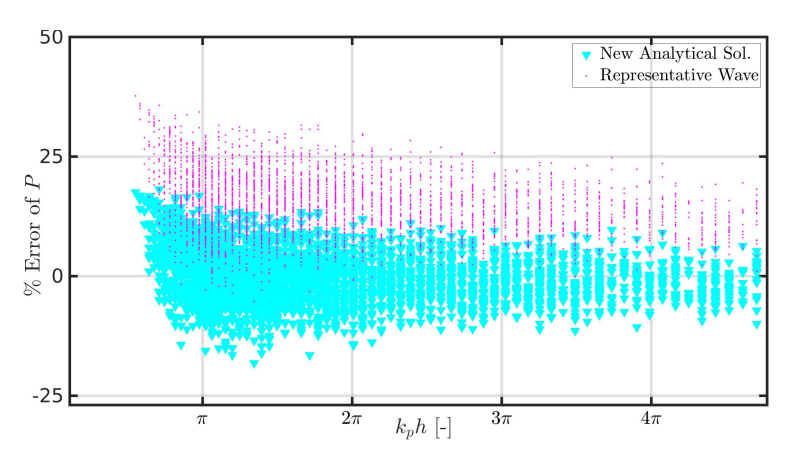
All of the wave energy spectra obtained were initially evaluated to narrow down the focus on spatial coverage and temporal variation of the problem. Beside allowing the selection of 16 locations, this attempt leads to a very important guideline that any quest for wave power in the coastal ocean of Thailand should consider only waves under two regional monsoons as the in- and out-of-the season wave power ratios are about 7:2 on average. The coastal areas in the eastern Thai Gulf and on the Andaman coast, which feature some large fetches on their west, are exposed to the southwest monsoon initiated in the Indian ocean during June to October. The other part along Thai Gulf features a wide and long fetch on the east and will experience much larger waves under the northeast monsoon during November to April. Apart from offering higher wave power, the occurrence of monsoon waves and their principal directions are also more predictable which would accommodate any further study on related techniques and power harvesting schemes.

Figure 8.2a shows an example of magnitudes and variations of 24-hr moving average wave power found at Location A, Narathiwas, which is furthest south on Thai Gulf. During the regional northeast monsoon, the averaged power is shown to be as high as 5 kW/m but it is also fluctuating greatly over the time. The estimates in comparison were produced from the three different techniques which are the representative wave approach, the numerical integration, and the new analytical solution. Taking the numerically integrated power as exact results, the estimation errors induced by the other two techniques are illustrated in Figure 8.2b. Initially, the errors tend to decrease as the proximal water depth $k_n h$ increases, agreeing with findings from all the previous tests. For the lower end of $k_p h < 2\pi$ here, the new solution is associated with around $\pm 15\%$ errors while those of the representative approach are in a range of 0 to 30%. Although both ranges become narrower in the upper part of $k_p h$, it is clearly observed that the errors from the new solution are almost symmetric about the zero-error line, but the representative approach is always involved with overestimation. Such a difference can bring a significant outcome when applying each technique in the study of wave energy and power. Any estimation bias must certainly be taken care of, but such a symmetric deviation as offered by the new solution can allow a neutral mean power over a duration, thus providing a very precise estimate of the wave power potential. Generally, this specific quantification is the first principal task in any evaluation of wave power resources.

Figure 8.3a illustrates a similar example of 24-hr moving average wave power at Location N, or Phuket, a famous island in the Andaman sea. Being on the other side of the coast, this



(a) 24-hr moving average wave power during northwest monsoon



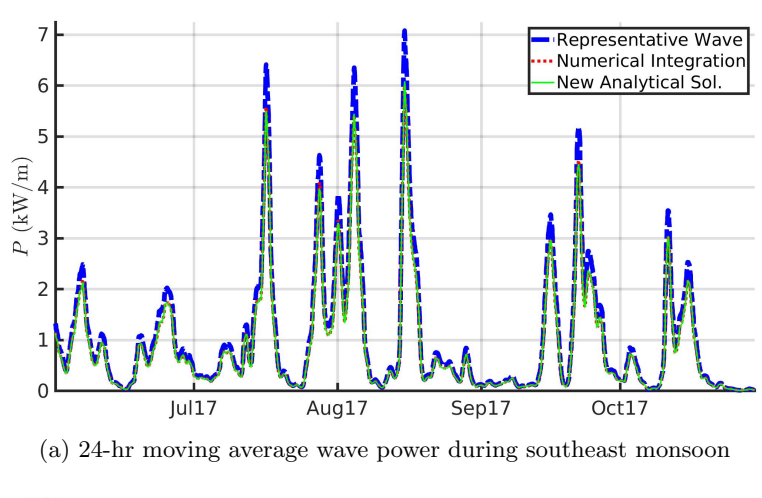
(b) Errors relative to the results from full numerical integration

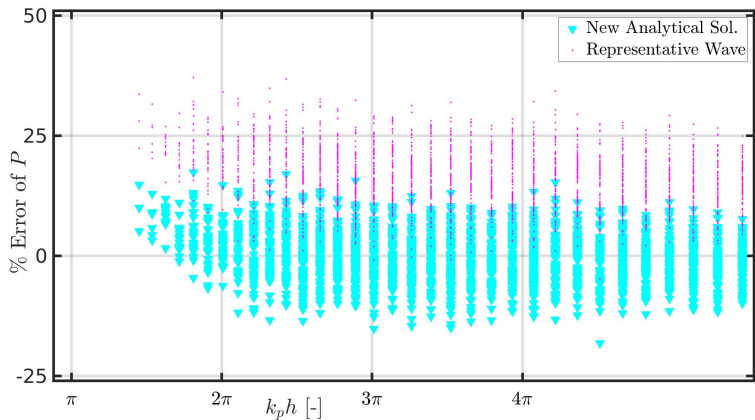
Figure 8.2: Evaluation on the magnitudes of wave power at Location "A" (Narathiwas) and estimated errors from the two different techniques.

location is exposed to southwest monsoon from the Indian ocean. The averaged power is therefore shown for June to October during which multiple peaks were observed between 6 to 7 kW/m. The fluctuation of the power is as high as that of the previous instance and, in fact, this characteristic should be anticipated for any locations around this part of the ocean according to the regional wave climatology. The estimates allowed by the three different techniques are compared and the estimation errors induced by the representative approach and the new analytical solution are illustrated in Figure 8.2b. Typical trends of the errors still persist but their reductions following the increase of $k_p h$ do not turn up clearly since all wave spectra fall into the deep-water regime. For the entire part of $k_p h > 2\pi$, a range of $\pm 15\%$ of the errors is observed for the new solution while a range of 0 to 30% is found for the representative approach. Noticeably, these approximated errors are the same as those of the first example in Figure 8.2b but the ranges of $k_p h$ between the two cases are different. For a comparison in the same range of $k_p h$, the performance of the new solution seems to be greater in the previous case. This variation may occur as the two sets of simulated wave spectra differ from each other. The coastal sea at Location N in Figure 8.3 features larger and steeper waves which are often associated with longer wave periods. A significant portion of energy may distribute in the low-frequency end of the domain thus leading to an irregular and more peaky wave energy spectrum. This deviation and the increase in the sea steepness can directly affect the performance of the new solution which relies on a typical spectral form through the use of a parameterized wave spectrum.

8.2 Potential Power along the Coasts

Average wave power potentials found at all of the locations during their monsoon periods are summarized in Figure 8.4. These season-averaged values appear to be relatively low, ranging from 0.3 to 1.5 kW/m, as opposed to the maximum daily average which could be as high as 10 kW/m. Initially, this fact implies that the standard deviations of the power can be multiple times of the average values. Beside the temporal fluctuation, the power magnitudes also differ greatly among the locations. The Southern Thai Gulf is the region that sees the greatest spatial variation of the wave power potentials, including the most promising spot at Location E and a few very low potential sites such as Locations B and C. Most of the locations in the Eastern Thai Gulf do not offer any impressive magnitude of the potential with the zonal maximum found to be slightly lower than 0.7 kW/m. The sites in the Andaman Sea may not seem to offer much greater potentials but the resulting mean values between 0.6 to 1.0 kW/m can be considerable and are also the most invariant





(b) Errors relative to the results from full numerical integration

Figure 8.3: Evaluation on the magnitudes of wave power at Location "N" (Phuket) and estimated errors from the two different techniques.

numbers in a particular coastal zone. The true potential of wave power in this region is still widely open for a more detailed evaluation. The temporal and spatial coverages certainly need to be extended and a more circumspect investigation is required on their variations. A complete multi-dimensional, statistical analysis is possibly the most appropriate approach for any further attempts on the problem.

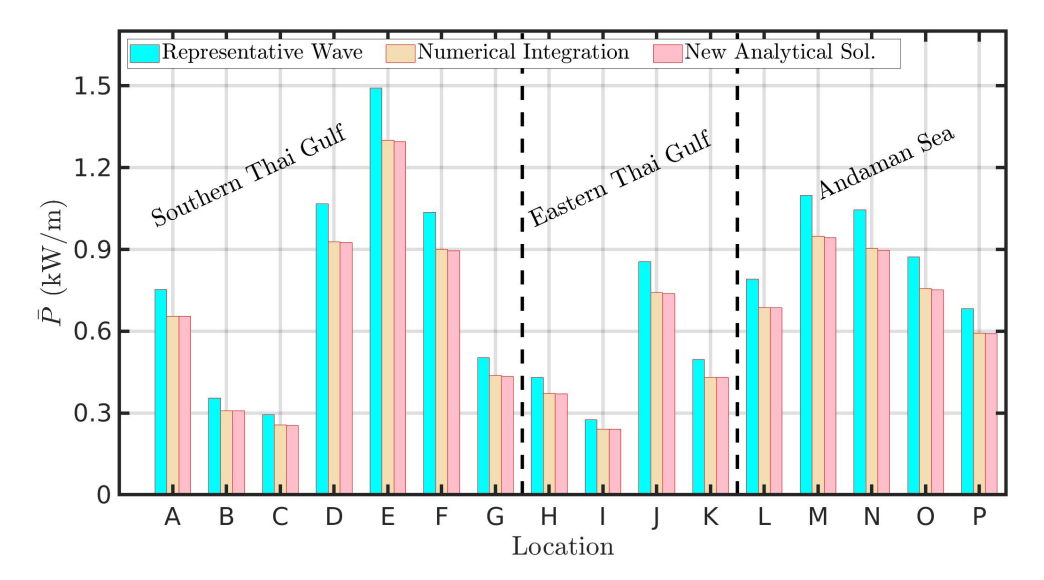


Figure 8.4: Average wave power potential found during the monsoon season of each of the locations. The southern Thai Gulf is evaluated under the northwest monsoon from Nov 2017 to April 2018; the other two zones are evaluated under the southeast monsoon from Jun 2017 to Sep 2017.

For the main purpose here on the application of the new solution, the magnitudes of wave power potentials yielded by the three available methods are compared and illustrated in Figure 8.4. The comparison result shows that the representative wave approach tends to provide around 10 to 15% higher estimates than the other two techniques. Surprisingly, the estimation results allowed by the new analytical solution almost match with those of the numerical integration at every location investigated. This encouraging outcome is possible as a consequence of the estimation with symmetrical biases, from which a neutral mean can be determined. Since the underlying wave spectra were also simulated, the numerical technique may not provide actual values of the power but such resulting potentials should still be accepted as the best estimates. That is, the wave model is believed to allow an accurate random wave field in the sea. This given hypothesis can be met to

different degrees in practical, but its effectiveness over the narrow-banded assumption can always be warranted. For the objective here in determining the wave power potential, the performances of the new analytical solution and the numerical technique should therefore be considered to be equal as they both provide almost identical results.

The resulting numbers and the facts discovered here can be digested to summarize several interesting cases on the capabilities of the new solution and the traditional representative wave approach. One is when the energy distribution in the random sea perfectly follows the form of a narrow-banned spectrum. In this idealistic case, both of the techniques will perform equally well as the actual spectrum can be represented based on their underlying principles, i.e. using some bulk wave parameters or a parameterized wave spectrum. Another case, the most common in nature, occurs when the random wave field features a typical pattern of energy distribution but with some irregularities. Almost all of the test cases in this study fall into this scenario and therefore, according to the results shown thus far, the mean accuracy of the new solution can be pronounced to be up to 15%superior than that of the representative wave approach. It is also a valid question whether the new solution can be outperformed in any circumstance. This unfavorable case is, in fact, possible but only when the sea spectrum is so irregular that no assumption can be made for its representation. Under this rare condition, accounting for only 3% to 8% in all of the analyzes in this study, the representative wave approach can offer a more accurate result but only by random chance rather than by its basis principle. With all these facts, the new analytical solution can be confidently applied in any practical estimation, especially for wave power as possible errors from discrete estimates can be averaged-out when reproducing the mean potential power.

LOCATION		^{o}N	^{o}E	$\bar{h}(m)$	LOCATION		^{o}N	^{o}E	$\bar{h}(m)$
A	NARATHIWAS	6.507	101.852	14.4	I	RAYONG(1)	12.624	100.998	9.7
В	SONGKHLA	6.967	100.820	9.1	J	RAYONG(2)	12.492	101.588	19.9
С	NAKORNSRI	8.287	100.279	6.13	K	CHANBURI	12.494	101.954	8.9
D	CHUMPON	10.506	99.269	17.4	L	PHANGHA(1)	9.106	98.155	16.9
Е	PRACHUB(1)	11.042	99.506	19.9	М	PHANGHA(2)	8.570	98.152	41.4
F	PRACHUB(2)	11.802	99.900	22.3	N	PHUKET	7.718	98.293	39.2
G	PRACHUB(3)	12.543	100.045	17.7	О	KRABI	7.468	98.994	28.3
Н	PATTAYA	12.867	100.847	22.5	Р	TRANG	7.245	99.282	16.2

Table 8.1: Information of 16 locations in the coastal ocean of Thailand considered for practical application of the new formula.

9 Conclusion of the Study

Ocean waves have recently been introduced as a flourishing source of alternative power due to their abundance and reliability. Evaluation of the wave power potential has been conducted worldwide with some early efforts in North America and Europe. In any attempts, the first and foremost information needed is certainly the intrinsic wave power potential which helps provide an outlook on the feasibility. This requirement challenges many researchers to quest for optimal and practical means in estimating the power potential in such an enormous and highly varying environment.

In current practice, two traditional estimation methods are often applied which include a full wave spectrum integration and a representative wave approach based on some nominal wave parameters. These two options are rather different in terms of implementation as the former relies on a numerical technique while the latter offers a closed-form analytical solution. The present research work is aimed at introducing a new formula for the estimation of total wave power P, which allows an accuracy and precision comparable to that of the numerical method but appears in a practical form of analytical solution. The key technique in the formulation is the utilization of a parameterized wave spectrum for imitating the random sea. A few implicit terms and functions in the full spectral expression are then simplified using an alternative wave dispersion relation and mathematical asymptotes. The derivation is finally achieved via an integration relying on the linear wave theory to obtain the new analytical formula from which the total wave power can be estimated based on the water depth and basic wave parameters including statistical wave height and wave period.

To ensure its capability, the new solution was verified by investigating all of the steps involved in its formulation. The verification revels that the simplification and asymptotic techniques applied can induce some errors but their effects on the resulting wave power are insignificant. Besides, a large set of synthetic wave spectra based on up to 26,000 realizations were applied to evaluate the new formula under different conditions of random waves. In comparison to the representative wave approach, the synthetic test proves that the new solution can offer greater estimation accuracy and precision in the mid-intermediate to deep water condition in which the proximal water depth factor k_ph for this applicable range can be defined as $k_ph > \pi/4$.

The new formula was validated using two reliable sources of field wave spectra. First, its estimation performance and sensitivity on diverse sea states were investigated with available data from a nearshore wave buoy. It was demonstrated that the new solution can estimate the total wave power within about $\pm 12\%$ errors while the representative wave approach can produce up to 40% errors. The performance of the new formula seems to be affected by the sea steepness and the spectral width factors $(S_p \text{ and } \nu)$ but such an impact should be limited within the applicable range of new solution declared in terms of the relative water depth $(k_p h)$. For more than 90% of the tests, regardless of the sea states, the new formula still allow more accurate estimates than the representative wave approach. The second validation of new formula employed eight independent sets of wave energy spectra recorded by the National Data Buoy Center (NDBC) along the US Atlantic Coast and the Gulf of Mexico. In this case, the superior of the new formula to the representative wave approach can be confirmed once again based on the offsets in the mean estimation errors and the standard deviations of around 15% and 3%, respectively.

After the verification and the validation, the new formula was demonstrated for practical use in the estimation of wave power in the coastal sea of Thailand. A modeling suit was adopted to simulate hourly wave data over a year at 16 locations along both sides of the national coast. An initial analysis based on the data leads to an important remark that only the waves under two regional monsoons should be considered as their power delivery could be up to 3 times higher than that of the off-season waves. For the main purpose in this study, hourly estimates of wave power from the representative wave approach, the numerical integration, and the new analytical solution were first compared at each of the locations. In general, the new solution was found to produce around $\pm 15\%$ errors while the representative approach was associated with errors in a range of 0 to 30%. Both of such error ranges were found to be narrower in deeper water, in terms of the proximal factor $k_p h$,

which are in accordance with the other findings based on synthetic and available measured wave spectra.

For all of the locations considered, average magnitudes of wave power during the monsoon seasons were computed and the resulting power potentials were found to be relatively small around 0.3 to 1.5 kW/m. Both of the temporal and spatial variations of the regional wave power potentials were found to be significantly high based on the standard deviations. The applicability and the performance of the new solution were proven through a comparison among wave power potentials allowed by the three available methods. The outcome was very encouraging as the estimations allowed by the new analytical solution and the numerical integration were almost identical, while the representative approach tended to yield around 10 to 15% higher estimates. This favorable result is achievable as the new solution is involved with limited and symmetrical estimation biases which can be averaged out in the computation of the mean. Such a neutral deviation can always lead to a precise estimate of the mean wave power potential which is a primary indicator in any evaluation of wave power resources.

The superiority of the new analytical formula over the representative wave approach can be explained based on findings from all of the tests. In general, the information of random waves can be derived into a wave energy spectrum which can also be imitated via use of a parameterized wave spectrum which is the backbone of the new solution. Actual wave spectra in the nature may vary greatly but their shapes and frequency bands are bounded, and most parameterized wave spectra offer some dependable flexibility to replicate the variation. Whereas, the representative wave approach only considers few basic wave parameters assuming a narrow-banded wave field, therefore its estimation could only be as accurate as the others' only if this rare and idealistic condition becomes true. The most common wave spectra in the field are certainly those which feature a typical energy distribution with some irregularities, and almost all of the wave spectra in every test here fell into this category. With this fact, the test results should provide a sufficient confidence interval in any practical application of the new formula.

The new analytical formula developed in this study should be able to serve as an effective tool in the estimation of total power of surface waves in the ocean. Besides a much-required means in wave power resource assessment, this type of solution can also be incorporated in a module of wave power estimation for input or computing parameters in any wave modeling system. In standalone form, the new formula which appears in a closed analytical form can readily be executed by coastal and ocean engineers in many practical applications. The

new body of knowledge achieved in this study is expected to be extended in two promising directions. One is on the improvement of the new formula, focusing on enhancing its applicable range and estimation performance. The other is on a very widely-open topic which is the assessment of wave power potential of Thailand which was conducted initially here to demonstrate the use of the new formula. A complete evaluation on the magnitude and variation of the wave power in this region is still certainly needed, at least for a critical justification on whether such an alternative power around the equator is worth considering despite being infamous for its low wave power density.

10 REFERENCES

- Arinaga, R. A., Cheung, K. F., 2012. Atlas of global wave energy from 10 years of reanalysis and hindcast data. Renewable Energy 39 (1), 49–64.
- Booij, N., Haagsma, I.J.G.and Holthuijsen, L., Kieftenburg, A., Ris, R., Van Der Westhuysen, A., Zijlema, M., 2004. SWAN Cycle III version 40.41 User Manual. Tech. rep., Delft University of Technology, 115 p.
- Booij, N., Ris, R. C., Holthuijsen, L. H., 1999. A third-generation wave model for coastal regions: 1. Model description and validation. J. of Geophysical Res.- Oceans 104 (C4), 7649–7666.
- Boronowski, S., Wild, P., Rowe, A., van Kooten, G. C., 2010. Integration of wave power in Haida Gwaii. Renewable Energy 35 (11), 2415–2421.
- Bouws, E., Gunther, H., Rosenthal, W., Vincent, C. L., 1985. Similarity of the wind wave spectrum in finite depth water 1. Spectral Form. J. of Geophysical Res.- Oceans 90 (1), 975–986.
- Cahill, B., Lewis, T., 2014. Wave period ratios and the calculation of wave power. In: the 2nd Marine Energy Technology Symposium METS2014, WA, USA.
- Cornett, A. M., et al., 2008. A global wave energy resource assessment. In: The 18th International Offshore and Polar Engineering Conference. International Society of Offshore and Polar Engineers.
- Dean, R. G., Dalrymple, R. A., 1991. Water Wave Mechanics for Engineers and Scientists. Adv. Series on Ocean Eng., Vol. 2. World Scientific, Singapore.
- Defne, Z., Haas, K. A., Fritz, H. M., 2009. Wave power potential along the Atlantic coast of the Southeastern usa. Renewable Energy 34 (10), 2197–2205.
- Defne, Z., Haas, K. A., Fritz, H. M., 2011. Numerical modeling of tidal currents and the effects of power extraction on estuarine hydrodynamics along the georgia coast, usa. Renewable Energy 36 (12), 3461–3471.
- Eckart, C., 1952. The propagation of gravity waves from deep to shallow water. In: Gravity waves, National Bureau of Standards Circular 521. Vol. 1. pp. 165–173.

- Falnes, J., 2007. A review of wave-energy extraction. Marine Structures 20 (4), 185–201.
- Fernández, J., Salcedo-Sanz, S., Gutiérrez, P. A., Alexandre, E., Hervás-Martínez, C., 2015. Significant wave height and energy flux range forecast with machine learning classifiers. Engineering Applications of Artificial Intelligence 43, 44–53.
- Gonçalves, M., Martinho, P., Soares, C. G., 2014. Wave energy conditions in the western french coast. Renewable Energy 62, 155–163.
- Hasselman, K., Barnett, T. P., Bouws, E., Carlson, D. E., Hasselmann, P., 1973.
 Measurements of wind-wave growth and swell decay during the Joint North Sea Wave Project (JONSWAP). Tech. Rep. No. 12, Dt. Hydrogr. Z.
- Hughes, M. G., Heap, A. D., 2010. National-scale wave energy resource assessment for australia. Renewable Energy 35 (8), 1783–1791.
- Iglesias, G., Carballo, R., 2011. Choosing the site for the first wave farm in a region: A case study in the Galician Southwest (Spain). Energy 36 (9), 5525–5531.
- Jacobson, P. T., Hagerman, G., Scott, G., 2011. Mapping and assessment of the united states ocean wave energy resource. Tech. rep., Electric Power Research Institute, CA, USA.
- Kirby, J. T., Dalrymple, R., Shi, F., 2005. REF/DIF S version 1.3: Documentation and users manual. Tech. rep., Research Report NO. CACR-04-01. Center for Applied Coastal Research, Univ. of Delaware.
- Lawless, M., Rodger, D., 2013. Development of the european tidal database and its potential application to marine renewables. J. of Coastal Research 65 (sp2), 1629–1632.
- Lindroth, S., Leijon, M., 2011. Offshore wave power measurements- A review. Renewable and Sustainable Energy Reviews 15 (9), 4274–4285.
- Longuet-Higgins, M., 1975. On the joint distribution of the periods and amplitudes of sea waves. J. of Geophysical Res.- Oceans 80 (18), 2688–2694.
- Mofor, L., Goldsmith, J., Jones, F., 2014. Ocean energy: Technology readiness, patents, deployment status and outlook. Tech. rep., International Renewable Energy Agency (IRENA) Report, Paris.

- Mork, G., Barstow, S., Kabuth, A., Pontes, M. T., 2010. Assessing the global wave energy potential. In: ASME 2010 29th International Conference on Ocean, Offshore and Arctic Engineering. American Society of Mechanical Engineers, pp. 447–454.
- Pawlowicz, R., Beardsley, B., Lentz, S., 2002. Classical tidal harmonic analysis including error estimates in MATLAB using T_TIDE. Computers & Geosciences 28 (8), 929–937.
- Pierson, W. J., Moskowitz, L., 1964. Proposed spectral form for fully developed wind seas based on similarity theory of S. A. Kitaigorodskii. J. of Geophysical Res.- Oceans 69 (24), 5181–5190.
- Pontes, M., 1998. Assessing the european wave energy resource. J. of Offshore Mechanics and Arctic Engineering 120 (4), 226–231.
- Reikard, G., 2013. Integrating wave energy into the power grid: Simulation and forecasting. Ocean Engineering 73, 168–178.
- Reikard, G., Robertson, B., Buckham, B., Bidlot, J.-R., Hiles, C., 2015. Simulating and forecasting ocean wave energy in western canada. Ocean Engineering 103, 223–236.
- Sawin, J. L., Sverrisson, F., Chawla, K., Lins, C., Adib, R., Hullin, M., Leitner, S., Mazzaccaro, S., Murdock, H., Williamson, L. E., et al., 2015. Renewables 2015 global status report. Tech. rep., Renewable Energy Policy Network for the 21st Century.
- Sawin, J. L., Sverrisson, F., Chawla, K., Lins, C., Adib, R., Hullin, M., Leitner, S., Mazzaccaro, S., Murdock, H., Williamson, L. E., et al., 2016. Renewables 2016 global status report. Tech. rep., Renewable Energy Policy Network for the 21st Century.
- Sierra, J., Martín, C., Mösso, C., Mestres, M., Jebbad, R., 2016. Wave energy potential along the Atlantic coast of Morocco. Renewable Energy 96, 20–32.
- Skamarock, W. C., Klemp, J. B., Dudhia, J., Gill, D. O., Barker, D. M., Wang, W., Powers, J. G., 2008. A description of the advanced research wrf version 3. ncar technical note-475+str. Tech. rep.
- Soares, C. G., Carvalho, A., 2003. Probability distributions of wave heights and periods in measured combined sea-states from the Portuguese coast. J. of Offshore Mechanics and Arctic Eng. 125 (3), 198–204.

- Sørensen, H. C., Russell, I., 2006. Life cycle assessment of the wave energy converter: wave dragon. In: Int Conf Ocean Energy. Fron Innovation to Industry. OTTI, Bremerhaven, Germany.
- Srisuwan, C., Rattanamanee, P., Rattanapitikon, W., 2017. Analytical formulas for estimation of phase-averaged parameters of random waves. Ocean Engineering 133, 23 35.
- Svendsen, I. A., 2006. Introduction to nearshore hydrodynamics. Vol. 24. World Scientific.
- SWAN Team, 2011. Swan cycle iii version 40.85 user manual. delft university technology, faculty of civil engineering and geosciences. Tech. rep.
- Thomson, R., Harrison, G., Chick, J., 2011. Full life cycle assessment of a wave energy converter. In: IET Conference Proceedings. The Institution of Engineering & Technology, Edinburgh, UK.
- URS, 2009. Wave power feasibility study report. Tech. rep., Rep. No. 28067508. San Francisco Public Uitlities Commission, The City and County of San Francisco.
- van Nieuwkoop, J. C., Smith, H. C., Smith, G. H., Johanning, L., 2013. Wave resource assessment along the Cornish coast (UK) from a 23-year hindcast dataset validated against buoy measurements. Renewable Energy 58, 1–14.
- Work, P., Srisuwan, C., 2010. Identification of swell in nearshore surface wave energy spectra. The International J. of Ocean and Climate Systems 1 (2), 51–66.
- Work, P. A., 2008. Nearshore directional wave measurements by surface-following buoy and acoustic doppler current profiler. Ocean Eng. 35 (8-9), 727–737.
- Work, P. A., Haas, K. A., Defne, Z., Gay, T., 2013. Tidal stream energy site assessment via three-dimensional model and measurements. Applied Energy 102, 510–519.



Appendix I: Output from the Research Project

Output จากโครงการวิจัยที่ได้รับทุนวิจัย

1. ผลงานตีพิมพ์ในวารสารวิชาการนานาชาติ

"Srisuwan, C., Rattanamanee, P., Rattanapitikon, W. (2020). Analytical formula for estimation of surface wave power with application in the coastal ocean of Thailand. Ocean Engineering (ELSEVIER), Vol. 204, 107273."

Database: ISI Web of Science

Quartile: 1st, all listed fields (CIVIL/MARINE/OCEAN)

5-Year Impact Factor: 3.067

Link: https://www.sciencedirect.com/science/article/pii/S0029801820303206

by 1) Department of Civil Engineering, Faculty of Engineering, Prince of Songkla University.

This research project has contributed to a new analytical solution which can be applied for an estimation of surface wave power in the coastal ocean. The formula as well as important research findings have now been added to the graduate-level lectures, in the MS and PhD curricula, at the Department of Civil Engineering, Prince of Songkla University. The courses in which these new contents appear include: 220-540 Linear Water Wave Mechanics, 220-543 Nearshore Hydrodynamics, and in the programing session in 220-580 Research Methodology in Civil Engineering.

and 2) All interested parties in the field of coastal and ocean engineering.

The new analytical tool accomplished in this research has led to a production of an article titled "Analytical formula for estimation of surface wave power with application in the coastal ocean of Thailand". This article has been published in Ocean Engineering (Vol. 204) which is ranked in the 1st quartile as being one of the most prestigious journals in the subject field of any related field (Marine/Ocean/Civil Engineering and Oceanography). Available online in the ScienceDirect and ISI Web of Science databases, this article can be assessed by all interested persons from anywhere and they can make the most of all of the outputs from this research project.

and 3) Energy Investors and Policy Makers.

In the final chapter in this project, an overview of the surface wave energy potential is provided for the entire coastal zone of Thailand. The conclusion on the potential can help identify large spatial extent and high temporal variation of this specific type of energy. Local wind influences due to the Southwest monsoon and the Northeast monsoon can be focused. Also, a rank of suitable locations according to their wave powers is given and ready to be adopted for initial site selection after which a detailed assessment can be executed.



Appendix II: Article Published in Ocean Engineering

ELSEVIER

Contents lists available at ScienceDirect

Ocean Engineering

journal homepage: www.elsevier.com/locate/oceaneng



Highlights



Analytical formula for estimation of surface wave power with application in the coastal ocean of Thailand

Ocean Engineering xx (xxxx) 107273

Chatchawin Srisuwan*, Payom Rattanamanee, Winyu Rattanapitikon

- Analytical formula based on parameterized wave spectrum for wave power estimation.
- · Accuracy and precision improving around 15% and 5% from traditional approach.
- · Synthetic tests showing applicability of the formula in intermediate to deep water.
- · Tests with reliable field datasets confirming the capability of the new formula.
- · Application of the new formula for its utility in evaluating wave power potential.

Graphical abstract and Research highlights will be displayed in online search result lists, the online contents list and the online article, but will not appear in the article PDF file or print unless it is mentioned in the journal specific style requirement. They are displayed in the proof pdf for review purpose only.



Contents lists available at ScienceDirect

Ocean Engineering

journal homepage: www.elsevier.com/locate/oceaneng



Analytical formula for estimation of surface wave power with application in the coastal ocean of Thailand

Chatchawin Srisuwan a,*, Payom Rattanamanee a, Winyu Rattanapitikon b

- ^a Department of Civil Engineering, Faculty of Engineering, Prince of Songkla University, Hat Yai, 90110, Thailand
- ^b Sirindhorn International Institute of Technology, Thammasat University, Pathum Thani, 12121, Thailand

ARTICLE INFO

Keywords: Renewable ocean energy Wave energy flux Wave power density Wave energy spectra Ocean wave modeling

ABSTRACT

Two common techniques in determining surface wave power include a full wave spectrum integration and a representative wave approach. Under the concept of spectral wave parameterization, a new estimation formula is introduced in this study to capitalize the advantages of both the numerical method and the closed-form solution. The formula was verified using synthetic wave data and its applicable condition is recommended to be in the upper-intermediate to deep water environment. Validation against reliable field wave data showed that the new solution can outperform the representative wave approach by allowing higher estimation performance around 5%–15% on average. The new formula was applied for a practical estimation of wave power in Thailand. While the resulting wave power was found to be relatively low around 0.3 to 1.5 kW/m, the utility of the new solution can be warranted according to its consistency with the full numerical technique. This encouraging outcome is achievable as the deviation of the resulting estimates is limited and symmetric about a neutral mean. In summary, the superiority of the new analytical formula can be attributed to its dependable replication of typical random wave field and its adaptability to irregular wave energy distribution in the nature.

1. Introduction

Alternative energy from the ocean contributes less than 0.1% of the renewable energy, with most of the present development projects found in European countries (Mofor et al., 2014; Sawin et al., 2015). Tidal power is to date the most advanced topic in the field since tides are deterministic and feature greatest magnitudes close to the shoreline, adding some reliability and practicality to the energy conversion (e.g. Define et al., 2011; Lawless and Rodger, 2013; Work et al., 2013). The harvest of energy from irregular surface waves usually has to be performed in a harsh environment under some random conditions. State-of-the-art technologies have recently been developed to allow conversion of renewable energy from the waves which are induced everywhere in the ocean which covers more than 70% of the earth surface (e.g. Sørensen and Russell, 2006; Thomson et al., 2011).

Ocean wave energy is associated with relatively high spatial and temporal variations but, despite being a debatable topic, is more persistent than wind and solar energy (Falnes, 2007; Reikard, 2013). A feasibility study in a region always involves characterization and mapping of the available energy as initial tasks, allowing optimization for the energy converting scheme, and minimizing risk in the operation (Iglesias and Carballo, 2011). Magnitudes, time periods, and propagation directions of waves are the primary factors required in the

estimation of wave energy flux and its total, non-directional quantity that represents the local wave power density (Jacobson et al., 2011). Advanced numerical models have also been introduced for predicting these parameters, mainly to overcome spatial limitation in launching field wave measurement campaigns (e.g. Arinaga and Cheung, 2012; Reikard et al., 2015).

A numerical solution can be executed to integrate energy fluxes contributed by random waves with different magnitudes and frequencies. This method is usually applied where wave energy spectra are available in the target area (e.g. van Nieuwkoop et al., 2013; Gonçalves et al., 2014). The other common implementation relies on the assumption of a narrow-banded wave field with some nominal leading waves (e.g. Hughes and Heap, 2010). This latter technique, commonly referred to as a representative wave approach, allows a simple closed-form equation for the computation of the total energy flux of the wave field. For deep water waves, the approach can further be simplified and only the nominal wave height and wave period are required in the estimation (e.g. Cornett et al., 2008; Fernández et al., 2015).

Scarcity of quality spectral wave data often leads to an application of the representative wave approach which offers an ease of use and practicality. Define et al. (2009) performed a regression analysis and found that a reduction factor of 0.61 was appropriate in the estimation

E-mail addresses: chatchawin.s@psu.ac.th (C. Srisuwan), payom.r@psu.ac.th (P. Rattanamanee), winyu@siit.tu.ac.th (W. Rattanapitikon).

https://doi.org/10.1016/j.oceaneng.2020.107273

Received 8 December 2019; Received in revised form 28 February 2020; Accepted 17 March 2020

^{*} Corresponding author.

C. Srisuwan et al. Ocean Engineering 204 (2020) 107273

Nomenclature						
η	Instantaneous water surface level (L)					
γ^{δ}	Peak enhancement factor in JONSWAP					
	spectrum [–]					
ω	Wave angular frequency (T^{-1})					
$oldsymbol{\phi}_k$	Depth-dependency factor in TMA spectrum					
	[-]					
θ	Coefficient in parameterized wave spectrum [–]					
\vec{u}	Total flow velocity due both wave and current (LT^{-1})					
C	Wave celerity (LT ⁻¹)					
$C_{ m g}$	Wave group celerity (LT ⁻¹)					
$\stackrel{g}{D}$	Directional spreading function of wave					
	spectrum [–]					
E	Directional surface wave energy spectrum (L ² T)					
E_T	Total energy of surface water wave $(ML^2 T^{-2})$					
f	Wave frequency (T^{-1})					
f_H	High frequency cutoff (T ⁻¹)					
f_L	Low frequency cutoff (T^{-1})					
f_p	Peak wave frequency (T^{-1})					
F_x, F_y	Wave-induced mass flux in x or y direction					
•	$(ML^2 T^{-3})$					
F_{α}	Wave energy flux in α direction (ML ² T ⁻³⁾					
H	Surface wave height (L)					
h	Mean water depth (L)					
H_s	Significant wave height (L)					
H_{rms}	Root-mean-square height of random waves (L)					
k	Wave number (L^{-1})					
k_p	Wave number evaluated at peak wave frequency (L^{-1})					
L	Wave length (L)					
P	Total wave power density of the wave field $(ML^2 T^{-3})$					
R^2	Coefficient of determination [-]					
S_{η}	Nondirectional surface wave energy spectrum (L ² T)					
T	Energy period of the wave field (T)					
T_e u	Nondimensional parameter equal to					
u_L	$(\omega^2 h)/g$ [–] Nondimensional parameter u evaluated at					
	f_L [-]					
u_H	Nondimensional parameter u evaluated at f_H [–]					
BIAS	Slope of a linear line fitted through comparison between two datasets [–]					
Err.	Error in estimation as percentage of mean measured value (%)					
RMSD	Root-mean-square deviation as percentage					
	of mean measured value (%)					
Std.	Standard deviation of Err. as percentage of mean measured value (%)					

where the significant wave height and mean wave period were the nominal wave parameters. The adjustment may alternatively be achieved via an introduction of an adjusting sea state parameter derived from the zeroth and first negative moments of the frequency spectrum or the weighted average of the wave energy (e.g. Boronowski et al., 2010). Analyses based on field wave data, however, reveal that this conversion technique could lead to an underestimation of wave power by up to 18% since the wave power computed using the nominal wave does not match the actual energy spectrum in a random sea (Cahill and Lewis, 2014).

In the present study, the ultimate goal is to introduce a novel analytical formula for the estimation of wave power density. The derivation is first illustrated for the new solution which appears in closed form for practicality while considering incremental components of random wave energy similar to applying a numerical technique. Using reliable spectral wave data, the formula is verified and validated to assure its estimation capability, in comparison to the representative wave approach. An application of the new solution is subsequently demonstrated by estimating wave power potential along the coasts of Thailand. Beside the demonstration, an outlook of wave power potential can be obtained for feasible sites in the country where, to the authors' knowledge, no characterizing or mapping of the local wave power has ever been attempted before. Based on all of the results, conclusions of the study are finally drawn to summarize underlying principles, estimation performance, and practical utilities of the new formula.

2. Estimation of wave energy flux and wave power density

The underlining physics of surface water waves and associated energy are reviewed briefly here since there are implications for estimation of wave power density. Several techniques commonly used in the estimation are reviewed as later on they will be compared to the new formula developed in the present research effort.

2.1. Definition and monochromatic assumption

Surface water waves develop and grow as wind blows across a flat ocean surface. The displacement of the fluid mass against its vertical equilibrium results in gravitational potential energy. The oscillatory wave-induced pressure also causes a water particle to orbit and initiates kinetic energy under the waves. Fig. 1 illustrates a progressive wave with important parameters involved with its motion. According to the definition, the potential and kinetic wave energies can be combined to represent the total surface wave energy (e.g. Svendsen, 2006)

$$E_T = \frac{1}{2L} \left[\int_x^{x+L} \rho g(h+\eta)^2 \, dx \right] + \frac{1}{2L} \left[\int_x^{x+L} \int_{-h}^{\eta} \rho(u_x^2 + u_z^2) \, dz \, dx \right]$$
 (1)

in which u_x and u_z are the wave-induced velocities in the x and z components, respectively. The other symbols and coordinates are as defined in Fig. 1. The total amount of wave energy (E_T) here is a phase-averaged scalar per unit area since the integrals are evaluated over the wave for both the potential energy in the first term and the kinetic energy on the second term.

The rate at which the wave energy is transferred with the propagating wave is referred to as the wave energy flux or wave power. Through a vertical section, this rate is the quantity of work being done due to the presence of the wave which can be described following

$$F_{\alpha,t} = \int_{-h}^{\eta} \left[p + \rho g z + \frac{\rho}{2} (\vec{u} \cdot \vec{u}) \right] u_{\alpha} \, dz \, n_{\alpha} \tag{2}$$

where p is the wave-induced pressure; \vec{u} is the total flow velocity due to both wave and current; and u_{α} is the horizontal velocity in the direction of interest with n_{α} as its normal unit vector. These directional aspects imply that the resulting value of the flux F depends on the angle between wave propagation direction and a referenced frame such as a bathymetric contour or the coastline.

An appropriate choice of wave theory may be selected to describe the parameters involved in the exact expressions in Eqs. (1) and (2). If

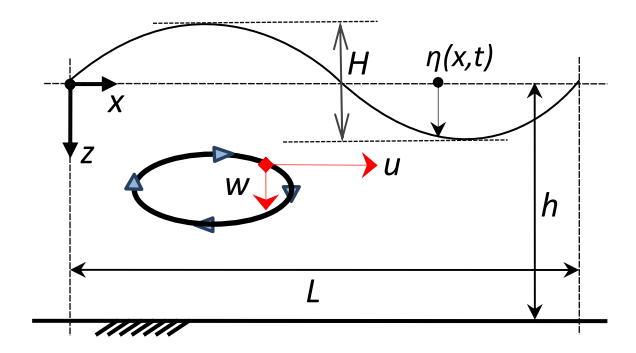


Fig. 1. Progressive wave and basic wave parameters associated with wave energy and power.

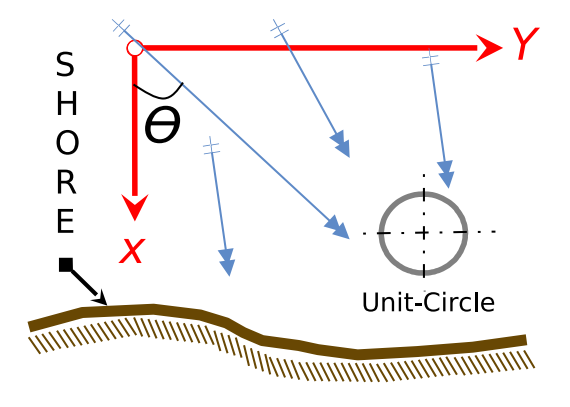


Fig. 2. Plan view of waves propagating towards the shoreline and the unit-circle power estimation concept.

the linear wave theory is adopted (e.g. Dean and Dalrymple, 1991), the integral terms that represent the potential and the kinetic wave energies can be evaluated to yield the total energy under a monochromatic wave

$$E_T = \frac{1}{8}\rho g H^2 \tag{3}$$

where H is the wave height and E_T is given per unit area of the sea surface. Note that some higher order terms are truncated in the linear wave theory such that the integration is limited only to the mean water level (z=0). Considering an x coordinate normal to the shoreline (see Fig. 2), the use of the linear wave theory can aid the evaluation of the energy flux to yield

$$F_x = E_T \cdot C_g \cos(\theta);$$
 and $F_y = E_T \cdot C_g \sin(\theta)$ (4)

in which F_x and F_y are the shore-normal and shore-parallel components of the energy flux, respectively. The group celerity C_g indicates the speed at which the energy is being transmitted, which is given as

$$C_g = \frac{C}{2} \left[1 + \frac{2kh}{\sinh(2kh)} \right] \tag{5}$$

where k is the wave number equal to $2\pi/L$. Each component of the energy flux given in Eq. (4) has the unit of watt per a unit meter of wave crest. The amount of the total power (P) available in the wave can therefore be represented by $P = \sqrt{F_x^2 + F_y^2}$. This quantity is often referred to as "wave power density" or "wave power potential" of the sea surface which is widely accepted as a standard parameter in the estimation of the wave energy resources all over the world (e.g. Pontes, 1998; Define et al., 2009; Mork et al., 2010).

2.2. Estimation of power density of random waves

An actual wave field in the ocean consists of random waves with different frequencies (f) and directions (θ). The linear wave theory can

still be applied to describe individual characteristics of all of the waves that contribute to the net available wave power. For example, by use of the concept of wave energy spectra, the shore-normal component of energy flux (F_x) given earlier for a monochromatic wave in Eq. (4) can be revised as

$$F_{x} = \rho g \int_{0}^{2\pi} \int_{0}^{\infty} E(f,\theta) C_{g}(f) \cos\theta \, d\theta \, df \tag{6}$$

where E is the directional wave energy spectrum; and C_g are now the frequency-dependent wave group celerities. The integrals in Eq. (6) are to be evaluated numerically over all possible wave frequencies f and directions θ . The evaluation result should be referred to as a spectral estimate of the parameter since dynamic wave parameters such as the orbital velocities are not considered directly. In wave measurement and analysis, however, it is always interpreted as a measured result due to a lack of means to quantify the energy flux directly.

The total available power in the wave field can still be computed as a scalar sum of energy fluxes of random waves in their propagation directions, i.e. resembling a sink of transmitted wave energy. The wave power density may therefore be redefined as the rate at which the wave energy is aggregated across a circular domain with unit length diameter (Jacobson et al., 2011). Note that wave power density holds the unit of watt per meter which is basically the width of a vertical plane bisecting the unit circle (see also Fig. 2).

In practice, the estimation of the wave power density can be achieved via two traditional methods. The first technique is to reproduce the spectral estimates based on available wave energy spectra ${\it E}$ which is represented by

$$E(f,\theta) = S_{\eta}(f) D(f,\theta) \tag{7}$$

where S_{η} is a non-directional energy spectrum, and $D(f,\theta)$ is a directional spreading function. Under the unit-circle concept, the wave power density can be obtained by integrating the energy fluxes over all possible wave directions assuming conservation of wave energy flux such that

$$\int_0^{2\pi} D(f,\theta) \, d\theta = 1 \tag{8}$$

which subsequently allows the expression of the total wave power density to follow

$$P = \rho g \int_0^\infty S_{\eta}(f) C_g(f) df \tag{9}$$

where $C_g(f)$ is the group celerity of an individual wave with frequency f. By use of this equation, within the limitations of linear wave theory, an accurate estimation of the wave power density can be achieved if the local wave energy spectra are made available. Many advanced techniques can be launched to serve to measure the wave spectra but wave power assessments will still be limited by spatial and temporal extents of the measurement. The wave spectra may also be attributed by both sea and swell, but the former which is locally generated is of primary interest when assessing surface wave energy.

Given the limitation in in-situ measurement of wave spectra, predictive or parameterized equations for the wave spectra may optionally be utilized for the provision of the required sea spectrum information. For fully-developed surface waves in deep water, Pierson and Moskowitz (1964) suggested that the distribution of energy with frequency could be described using the well-known Pierson–Moskowitz (PM) wave spectrum

$$S_{\eta}^{PM}(f) = \vartheta g^2 (2\pi)^{-4} f^{-5} \exp\left[-\frac{5}{4} \left(\frac{f}{f_p}\right)^{-4}\right]$$
 (10)

in which f_p represents the peak wave frequency, and ϑ is an empirical constant that controls the magnitude of the spectral wave energy. Since its introduction, the PM wave spectrum has gone through two major modifications. The first adjustment led to the JONSWAP wave spectrum (Hasselman et al., 1973), in which the fetch and duration

limits are considered in the formation of the spectrum. The effect of finite water depth on the wave field was later accounted for in the second modification (Bouws et al., 1985), resulting in the TMA spectrum that follows

$$S_{\eta}^{TMA}(f) = S_{\eta}^{PM} \gamma^{\delta} \phi_{k} \tag{11}$$

in which γ^δ is the peak enhancement factor imposed in the JONSWAP spectrum to account for the fetch and the duration. The factor ϕ_k which is introduced into the TMA spectrum to represent the water depth dependency can be expressed as

$$\phi_k(f,h) = \left[k(f,h)^{-3} \frac{\partial k(f,h)}{\partial f} \right] / \left[k(f,\infty)^{-3} \frac{\partial k(f,\infty)}{\partial f} \right]$$
 (12)

where k(h) and $k(\infty)$ are the wave numbers evaluated for the local water depth and deep water, respectively. Once parameterized, a wave spectrum can readily be employed for the estimation of wave power density following the integral expression in Eq. (9). This wave parameterization technique is applied not only for an explicit determination of wave spectra, but also for specification of input waves in many numerical models (e.g. Booij et al., 2004; Kirby et al., 2005).

The other common approach in the estimation of the wave power density is referred to as a representative wave approach in which some leading waves are used to represent the random wave field. For example, if the wave energy spectrum S_{η} is assumed to feature a narrowed-banded distribution, the total wave energy can be represented through the root-mean-squared wave height (H_{rms}) which subsequently allows the wave power density that follows

$$P = \frac{1}{8} \rho g H_{rms}^2 C_g(f_m) \tag{13}$$

in which C_g is the wave group celerity evaluated at the energy-weighted mean wave frequency (f_m) . Under deep water conditions, all of the waves will feature depth-independent phase speeds. This characteristic eliminates the effect of the water depth on the group celerity in the total wave power, allowing a revision of Eq. (13) to become

$$P = \frac{\rho g^2 H_s^2 T_e}{64\pi}$$
 (14)

in which H_s is the significant wave height approximately equal to $\sqrt{2}H_{rms}$; and T_e is given as the energy period of the wave field. By definition, T_e is the period of a monochromatic wave which features the same amount of wave energy as the random sea of interest (Iglesias and Carballo, 2011). It is often related to a spectral wave period, for example $T_e = \delta T_m$, where δ is an adjusting factor and T_m is the mean wave period. Based on wave spectra at 12 stations along the US coasts, Cahill and Lewis (2014) found that the value of δ could range from 1.21 to 1.38 when the average zero-crossing period was taken as the mean period T_m . This variation was reported to originate as a result of different site characteristics and prevailing wave conditions.

Both of the typical estimation techniques feature advantages and disadvantages. The spectral-based numerical method, while capable of providing accurate results, is often subject to limited availability of local spectral wave data. The method also does not permit a closed-form analytical solution for the estimation even with the parameterization of wave spectra. A straightforward and wider applicability can be found for the representative wave approach in which a simple explicit formula is allowed. This approach, however, may not sufficiently account for contributions from all individual waves in the field. Adjustment to the estimation result may be conducted, but this effort could be subjective since it does not always consider different site and wave climate conditions.

3. New analytical solution

Development of the new solution for estimation of wave power density based on the wave spectrum concept is described in this section. The keys in the problem formulation and the evaluation of the solution are illustrated for the first time below.

3.1. Problem formulation

The advantages of the representative wave approach and the spectral-based numerical integration are adopted in the determination of the new solution in this study. This consideration requires that the new solution be in closed analytical form which is more practical to use, while features a wide applicable range and offers improved estimation accuracy based on the random wave field. The governing equation here therefore follows the spectral-based expression of the wave power density, which can be redefined here for convenience as

$$P = \rho g \int_{f_L}^{f_H} S_{\eta}(f) C_g(f) df \tag{15}$$

in which f_L and f_H represent the lower bound and the upper bound of the applicable frequency range, respectively. To determine the wave power density P, an appropriate choice of the energy spectrum S_η has to be substituted into Eq. (15) for an evaluation. Here, the condition of interest is a fully-developed sea in arbitrary water depths, which is the most common scenario in the evaluation of potential wave power (e.g. Sierra et al., 2016). The distribution of wave energy with frequency in this case can be described by aids of the wave-spectrum parameterization technique following

$$S_{\eta}(f) = \vartheta g^{2} (2\pi)^{-4} f^{-5} \exp\left(-\frac{5}{4} \left(\frac{f}{f_{p}}\right)^{-4}\right) \cdot \phi_{k}(f, h)$$
 (16)

where ϕ_k is the depth-dependency factor given previously in Eq. (12); and θ is the only constant controlling the amount of the energy. Due to the limitation of water depth on surface wave generation, the factor ϕ_k will impose a decrease of the wave energy across the frequency domain before its value approaches unity under the deep water condition.

With the combination of the energy distribution, the depth dependency, and the wave celerity terms, Eq. (15) will be in a fairly complex form and must be reformulated in order for it to allow an analytical closed form solution for the wave power density. The first modification on the original expression is applied on the depth-dependency factor ϕ_k in which the wave number k can be described following the linear wave dispersion relation in the absence of mean current

$$k = \frac{\omega^2}{g \tanh(kh)} \tag{17}$$

which allows the factor ϕ_k to be rearranged into a new form that follows

$$\phi_k(f,h) = \left(\frac{\omega^5}{2g^2}\right) \left(k^{-3} \frac{\partial k}{\partial \omega}\right) \tag{18}$$

Despite this substitution, a complete evaluation of the factor ϕ_k is still not viable since the wave number k is not in an explicit form in the dispersion relation. A closed-form expression is therefore needed for k in Eq. (18) and the solution suggested by Eckart (1952) is used, which follows

$$k = \frac{u}{h\sqrt{\tanh u}} \tag{19}$$

where u is a non-dimensional factor equal to $(\omega^2 h)/g$. The validity of this expression is discussed in detail in the next section (Fig. 4). Initially, the maximum error between the exact values and the approximations of the wave number is found to be around 5% for intermediate water depth and is negligible in the shallow or deep water regime. Following this approximation, a rearrangement of the derivative term in Eq. (18) can be achieved to allow

$$\phi_k(f, h) = \tanh(u) + \frac{u}{2} \left[\tanh^2(u) - 1 \right]$$
 (20)

This new expression can then be inserted into Eq. (16) for the parameterization of the wave spectrum S_{η} which is one term in the estimation of the wave power density P in Eq. (15). The other term is the wave group celerity C_g or the speed at which the wave energy is being transferred. This factor can also be expressed in an explicit form by

use of Eckart's approximation in Eq. (19). These attempts will allow a new integral form of the wave power density, given with respect to the non-dimensional factor u as

$$P = A \int_{u_L}^{u_H} u^{-7/2} e^{-Bu^{-2}} \left[(\tanh u)^{3/2} + \frac{u}{2} \left((\tanh u)^{5/2} - (\tanh u)^{1/2} \right) \right] du$$
(21)

in which A and B are groups of constants from the original expressions of S_n and C_g , and from the transformation of df to du, which follow

$$A = \frac{\theta \rho g^{(5/2)} h^{(5/2)}}{4}; \quad \text{and} \quad B = \frac{5h^2}{4\omega_p^{-4} g^2}$$
 (22)

where ω_p is the peak angular wave frequency $(2\pi f_p)$, and the new integral limits u_L and u_H are the values of u at the low and the high frequency cutoffs, respectively. Note that the mean current is not considered in the formulation thus far as its effect should be rather insignificant far away from the shoreline where the wave power is of interest. Next, a closed-form analytical solution for the wave power density P can finally be obtained from the evaluation of Eq. (21).

3.2. Evaluation of analytical formula

The only task left now is to perform an integration on Eq. (21) which, however, is not trivial due to the nonlinear combination of the power, the exponential, and the hyperbolic tangent functions in the equation. To resolve this complexity, an asymptotic analysis will be applied and a nominal expression will be introduced to simplify the equation into an integrable format. This technique will be similar to that of Srisuwan et al. (2017) suggested for another set of waves parameters for different types of application.

The analysis is focused on the group of the hyperbolic tangent functions of which the resulting values are shown in Fig. 3. Over a wide range of the non-dimensional factor u, the following approximation can be made

$$(\tanh u)^{3/2} + \frac{u}{2} \left[(\tanh u)^{5/2} - (\tanh u)^{1/2} \right] \approx \frac{u}{2}, \quad \text{for } 0 < u \le u_*$$
 (23)

and

$$(\tanh u)^{3/2} + \frac{u}{2} \left[(\tanh u)^{5/2} - (\tanh u)^{1/2} \right] \approx 1, \quad \text{for} \quad u > u_*$$
 (24)

where u_* is the threshold value at which the behavior of the function appears to change, which is clearly observed at u=2.0 here. These asymptotes for the tanh terms can be substituted into Eq. (21) so that the expression of the wave power density is separated into two integral terms following

$$P = A \left[\frac{1}{2} \int_{u_I}^{u_*} u^{-5/2} e^{-Bu^{-2}} du + \int_{u_*}^{u_H} u^{-7/2} e^{-Bu^{-2}} du \right]$$
 (25)

These terms can be rearranged for partial integration with substitution of parameters. An aid of special functions is also required to express the definite integrals that involve a nonlinear combination of the power function of u and the exponential function $\exp\left[f(u)\right]$. Non-elementary gamma functions can be applied for the purpose here, of which the definitions are given following

$$\Gamma(\lambda, \beta) = \int_0^\beta e^{-u} u^{(\lambda - 1)} du \tag{26}$$

and

$$\tilde{\Gamma}(\lambda,\beta) = \int_{0}^{\infty} e^{-u} u^{(\lambda-1)} du \tag{27}$$

where Γ and $\tilde{\Gamma}$ are respectively the lower and the upper incomplete gamma functions distinguished by their integral limits. In the present problem with certain integral limits among u_L , u^* , and u_H , a pair of these gamma functions can be employed on each of the integral terms.

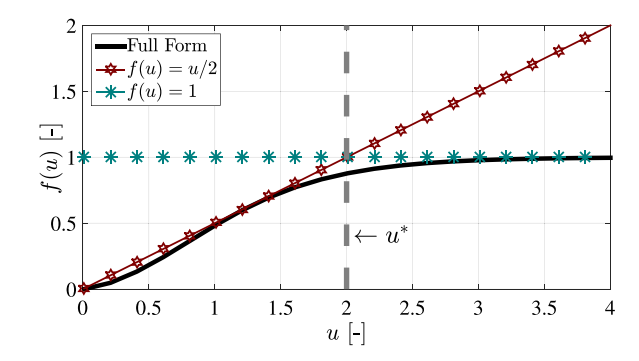


Fig. 3. Exact values from the full hyperbolic term compared to approximates allowed by asymptotic formulas employed in the new formula derivation.

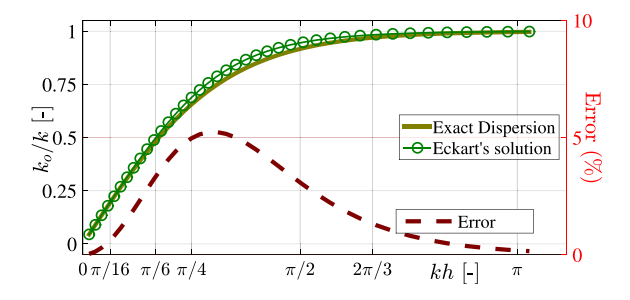


Fig. 4. Comparison between exact and approximation solutions of dispersion relation. Error is shown in percent respect to the right axis.

With all the preparations and the use of these special functions, Eq. (25) can be evaluated to yield

$$P = \frac{A}{4} \left[\frac{\sqrt{u_H} \exp\left(\frac{-B}{u_*^2}\right) - \sqrt{u_*} \exp\left(\frac{-B}{u_H^2}\right)}{B\sqrt{u_* u_H}} + \frac{\Gamma\left(\frac{3}{4}, \frac{B}{u_L^2}\right) - \Gamma\left(\frac{3}{4}, \frac{B}{u_*^2}\right)}{B^{(3/4)}} + \frac{\Gamma\left(\frac{1}{4}, \frac{B}{u_*^2}\right) - \Gamma\left(\frac{1}{4}, \frac{B}{u_H^2}\right)}{2B^{(5/4)}} \right]$$
(28)

which is a new closed-form, analytical equation for estimation of the wave power density. This full solution can be simplified into a more compact expression if all of the waves in the entire spectrum are considered. In this case, the lower and upper bounds u_L and u_H will respectively shift to 0 and ∞ , allowing the alternative formula that follows

$$P = A \left[\frac{-\exp(-B/4)}{4B\sqrt{2}} + \frac{\tilde{\Gamma}(3/4, B/4)}{4B^{(3/4)}} + \frac{\Gamma(1/4, B/4)}{8B^{(5/4)}} \right]$$
(29)

in which the constant value of u^* is already substituted into the equation. The newly-introduced formulas in Eqs. (28) and (29) here can be executed in any programs that include gamma functions which are very common in most scientific computing environments. It is worthwhile to recall that these formulas were achieved via use of a 1-D non-directional parameterized wave spectrum and a few simplifications based on linear wave theory. In the next sections, these adopted techniques will be verified and the new formulas will be validated against various sets of reliable wave data.

4. Verification of the new formula

The derivation of the new analytical formula introduced above involves a few assumptions and approximations. In this section, their

implications are investigated focusing on behaviors of a few important terms and the final solution. First of all, the approximate wave dispersion relation in Eq. (19) needs to be investigated as it is applied throughout the formulation. Fig. 4 illustrates a non-dimensional wave number $k_{\rm o}/k$ as a function of the relative water depth (kh), comparing the values yielded by the approximation and the full dispersion relation. The comparison shows a small maximum error of around 5%. Therefore, any direct use of the approximate expression for determining wave number should be acceptable, provided that eventual impact on the final result is also examined.

In the formulation of the new solution, the approximate dispersion relation is applied specifically on the hyperbolic tangent (tanh(u)) and the wave celerity (C_{σ}) . Possible influences from such modified terms may be best investigated based on the resulting wave power from several estimation options shown in Fig. 5a. The magnitudes of wave power allowed by the exact solution is adopted as a basis and the percent differences from the other alternatives are illustrated in Fig. 5b. For a sole inclusion of the approximated wave group celerity (C_p) , an underestimation of the wave power of up to 30% is found where the relative water depth $k_p h$ is equal to $\pi/4$ before it diminishes to zero as the value of $k_n h$ approaches 2π . The asymptotic form of tanh, meanwhile, leads to around 25% overestimation of the wave power in shallow water which then plummets to zero in deep water. Beyond the upper-intermediate water limit $(k_n > \pi/4)$, the magnitudes of wave power yielded by the new solution are only associated with some errors smaller than 5%. Whereas, the use of representative wave approach results in around 15 to 25% overestimation of the wave power.

The comparisons made in Fig. 5 may lead to two initial findings. One is that the new solution does not perform well in shallow water as the possible error can be excessive. The other conclusion is on the superiority of the new analytical formula over the traditional representative wave approach. To reassure its performance and applicability, the new solution in complete form is tested again by use of up to 26,000 synthetic wave spectra, each specified with a different combination of peak wave period (T_p) and water depth (h). One focus here is therefore to investigate the dependencies of the estimation accuracy and precision on the most influential factor which is the relative water depth (k_ph) .

Fig. 6 illustrates the relative density or the percentage of cases found according to the computed errors on P for many ranges of k_p . In each case, the results from the new analytical formula are compared to those of the representative wave approach, both evaluated against the exact values of P allowed by the numerical solution. In the upper range of $k_p h > 5\pi/4$, the new solution tends to lead to a fairly normal distribution of the tests of which the errors are between 25% to -25%, implying overestimation and underestimation respectively. Meanwhile, the result allowed by the representative wave approach appears to dislocate somewhat to the overestimation part, implying that the representative wave approach overestimates the wave power by 10 to 15% on average.

In the next lower range of $\pi/3 < k_p h < 3\pi/4$, the new solution results in a more peaky distribution of the number of tests over the computed errors with a small underestimation bias of around 5 to 10%. These overall results agree with the fact that the new solution is based on a more flexible parameterized spectrum which can better constitute the distribution as opposed to the representative approach which relies only on a fixed narrow-banned spectral model.

Fig. 7 shows a comparison between the root-mean square deviation (RMSD) of the results from the new solution and the representative approach, both evaluated against the numerical solution results. Except only when $k_p h$ is smaller than $\pi/4$, the RMSD of the new solution always shows a lower value. The percent difference is found to be 3 to 10% for the range of $\pi/4 < k_p h < 3\pi/4$. Toward the deep water regime, this number tends to become a constant of around 7 to 8%.

To summarize, a certain applicable condition of the new solution should be specified to be where $k_p h > \pi/4$. This limit simply covers

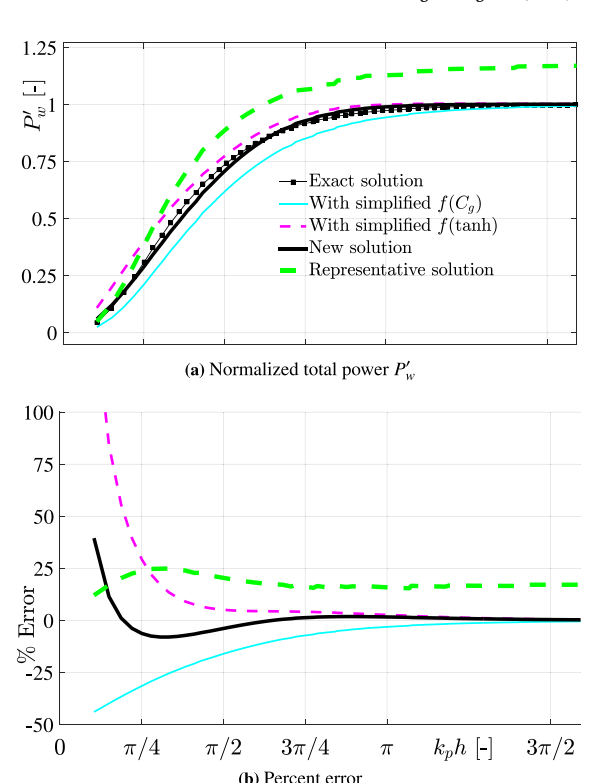


Fig. 5. Comparison on values of wave power estimated using different solutions and simplifications.

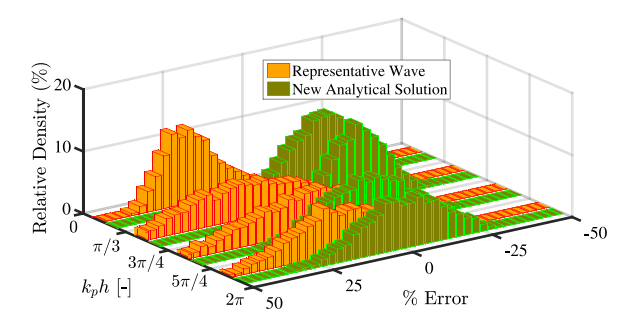


Fig. 6. Relative density of evaluation results on wave power P based on 26,000 synthetic tests given as functions of estimation errors and ranges of the relative water depth $k_c h$.

upper-intermediate to deep water environment, according to Dean and Dalrymple (1991) who defined the thresholds of shallow-water and deep-water waves to be at $kh < \pi/10$ and $kh > \pi$, respectively. In other words, the new solution should not be used wherever the depth is below the lower intermediate limit ($k_ph < \pi/4$). This prohibition should be especially strict for shallower water environment ($k_ph < \pi/10$). In practical, the new formula will offer very low estimation performance in such a range. More importantly, its formulation based on linear wave theory was not intended for describing shallow-water waves.

5. Validation

In the previous section, the new solution and associated terms are verified analytically and against synthetic data to explore its capability and applicable range. Here, the formula is to be validated using measured wave data from two reliable sources which will help disclose its performance and sensitivity under actual uncertainty and randomness of the wave field.

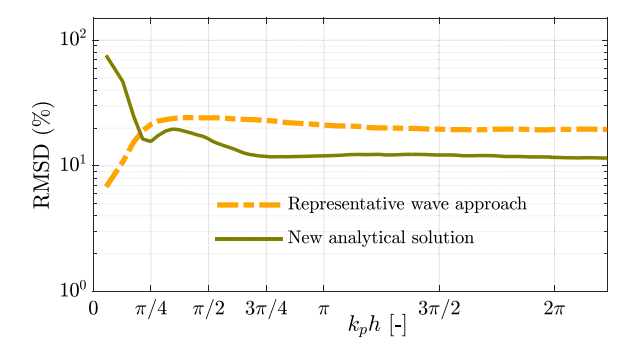


Fig. 7. Root-mean-square deviation (RMSD) found in the synthetic tests on the two different techniques given as a function of relative water depth $k_p h$.

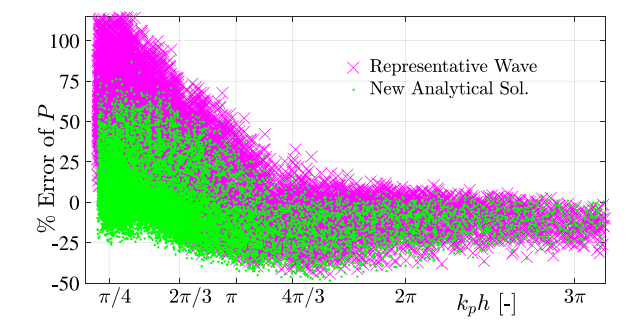


Fig. 8. Estimation errors of wave power as a function of relative water depth $k_p h$ in the validation of the two techniques against in-situ wave buoy data.

5.1. Nearshore wave buoy data

The first dataset utilized here was acquired by a surface-following wave buoy deployed at a site near the Savannah River in the State of Georgia, USA. This data collection offers more than 16,000 hourly records of spectral waves in a mean water depth of 13.6 m and a tidal range of 1.7 m, covering a wide variety of wave conditions for the proposed validation here. Regarding reliability, the data were also verified by 2.5-month coincident records from a collocated acoustic Doppler current profiler (ADCP). The full description and detailed analysis of the dataset can be found in Work (2008).

The data preparation here included a separation of sea and swell components in the original wave spectra which was necessary since the new solution was primarily developed to describe the local wind-induced waves or the sea. This first step was achieved using the technique outlined by Work and Srisuwan (2010), in which the separation frequency between sea and swell is identified based on the maximum sea steepness. Only the wave energy in the sea frequency band is considered as it is the primary target in the wave power estimation. The instantaneous water depths at the site, not available from the measurement but included in the new solution, were simulated using a tidal harmonic analyzing tool developed by Pawlowicz et al. (2002). Simulated depths were compared to available depth data from the ADCP and the difference between the two time series was found to be smaller than ±5%.

In a strict theory, the wave power reanalyzed from the available wave energy spectra should be referred to as the best estimate of P which is adopted as a basis in evaluating the results yielded by the new solution and the representative approach. In the use of the new solution, the only adjustable coefficient in the formula (θ) was specified such that the total wave energy was conserved. The estimation errors induced by each of the two techniques are illustrated in Fig. 8. Throughout the comparison, the new solution shows up to be the more accurate and more precise tool for the estimation compared to the representative wave approach.

The superiority of the new solution can be confirmed considering the statistical numbers summarized in Table 1, including the R-squared values, the mean percent errors, and the standard deviations found in each range of $k_p h$. In the table, the percent errors produced in the new solution are between 12 to -14% while the same type of numbers from the representative approach spread over 57 to -17%. At the lower limit of $k_p h < \pi/4$, the new solution may not be associated with excessive errors but it is still unrecommended for any application within this range, according to the underlying theory in the formulation and behaviors of the important terms discussed earlier in the verification.

The relative water depth $k_p h$ has been proven thus far to be highly influential to the performance of the new solution, but it could be possible that some other factors may play a vital role. The main focus here is on sensitive factors in the random wave spectra as any estimation techniques need to rely on them in some aspects. To investigate the sensitivity, the new solution is tested against two spectral factors which indicate the steepness and the energy-frequency spread in the wave spectrum. The former is referred to straight forwardly as the spectral steepness factor, representing an overall condition of the random wave field via

$$S_p = 2\pi^2 \left(\frac{H_{m0}}{gT_p^2}\right) \tag{30}$$

where H_{m0} and T_p are the spectral-based significant wave height and the peak wave period, respectively. This relationship may be interpreted more easily as a form of wave height to wave length ratio or a non-dimensional steepness of the wave field. The other indicator of interest is proposed for the quantifying the distribution of wave energy over the frequency bands, or simply the spectral width of the sea. Longuet-Higgins (1975) suggested that this physical characteristic can be measured using a single parameter ν which follows

$$v = \left(\frac{M_0 M_2}{M_z^2} - 1\right)^{1/2} \tag{31}$$

in which M_n is the nth moment of the random wave spectrum. A greater value of ν implies a wider frequency coverage or a broader distribution of wave energy. Values of ν between 0.3 to 0.5 are common for most wind-induced seas, including wave spectra parameterized using the TMA or the JONSWAP technique (e.g. Soares and Carvalho, 2003).

The deviation in the estimation results due to the steepness factor S_n is shown in Fig. 9a where both types of the estimates produce certain errors in a concave-up pattern over the values of the factor. The errors are greater for very small and very large values of S_p in which the tested wave spectra are believed to be somewhat irregular compared to a parameterized spectrum or a narrow-banded wave model. For example, the spectral shape can be more positively skewed in the case where waves with lower frequencies are dominant and such long period waves can cause the steepness to be very small. The influence on the spectral width of the wave field ν is examined in Fig. 9b. As the values of ν increase to around 0.3, both sets of the estimation errors rise at very similar rates from around 5% to 20% with those of the new solution being the lower group. Beyond that limit, the representative approach clearly becomes the less reliable method while the performance of the new solution improves significantly. It should not be surprising that the representative wave technique provides very poor results as it assumes a narrow-banded wave field.

Major findings from the validation using this wave buoy dataset can lead to a few conclusions. First, the best applicable range of the new solution previously specified to be where $k_p h > \pi/4$ could be reconfirmed. The solution might not fail in the test here with $k_p h < \pi/4$, but it is still not recommended for application due to a reliability reason. While the new formula is clearly most sensitive to $k_p h$, the spectral steepness factor (S_p) and the spectral width factor (v) may also be related to the solution performance. For both factors, the relations are fairly straightforward since the new solution performance will

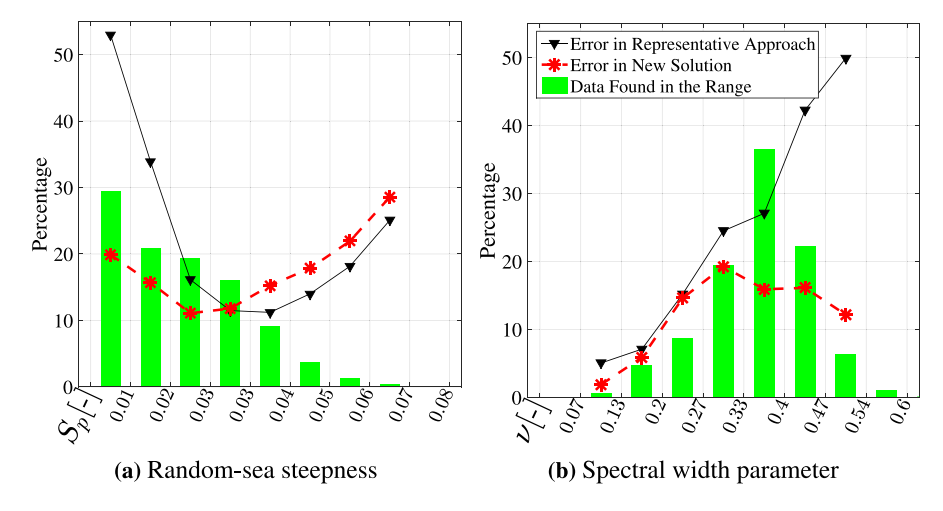


Fig. 9. Variations of the estimation errors found in the sensitivity tests based on two influential spectral factors. Both of the error and the data found in each range are presented in percentage respect to the vertical axis.

Table 1 Statistical factors computed per values of total wave power P yielded by the two different techniques based on data from the nearshore wave buoy. R^2 is the coefficient of determination, Err is the mean error in percent, Std is the standard deviation of error as percentage of the mean.

Analyzing technique:	Represe	ntative way	ve	New analytical solution		
Range ↓ / Factor →	R^2 [-]	Err. (%)	Std. (%)	R ² [-]	Err. (%)	Std. (%)
$0 < k_p h \le \pi/4$	0.58	57.74	24.74	0.91	12.68	17.49
$\pi/4 < k_p h \le \pi/2$	0.84	43.70	24.30	0.98	10.43	17.88
$\pi/2 < k_p h \le 3\pi/4$	0.97	17.36	22.41	0.96	2.28	19.30
$3\pi/4 < k_p h \le 3\pi/2$	0.91	-0.83	20.81	0.79	-10.42	18.59
$3\pi/2 < k_p h \le 3\pi$	0.78	-10.17	10.60	0.63	-14.20	10.29
$k_p h > 3\pi$	0.83	-17.34	7.29	0.89	-12.15	7.11

enhance if the two factors are within their common ranges specified in the model parameterized spectra. This reliance gives the new solution some flexibility in the estimation and it is the main explanation to its superiority over the representative wave approach.

5.2. NOAA wave buoys

To ensure its performance under wider field conditions, the new analytical solution is verified again here using wave energy spectra measured at eight locations along the US Atlantic Coast and the Gulf of Mexico. The data were achieved through a measurement campaign consisting of a network of wave buoys operated by the National Data Buoy Center (NDBC) of the US National Oceanic and Atmospheric Administration (NOAA). Initial details including specific positions of the measurement stations can be found in Table 2. About 7,000 hourly wave spectra recorded at each site were employed for the validation here.

The best estimates of wave power were first analyzed from the measured wave spectra using the exact integral method. The overall results can be separated into two sets for two groups of stations. The first includes those from Stations 1 to 4 which also feature waves in most intermediate water depths. The other set covers those from Stations 5 to 8 in which the waves were in the upper-intermediate water depth and beyond (See also Table 2 for ranges of $k_p h$). An example for the result from the first group is illustrated in Fig. 10a. The bias found may be noticed based on the linear straight line fitted through the comparison, which would feature a one-to-one slope for equality. In this case, the new solution appears to be the more accurate and more precise tool as the results are associated with a smaller degree of overestimation and also less scattered.

For the deeper stations (No.5–8), an example from the estimation of the wave power is illustrated in Fig. 10b. The results show that both of the representative wave and the new formulas seem to improve and provide the estimates which are more accurate and more precise than previously allowed for the shallower site in Fig. 10a. Still, the new analytical solution appears to be the superior option as its scattering is much narrower and the estimation bias is hardly noticeable. To provide a quantitative comparison, three statistical factors based on all of the results are considered including the mean absolute error, the estimation bias slope, and the standard deviation of the errors in terms of percentage of the mean. The differences between these factors from the representative wave approach and the new solution are computed and illustrated in Table 2.

The indicators presented in Table 2 can lead to a very clear conclusion for the gap between the capabilities of the two approaches. Considering the overall investigation, the mean error, the bias, and the standard deviation from the results from the new solution, are respectively about 0.13 to 0.18, 13 to 17%, and 2.3 to 6.6% lower than those of the representative wave approach. Regarding the applicable range, the new solution can be proved to deliver satisfactory estimates in any conditions in the validation here, but to adhere to the previous theoretical verification, the formula should be preserved for use at the relative water depth $k_p h > \pi/4$, or the upper-intermediate water depth and beyond. In all of the validation attempts, the findings are rather positive for the capability of the new analytical formula which should now be confident for practical use at any sites under the specified conditions.

6. Practical application

The new formula is employed for practical use here for the estimation of wave power in the coastal ocean of Thailand. The attempt was achieved at 16 locations in the Gulf of Thailand and the Andaman Sea, respectively on the east and the west of the nation's coastal ocean as shown in Fig. 11. Specific details including depths and coordinates of the locations can be found in Table 3.

The estimation was started by first modeling wind direction and speed over the entire region during May 2017 to April 2018 using the Weather Research and Forecasting (WRF) model (Skamarock et al., 2008). With available geographical information of the coastal ocean, the wind data were passed over to the third generation Simulating WAves Nearshore (SWAN) model (SWAN Team, 2011). The final simulation output was in the form of local wave energy spectra which can be processed further for important wave parameters including wave energy and power. It is worth noting that the new formula was

Table 2
Information of NDBC stations and statistical indicators found in the validation of the new analytical formula. Note that positive differences (Δ) indicate smaller values found in the new solution.

No.	Site specifi	ication		Statistical results			
	Sta. ID.	Position	h (m)	k _p h [-]	Δ BIAS [−]	△ Error (%)	△ Std. (%)
1.	41004	32.50N, 79.10W	38.4	0.90-30.6	0.13	14.44	2.29
2.	41008	31.40N, 80.87W	19.5	0.52 - 15.5	0.17	16.82	6.54
3.	41009	28.52N, 80.19W	40.5	0.85 - 32.3	0.13	14.62	3.55
4.	41013	33.44N, 77.74W	23.5	0.68 - 18.7	0.16	13.83	3.18
5.	41025	35.01N, 75.40W	68.3	1.53-49.6	0.18	16.90	3.27
6.	42019	27.91N, 95.35W	82.2	2.84-59.8	0.16	15.83	2.70
7.	42020	26.97N, 96.69W	79.9	2.76-52.7	0.17	16.14	2.56
8.	42036	28.50N, 84.52W	50.6	2.07-36.8	0.15	14.57	2.94

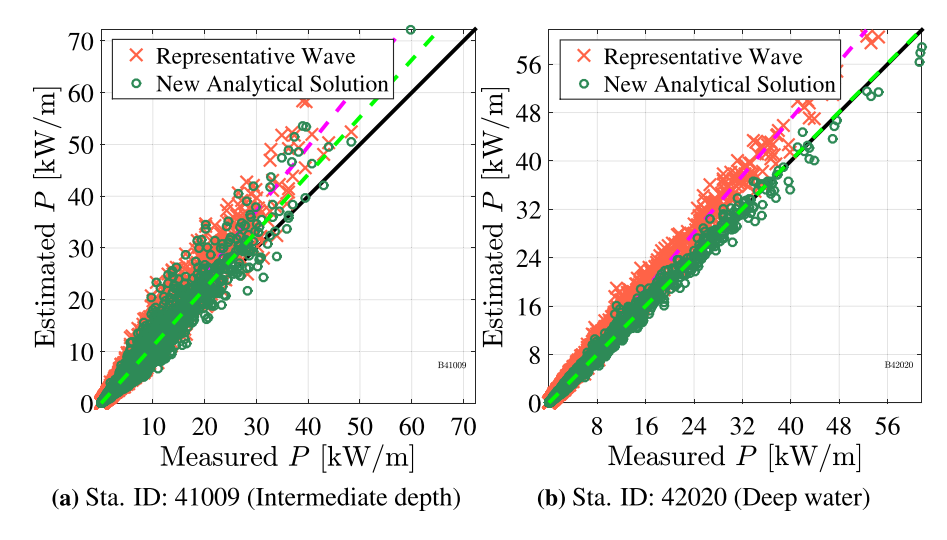


Fig. 10. Comparison between resulting values of total wave power *P* estimated using the two different techniques. The horizontal axes show values numerically integrated from measured random wave spectra. Summary on the comparison based on all of the datasets may be found in Table 2.

derived assuming fully-developed conditions which may not necessarily be the case in the SWAN model. Nevertheless, wave spectra in the monsoon seasons are considered here and they should approach a fully-developed stage as the model was implemented under strong and continuous winds. The improvement in the estimation allowed by the new formula will be proved to hold for any possible immaturity of the wave field.

All of the wave energy spectra obtained were initially evaluated to narrow down the focus on spatial coverage and temporal variation of the problem. This attempt leads to a very important guideline that any quest for wave power in the coastal ocean of Thailand should consider only waves under two regional monsoons as the in- and out-of-the season wave power ratios are about 7:2 on average. The coastal areas in the eastern Thai Gulf and on the Andaman coast, which feature some large fetches on their west, are exposed to the southwest monsoon initiated in the Indian ocean during June to October. The other part along Thai Gulf features a wide and long fetch on the east and will experience much larger waves under the northeast monsoon during November to April. Apart from offering higher wave power, the occurrence of monsoon waves and their principal directions are also more predictable which would accommodate any further study on power harvesting schemes and related techniques.

An example of magnitudes and variations of 24-hr moving average wave power in the study is shown in Fig. 12a for Location A, or Narathiwas, which is furthest south of Thai Gulf. During the regional northeast monsoon, the averaged power is shown to be as high as 5 kW/m but it is also fluctuating greatly over the season. The estimates in comparison were produced from the three different techniques which are the representative wave approach, the numerical integration, and the new analytical solution. Considering the numerically integrated power as exact results, the estimation errors induced by the other

two techniques are illustrated in Fig. 12b. Initially, the errors tend to decrease as the relative water depth $k_p h$ increases, agreeing with findings from all the previous tests with synthetic and measured data.

For the lower end of $k_ph < 2\pi$ here, the new solution is associated with around $\pm 15\%$ inaccuracy while those of the representative approach are in a range of 0 to 30%. Although both of these ranges decrease in the upper part of k_ph , it is observed that only the errors from the new solution are symmetric about the zero-error line, while the representative approach is always involved with overestimation. Such a difference can bring a significant outcome when applying each technique in the study of wave energy and power. Any estimation bias must certainly be taken care of, but such a symmetric deviation as offered by the new solution can still allow a neutral mean power over a duration, thus providing an accurate estimate of the local wave power density. Generally, this specific quantification is the first principal task in any evaluation of wave power potential.

Average wave power potentials found at all of the locations during their monsoon periods are summarized in Fig. 13. These seasonalaveraged values appear to be relatively low, ranging from 0.3 to 1.5 kW/m, as opposed to the maximum daily average which could be as high as 10 kW/m. Initially, this fact implies that the standard deviations of the power can be multiple times of such average values. Beside the temporal fluctuation, the power magnitudes also differ greatly among the locations. The southern Thai Gulf is the region that features the greatest spatial variation of the wave power potential, combining the most promising spot at Location E and a few very low potential sites such as Locations B and C. Most of the locations in the Eastern Thai Gulf do not offer any impressive magnitude of the potential with the zonal maximum found to be slightly lower than 0.7 kW/m. The sites in the Andaman Sea may not seem to offer much greater potentials but the resulting mean values between 0.6 to 1.0 kW/m can be considerable and are also the most invariant numbers in a particular coastal zone.

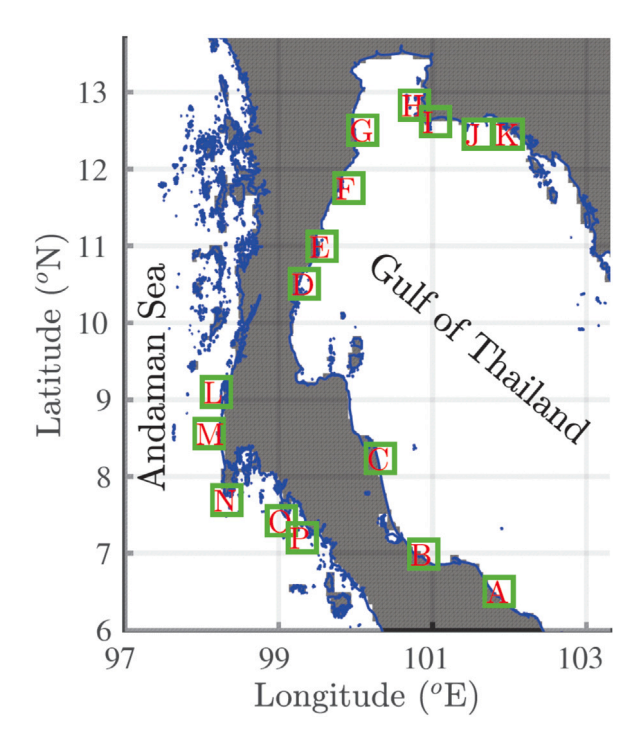


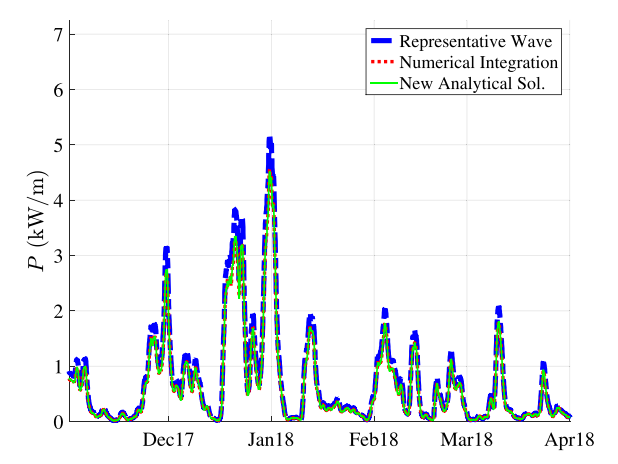
Fig. 11. Locations along the coastline of Thailand where the potential wave power is evaluated. Specific details including coordinates, depths, and the ranking of power potentials can be found in Table 3.

The actual final amount of wave power which can be harvested at a site is somewhat challenging to be estimated, as it is dependent primarily on allowable space and available technology. Feasibility studies of wave power projects have been attempted worldwide with some findings report that 20 kW/m of annual median power is the threshold for them to be commercially viable (Kofoed et al., 2006; Antonio, 2010). Such a number can however be subjective and highly varying since the local demand of power is a crucial factor and the cost associated with the power production drops sharply with time. In terms of usage in the present scenario here, the waves existing over a meter of the sea should be capable to power around 2–3 households with average electricity consumption, assuming a 50% power conversion efficiency.

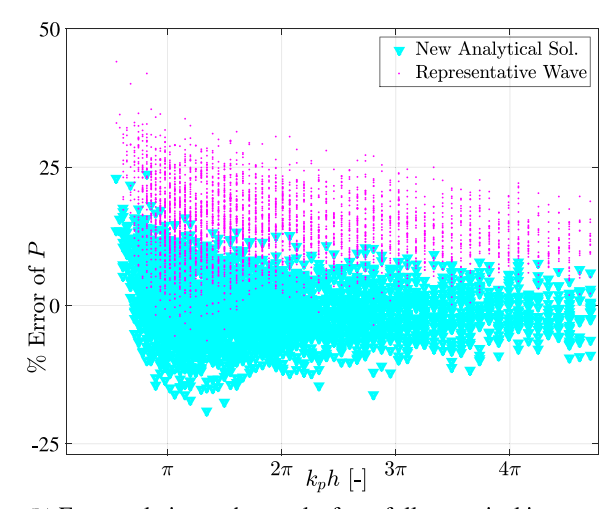
For the main purpose here on the application of the new solution, the magnitudes of wave power potential yielded by the three available methods are compared in Fig. 13. The comparison result shows that the representative wave approach tends to provide around 10 to 15% higher estimates than the other two techniques. The estimation results allowed by the new analytical solution almost match with those of the numerical integration at every location investigated. This encouraging outcome is achieved as a consequence of the estimation with symmetrical biases, from which a neutral mean can be determined. For the specific purpose here in determining the wave power potential, the performances of the new analytical solution and the numerical technique should therefore be considered to be closely comparable as they both provide almost identical results.

7. Conclusion and discussion

Ocean waves have recently been introduced as a promising source of alternative energy considering their abundance and reliability. For the estimation of wave power, two traditional methods are often applied including a full wave spectrum integration and a representative wave approach based on some nominal wave parameters. These two options are rather different in terms of implementation as the former relies



(a) 24-hr moving average wave power during northwest monsoon



(b) Errors relative to the results from full numerical integration

Fig. 12. Evaluation on the magnitudes of wave power at Location "A" (Narathiwas) and estimated errors from the two different techniques.

Table 3Information of 16 locations in the coastal ocean of Thailand considered for practical application of the new formula. The suitability rank is based on magnitude of evaluated wave power.

Location		°N	°E	h (m)	Suitability rank
#	Land area				
Α	NARATHIWAS	6.50	101.85	14.4	9th
В	SONGKHLA	6.96	100.82	9.1	14th
C	NAKORNSRI	8.28	100.27	6.13	15th
D	CHUMPON	10.50	99.26	17.4	3rd
E	PRACHUB(1)	11.04	99.50	19.9	1st
F	PRACHUB(2)	11.80	99.90	22.3	4th
G	PRACHUB(3)	12.54	100.04	17.7	11th
Н	PATTAYA	12.867	100.84	22.	13th
I	RAYONG(1)	12.62	100.99	9.7	16th
J	RAYONG(2)	12.49	101.58	19.9	6th
K	CHANBURI	12.49	101.95	8.9	12th
L	PHANGHA(1)	9.10	98.15	16.9	8th
M	PHANGHA(2)	8.57	98.15	41.4	2nd
N	PHUKET	7.71	98.29	39.2	5th
0	KRABI	7.46	98.99	28.3	7th
P	TRANG	7.24	99.28	16.2	10th

on a numerical technique while the latter offers a simple closed-form analytical solution. The present research work is aimed at introducing

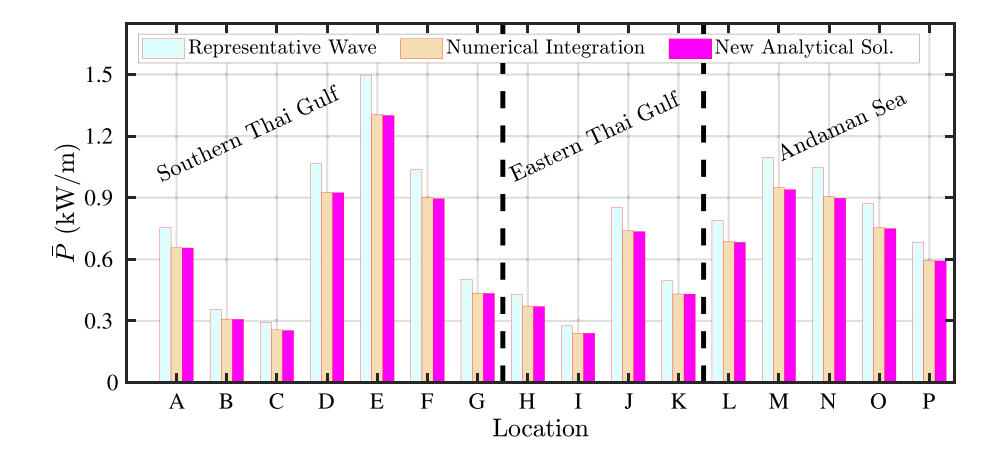


Fig. 13. Average wave power potential found during the monsoon season of each of the locations. The southern Thai Gulf is evaluated under the northwest monsoon from Nov 2017 to Apr 2018; the other two zones are evaluated under the southeast monsoon from Jun 2017 to Sep 2017.

a new formula for the estimation of total wave power that allows an accuracy and precision comparable to that of the numerical method but appears in a practical form of analytical solution.

The new solution was first verified by investigating all of the steps involved in its formulation. Besides, a large set of synthetic wave spectra based on up to 26,000 realizations were applied to evaluate the new formula under different conditions of random waves. In comparison to the representative wave approach, the synthetic test proves that the new solution can offer greater estimation accuracy and precision in the upper-intermediate to deep water condition over which the relative water depth factor $k_p h$ is greater than $\pi/4$. Therefore, this specific range of water depth is defined as the recommended applicable condition for the new formula.

The new formula was also validated using two reliable sources of field wave spectra. An investigation using available data from a nearshore wave buoy demonstrated that the new solution can estimate the total wave power within about $\pm 12\%$ errors while the representative wave approach can produce up to 40% errors. The second validation of new formula employed eight independent sets of wave energy spectra recorded by the National Data Buoy Center (NDBC) along the US Atlantic Coast and the Gulf of Mexico. In this case, the superior of the new formula to the representative wave approach can be confirmed once again based on the offsets in the mean estimation errors and the standard deviations of around 15% and 3%, respectively.

The new formula was demonstrated for practical use in the estimation of wave power in the coastal sea of Thailand. For the main purpose in this study, hourly estimates of wave power from the representative wave approach, the numerical integration, and the new analytical solution were compared at 16 target locations. In general, the new solution was found to produce around $\pm 15\%$ errors while the representative approach was associated with errors in a range of 0 to 30%. Both of such error ranges were found to be narrower in deeper water which are in accordance with the other findings based on synthetic and available measured wave spectra.

The applicability and the performance of the new solution were proven through a comparison among wave power potentials allowed by the three available methods. The outcome was very encouraging as the estimations allowed by the new analytical solution and the numerical integration were almost identical. Meanwhile, the representative approach tended to yield around 10 to 15% higher estimates. This favorable result is achievable as the new solution is involved with limited and symmetrical estimation biases which can be averaged out in the computation of the mean. Such a neutral deviation can always lead to a precise estimate of the mean wave power potential which is a primary indicator in any evaluation of wave power resources.

The new analytical formula developed in this study should be able to serve as an effective tool in the estimation of total power of surface waves in the ocean. Beside a much-required means in wave power resource assessment, this type of solution can also be incorporated in a module of wave power estimation as input or computing parameters in any wave modeling system. The new body of knowledge achieved in this study is expected to be extended in two promising directions. One is on the improvement of the new formula, focusing on enhancing its applicable range and estimation performance. The other is on a very widely-open topic which is the assessment of wave power potential of Thailand and perhaps the entire Southeast Asia.

Declaration of competing interest

The authors declare that they have no known competing financial interests or personal relationships that could have appeared to influence the work reported in this paper.

CRediT authorship contribution statement

Chatchawin Srisuwan: Conceptualization, Methodology, Formal analysis, Validation, Writing - original draft, Writing - review & editing. Payom Rattanamanee: Resources, Investigation, Project administration. Winyu Rattanapitikon: Writing - review & editing, Supervision, Funding acquisition.

Acknowledgments

This research project was supported by the Thailand Research Fund (TRF) and the Office of the Higher Education Commission (OHEC), Thailand as part of the research contract number MRG6180102. The authors are gratified by the kind assistance from all senior scholars and supporting staffs at the TRF and the OHEC agencies.

References

Antonio, F.d.O., 2010. Wave energy utilization: A review of the technologies. Renew. Sustain. Energy Rev. 14 (3), 899–918.

Arinaga, R.A., Cheung, K.F., 2012. Atlas of global wave energy from 10 years of reanalysis and hindcast data. Renew. Energy 39 (1), 49-64.

Booij, N., Haagsma, L., Kieftenburg, A., Ris, R., Van Der Westhuysen, A., Zijlema, M., 2004. SWAN Cycle III Version 40.41 User Manual. Technical Report, Delft University of Technology, p. 115.

Boronowski, S., Wild, P., Rowe, A., van Kooten, G.C., 2010. Integration of wave power in Haida Gwaii. Renew. Energy 35 (11), 2415–2421.

Bouws, E., Gunther, H., Rosenthal, W., Vincent, C.L., 1985. Similarity of the wind wave spectrum in finite depth water 1. spectral form. J. Geophys. Res.- Oceans 90 (1), 975–986

Cahill, B., Lewis, T., 2014. Wave period ratios and the calculation of wave power. In: The 2nd Marine Energy Technology Symposium METS2014, WA, USA.

C. Srisuwan et al.

- Cornett, A.M., et al., 2008. A global wave energy resource assessment. In: The 18th International Offshore and Polar Engineering Conference. International Society of Offshore and Polar Engineers.
- Dean, R.G., Dalrymple, R.A., 1991. Water Wave Mechanics for Engineers and Scientists. In: Adv. Series on Ocean Eng., Vol. 2., World Scientific, Singapore.
- Defne, Z., Haas, K.A., Fritz, H.M., 2009. Wave power potential along the Atlantic coast of the Southeastern USA. Renew. Energy 34 (10), 2197–2205.
- Defne, Z., Haas, K.A., Fritz, H.M., 2011. Numerical modeling of tidal currents and the effects of power extraction on estuarine hydrodynamics along the Georgia coast, USA. Renew. Energy 36 (12), 3461–3471.
- Eckart, C., 1952. The propagation of gravity waves from deep to shallow water. In: Gravity Waves, Vol. 521. National Bureau of Standards Circular, pp. 165–173.
- Falnes, J., 2007. A review of wave-energy extraction. Mar. Struct. 20 (4), 185-201.
- Fernández, J., Salcedo-Sanz, S., Gutiérrez, P.A., Alexandre, E., Hervás-Martínez, C., 2015. Significant wave height and energy flux range forecast with machine learning classifiers. Eng. Appl. Artif. Intell. 43, 44–53.
- Gonçalves, M., Martinho, P., Soares, C., 2014. Wave energy conditions in the western french coast. Renew. Energy 62, 155–163.
- Hasselman, K., Barnett, T.P., Bouws, E., Carlson, D.E., Hasselmann, P., 1973. Measurements of wind-wave growth and swell decay during the Joint North Sea Wave Project (JONSWAP). Technical Report No. 12, Dt. Hydrogr. Z..
- Hughes, M.G., Heap, A.D., 2010. National-scale wave energy resource assessment for Australia. Renew. Energy 35 (8), 1783–1791.
- Iglesias, G., Carballo, R., 2011. Choosing the site for the first wave farm in a region: A case study in the Galician Southwest (Spain). Energy 36 (9), 5525–5531.
- Jacobson, P.T., Hagerman, G., Scott, G., 2011. Mapping and Assessment of the United States Ocean Wave Energy Resource. Technical Report, Electric Power Research Institute, CA, USA.
- Kirby, J.T., Dalrymple, R., Shi, F., 2005. REF/DIF S version 1.3: Documentation and user's manual. Technical Report. Research Report NO. CACR-04-01, Center for Applied Coastal Research, Univ. of Delaware.
- Kofoed, J.P., Frigaard, P., Friis-Madsen, E., Sorensen, H.C., 2006. Prototype testing of the wave energy converter wave dragon. Renew. Energy 31 (2), 181–189.
- Lawless, M., Rodger, D., 2013. Development of the European tidal database and its potential application to marine renewables. J. Coast. Res. 65 (sp2), 1629–1632.
- Longuet-Higgins, M., 1975. On the joint distribution of the periods and amplitudes of sea waves. J. Geophys. Res.- Oceans 80 (18), 2688–2694.
- Mofor, L., Goldsmith, J., Jones, F., 2014. Ocean Energy: Technology Readiness, Patents, Deployment Status and Outlook. Technical Report, International Renewable Energy Agency (IRENA) Report, Paris.
- Mork, G., Barstow, S., Kabuth, A., Pontes, M.T., 2010. Assessing the global wave energy potential. In: ASME 2010 29th International Conference on Ocean, Offshore and Arctic Engineering. American Society of Mechanical Engineers, pp. 447–454.

- Pawlowicz, R., Beardsley, B., Lentz, S., 2002. Classical tidal harmonic analysis including error estimates in MATLAB using T_TIDE. Comput. Geosci. 28 (8), 929–937.
- Pierson, W.J., Moskowitz, L., 1964. Proposed spectral form for fully developed wind seas based on similarity theory of S. A. Kitaigorodskii. J. Geophys. Res.- Oceans 69 (24), 5181–5190.
- Pontes, M., 1998. Assessing the european wave energy resource. J. Offshore Mech. Arct. Eng. 120 (4), 226–231.
- Reikard, G., 2013. Integrating wave energy into the power grid: Simulation and forecasting. Ocean Eng. 73, 168–178.
- Reikard, G., Robertson, B., Buckham, B., Bidlot, J.-R., Hiles, C., 2015. Simulating and forecasting ocean wave energy in western Canada. Ocean Eng. 103, 223–236.
- Sawin, J.L., Sverrisson, F., Chawla, K., Lins, C., Adib, R., Hullin, M., Leitner, S., Mazzaccaro, S., Murdock, H., Williamson, L.E., et al., 2015. Renewables 2015 Global Status Report. Technical Report, Renewable Energy Policy Network for the 21st Century.
- Sierra, J., Martín, C., Mösso, C., Mestres, M., Jebbad, R., 2016. Wave energy potential along the atlantic coast of Morocco. Renew. Energy 96, 20–32.
- Skamarock, W.C., Klemp, J.B., Dudhia, J., Gill, D.O., Barker, D.M., Wang, W., Powers, J.G., 2008. A Description of the Advanced Research WRF Version 3. NCAR Technical note-475+ STR Technical Report, Citeseer.
- Soares, C., Carvalho, A., 2003. Probability distributions of wave heights and periods in measured combined sea-states from the Portuguese coast. J. Offshore Mech. Arct. Eng. 125 (3), 198–204.
- Sørensen, H.C., Russell, I., 2006. Life cycle assessment of the wave energy converter: Wave dragon. In: Int Conf Ocean Energy. Fron Innovation To Industry.. OTTI, Bremerhaven, Germany.
- Srisuwan, C., Rattanamanee, P., Rattanapitikon, W., 2017. Analytical formulas for estimation of phase-averaged parameters of random waves. Ocean Eng. 133, 23–35.
- Svendsen, I.A., 2006. Introduction to Nearshore Hydrodynamics, Vol. 24. World Scientific.
- SWAN Team, 2011. SWAN Cycle III Version 40.85 Technical Manual. Technical Report, Delft University Technology, Faculty of Civil Engineering and Geosciences.
- Thomson, R., Harrison, G., Chick, J., 2011. Full life cycle assessment of a wave energy converter. In: IET Conference Proceedings. The Institution of Engineering & Technology, Edinburgh, UK..
- van Nieuwkoop, J.C., Smith, H.C., Smith, G.H., Johanning, L., 2013. Wave resource assessment along the cornish coast (UK) from a 23-year hindcast dataset validated against buoy measurements. Renew. Energy 58, 1–14.
- Work, P.A., 2008. Nearshore directional wave measurements by surface-following buoy and acoustic Doppler current profiler. Ocean Eng. 35 (8–9), 727–737.
- Work, P.A., Haas, K.A., Defne, Z., Gay, T., 2013. Tidal stream energy site assessment via three-dimensional model and measurements. Appl. Energy 102, 510–519.
- Work, P., Srisuwan, C., 2010. Identification of swell in nearshore surface wave energy spectra. Int. J. Ocean Clim. Syst. 1 (2), 51–66.